



HAL
open science

Sulfate-radical Induced Removal of Organic Micro-pollutants from Aqueous Solution- Influence of Natural Water Constituents

Lei Zhou

► **To cite this version:**

Lei Zhou. Sulfate-radical Induced Removal of Organic Micro-pollutants from Aqueous Solution- Influence of Natural Water Constituents. Catalysis. Université de Lyon, 2017. English. NNT : 2017LYSE1171 . tel-01629838

HAL Id: tel-01629838

<https://theses.hal.science/tel-01629838>

Submitted on 6 Nov 2017

HAL is a multi-disciplinary open access archive for the deposit and dissemination of scientific research documents, whether they are published or not. The documents may come from teaching and research institutions in France or abroad, or from public or private research centers.

L'archive ouverte pluridisciplinaire **HAL**, est destinée au dépôt et à la diffusion de documents scientifiques de niveau recherche, publiés ou non, émanant des établissements d'enseignement et de recherche français ou étrangers, des laboratoires publics ou privés.



N°d'ordre NNT : 2017LYSE1171

THESE de DOCTORAT DE L'UNIVERSITE DE LYON

opérée au sein de

l'Université Claude Bernard Lyon 1

Ecole Doctorale ED206

Chimie de Lyon

Spécialité de doctorat :

Discipline : Chimie

Soutenue publiquement 27/09/2017, par :

Lei ZHOU

**Élimination induite par le radical sulfate de micro
polluants organiques en phase aqueuse-Influence des
constituants naturels de l'eau**

Devant le jury composé de :

RICHARD Claire, Directeur de Recherches CNRS, Université Clermont Auvergne

Présidente

WONG-WAH-CHUNG Pascal, professeur, Université Aix Marseille

Rapporteur

CHIRON Serge, Professeur, Université de Montpellier

Rapporteur

VULLIET Emmanuelle, Chargée de Recherche, Université Claude Bernard Lyon 1

Examinatrice

SLEIMAN Mohamad, Maître de Conférences, Sigma Clermont, Université Clermont Auvergne

Examinateur

CHOVELON Jean-Marc, Professeur, Université Claude Bernard Lyon 1

Directeur de thèse

FERRONATO Corinne, Maître de Conférences, Université Claude Bernard Lyon 1

Co-directrice de thèse

UNIVERSITE CLAUDE BERNARD - LYON 1

Président de l'Université

Président du Conseil Académique

Vice-président du Conseil d'Administration

Vice-président du Conseil Formation et Vie Universitaire

Vice-président de la Commission Recherche

Directrice Générale des Services

M. le Professeur Frédéric FLEURY

M. le Professeur Hamda BEN HADID

M. le Professeur Didier REVEL

M. le Professeur Philippe CHEVALIER

M. Fabrice VALLÉE

Mme Dominique MARCHAND

COMPOSANTES SANTE

Faculté de Médecine Lyon Est – Claude Bernard

Directeur : M. le Professeur G.RODE

Faculté de Médecine et de Maïeutique Lyon Sud – Charles Mérieux

Directeur : Mme la Professeure C. BURILLON

Faculté d'Odontologie

Directeur : M. le Professeur D. BOURGEOIS

Institut des Sciences Pharmaceutiques et Biologiques

Directeur : Mme la Professeure C. VINCIGUERRA

Institut des Sciences et Techniques de la Réadaptation

Directeur : M. X. PERROT

Département de formation et Centre de Recherche en Biologie Humaine

Directeur : Mme la Professeure A-M. SCHOTT

COMPOSANTES ET DEPARTEMENTS DE SCIENCES ET TECHNOLOGIE

Faculté des Sciences et Technologies

Directeur : M. F. DE MARCHI

Département Biologie

Directeur : M. le Professeur F. THEVENARD

Département Chimie Biochimie

Directeur : Mme C. FELIX

Département GEP

Directeur : M. Hassan HAMMOURI

Département Informatique

Directeur : M. le Professeur S. AKKOUCHE

Département Mathématiques

Directeur : M. le Professeur G. TOMANOV

Département Mécanique

Directeur : M. le Professeur H. BEN HADID

Département Physique

Directeur : M. le Professeur J-C PLENET

UFR Sciences et Techniques des Activités Physiques et Sportives

Directeur : M. Y.VANPOULLE

Observatoire des Sciences de l'Univers de Lyon

Directeur : M. B. GUIDERDONI

Polytech Lyon

Directeur : M. le Professeur E.PERRIN

Ecole Supérieure de Chimie Physique Electronique

Directeur : M. G. PIGNAULT

Institut Universitaire de Technologie de Lyon 1

Directeur : M. le Professeur C. VITON

Ecole Supérieure du Professorat et de l'Education

Directeur : M. le Professeur A. MOUGNIOTTE

Institut de Science Financière et d'Assurances

Directeur : M. N. LEBOISNE

Acknowledgement

This scientific thesis was accomplished at institut de recherches sur la catalyse et l'environnement de Lyon (IRCELYON), Université Claude Bernard-Lyon 1 in Lyon. Firstly, I wish to express my sincerely gratitude to my advisors, Pr. Jean-Marc Chovelon and Dr. Corinne Ferronato for guidance during the 3 years on both my research and life. And, I cordially express my thanks to Dr. Claire Richard and Dr. Mohamad Sleiman from institute de chimie de Clermont-Ferrand (ICCF) of Université Clermont Auvergne for their hosting from 2016 to 2017 to help finish this thesis. I am lucky to have four supervisors during my PhD, I would like to say without their guidance and encouragement, I could not obtain my scientific achievement. Their deep knowledge and huge enthusiasm in scientific research strongly influence me and will accompany with me in my following life and research activities.

This paper would not have been possible without the precious help of Ludovic Fine, the “Swiss Knife” in our lab. Species thanks to Emmanuelle Vulliet, Laure Wiest, and Robert Baudot and Guillaume Voyard for their experimental supporting. I also express my thanks to those who gave me various recommendations and technical supports during my research.

I gratefully acknowledge the China Scholarship Council (CSC) for the financial support to study at IRCELYON.

My thanks to my friends Chongyang Wang, Wenjun Hao, Wenzhang Fang and Junjie Pu in Lyon; Xiaoning Wang, Wenyu Huang, Jinlong Zha, Shengnan Li, Miao Wang and Yanan Yuan in Clermont-Ferrand for their help during the 3 years.

My special thanks should be given to my family, my parents, parents in law, especially my wife Dandan Fang for her deep love, silent support and tremendous sacrifice during these years of my studies. I sincerely hope the finish of this thesis would represent a good start to welcome our upcoming baby.

Abstract

Sulfate radical ($\text{SO}_4^{\cdot-}$) based advanced oxidation processes (AOPs) has been proved to be effective for the removal of many contaminants. In this thesis, we investigated the oxidation processes of iodinated X-ray contrast media diatrizoate (DTZ), β 2-adrenoceptor agonists salbutamol (SAL) and terbutaline (TBL) by reaction with $\text{SO}_4^{\cdot-}$ generated from the activation of persulfate (PS); in addition, the reactivity of $\text{SO}_4^{\cdot-}$ with natural organic matter (NOM) was also estimated.

Specifically, to determine the reactivity of $\text{SO}_4^{\cdot-}$ with NOM, laser flash photolysis (LFP) technique was applied to monitor the $\text{SO}_4^{\cdot-}$ decay and the formation of the transients from organic matters. Reaction rate constants comprised between 1530 and 3500 $\text{s}^{-1} \text{ mgC}^{-1} \text{ L}$ were obtained by numerical analysis of differential equations and the weighted average of the extinction coefficient of the generated organic matters radicals between 400 and 800 $\text{M}^{-1} \text{ cm}^{-1}$.

In the decomposition process of DTZ by UV-activated PS, major oxidation pathways include deiodination-hydroxylation, decarboxylation- hydroxylation and side chain cleavage. Results also indicated that DTZ degradation rate increased with increasing PS concentration. The presence of NOM inhibited DTZ removal rate, while, bicarbonate enhanced it, and chloride ions induced a negative effect above 500 mM.

For the degradation of SAL and TBL, phenoxyl radicals were proven to play a very important role from the initial step. Chloride exhibited no effect on the oxidation efficiencies of SAL and TBL, while bromide, bicarbonate and NOM all showed inhibitory effects.

Key words: Advanced oxidation process; Sulfate radical; Organic micro-pollutants; Laser flash photolysis; Natural organic matter.

RESUME

Les processus d'oxydation avancés à base du radical sulfate ($\text{SO}_4^{\bullet -}$) ont prouvé leur efficacité pour l'élimination de nombreux contaminants. Dans ce travail de thèse, nous avons étudié les processus d'oxydation et de dégradation par le radical sulfate activé à partir du persulfate (PS) pour les molécules suivantes : le diatrizoate, molécule utilisée comme produit de contraste radiologique iodé (DTZ), le salbutamol (SAL) et la terbutaline (TBL), agonistes des récepteurs β 2-adrénergiques. En outre, la réactivité de $\text{SO}_4^{\bullet -}$ avec la matière organique naturelle (NOM) a également été déterminée.

Plus précisément, pour déterminer la réactivité de $\text{SO}_4^{\bullet -}$ avec NOM, une technique de photolyse laser couplée à la spectroscopie (LFP) a été appliquée pour étudier l'évolution de $\text{SO}_4^{\bullet -}$ ainsi que la formation d'espèces transitoires à partir de la matière organique. Des constantes de vitesses comprises entre 1530 et 3500 $\text{s}^{-1} \text{mgC}^{-1} \text{L}$ ont été obtenues par analyse numérique des équations différentielles et des valeurs moyennes de coefficient d'absorption molaires comprises entre 400 et 800 $\text{M}^{-1} \text{cm}^{-1}$ ont été déterminées pour les espèces transitoires générées de la matière organique.

Dans le processus de décomposition de DTZ par PS activé par UV, les principales voies d'oxydation sont la dé-iodination-hydroxylation, la dé-carboxylation-hydroxylation et le clivage de la chaîne latérale. Les résultats ont également indiqué que la vitesse de dégradation du DTZ augmentait avec l'augmentation de la concentration en PS.

La présence de NOM a inhibé la dégradation de DTZ, tandis que le bicarbonate l'a amélioré. Pour les ions chlorure un effet négatif a été observé pour des concentrations supérieures à 500 mM.

Pour la dégradation du SAL et du TBL, il a été montré que les radicaux phénoxy jouaient un rôle majeur en début de réaction. Par ailleurs, le chlorure n'a pas eu d'effet tangible sur

l'efficacité d'oxydation de la SAL et du TBL, tandis que les ions bromures, bicarbonates et le NOM présentaient des effets inhibiteurs.

Mots clés: Processus d'Oxydation Avancé; Radical sulfate; Micro-polluants organiques; Photolyse Laser couplé à la spectroscopie, Matière organique naturelle.

Table of Contents

| | |
|--|----|
| List of Figures..... | 5 |
| List of Tables..... | 9 |
| General Introduction | 11 |
| Chapter I Organic micro-pollutants and advanced oxygen process..... | 15 |
| 1.1. Organic micro-pollutants in aquatic environment..... | 15 |
| 1.1.1 The occurrence of organic micropollutants | 15 |
| 1.1.2 Sources and fate of organic micro-pollutants in natural waters..... | 17 |
| 1.1.3. Environmental fate of organic micro-pollutants in natural waters..... | 19 |
| 1.1.4. Environmental risk of organic micro-pollutants..... | 25 |
| 1.2. Advanced oxidation process in water treatments..... | 26 |
| 1.2.1. Hydroxyl radicals ($\cdot\text{OH}$) based AOPs..... | 28 |
| 1.2.2. Sulfate radical ($\text{SO}_4^{\cdot-}$) based AOPs..... | 30 |
| 1.3. References..... | 37 |
| Chapter II Experiment Section..... | 55 |
| 2.1. Chemicals and materials..... | 55 |
| 2.2 Steady-state photolysis experiments..... | 57 |
| 2.3 Laser Flash Photolysis (LFP) experiments..... | 59 |
| 2.4 Analytical procedures..... | 59 |
| 2.5. Rate constants measurements..... | 61 |
| 2.6. Calculations..... | 62 |
| 2.7. References..... | 66 |
| Chapter III Reactivity of sulfate radicals with natural organic matters..... | 69 |
| 3.1. Results and discussion..... | 70 |

| | |
|--|------------|
| 3.1.1. Formation and identification of transient species..... | 70 |
| 3.1.2. Reactivity of $\text{SO}_4^{\bullet-}$ towards selected NOM..... | 71 |
| 3.1.3. Bleaching..... | 75 |
| 3.2. Conclusion..... | 75 |
| 3.3. References..... | 75 |
| Chapter IV Degradation of Diatrizoate by Photo-activated Persulfate | 79 |
| 4.1 Results and discussion..... | 81 |
| 4.1.1. Reaction kinetics. | 81 |
| 4.1.2. Identification of oxidizing species ($\text{SO}_4^{\bullet-}$ and $\cdot\text{OH}$)..... | 90 |
| 4.1.3. Degradation products and reaction pathways..... | 92 |
| 4.1.4. Impacts of natural water constituents..... | 96 |
| 4.2. Conclusion..... | 100 |
| 4.3. References. | 101 |
| Chapter V Degradation of β2-adrenoceptor Agonists Salbutamol and Terbutaline | |
| by Photo-activated Persulfat..... | 109 |
| 5.1 Results and discussion..... | 111 |
| 5.1.1. Formation and identification of transient species..... | 111 |
| 5.1.2. Reactivity of sulfate radical towards SAL and TBL..... | 114 |
| 5.1.3. UV/PS oxidation under simulated solar light..... | 115 |
| 5.1.4. Oxidation products..... | 119 |
| 5.1.5. Mechanisms of oxidation pathways..... | 120 |
| 5.1.6. Effects of natural water constitutues..... | 124 |
| 5.2. Conclusion..... | 135 |
| 5.3. References..... | 136 |

| | |
|---|-----|
| Chapter VI General conclusions and respects | 145 |
| Appendix..... | 149 |

List of Figures

| | |
|--|----|
| Figure 1.1. Representative sources and routes of micro-pollutants in the environment..... | 17 |
| Figure 1.2. Hydroxyl radicals formed according to advanced oxidation technologies..... | 28 |
| Figure 2.1. The scheme of applied SUNTEST photo-reactor..... | 58 |
| Figure 2.2. Incident light received by the solutions in the SUNTEST..... | 58 |
| Figure 2.3. Standard curve for PS concentration determination..... | 64 |
| Figure 3.1. Time profile absorbance monitored for PS (1) and PS + NLNOM (2) at 450 nm; time profile absorbance monitored at 600 nm for PS + NLNOM (3)..... | 70 |
| Figure 3.2. Excitation of a solution containing PS and NLNOM. Transient spectrum measured 50 μ s after the pulse end (A) and absorbance decay measured at 450 nm (B).... | 71 |
| Figure 3.3. Bleaching of the four selected NOMs by photo-activation of PS at 330 nm..... | 74 |
| Figure 4.1. Degradation of DTZ by UV, H ₂ O ₂ in dark, PS in dark, UV/H ₂ O ₂ and UV/PS.... | 81 |
| Figure 4.2. Decay of sulfate radical transient followed at 450 nm in the absence and presence of DTZ (A); the linear relationship of the pseudo-first order decay constant of SO ₄ ^{•-} (k , s ⁻¹) versus the concentration of DTZ (B)..... | 83 |
| Figure 4.3. Absorption spectrum of H ₂ O ₂ and PS at 50 mM from 250 to 350 nm..... | 84 |
| Figure 4.4. The UV-Vis spectrum of DTZ reaction solutions oxidized by UV/PS in a cell of pathlength 1 cm..... | 85 |
| Figure 4.5. Light intensity absorbed by PS during the reaction process..... | 86 |
| Figure 4.6. Degradation of DTZ by UV/PS (A) for various pH; (B) for different initial PS doses..... | 87 |
| Figure 4.7. Speciation of DTZ at different pH values..... | 89 |
| Figure 4.8. Degradation efficiencies of DTZ by UV/PS in the presence of different scavengers (EtOH and TBA) molar ratios..... | 91 |
| Figure 4.9. Proposed oxidation pathways of DTZ by simulated sunlight activated PS..... | 94 |

| | |
|---|-----|
| Figure 4.10. Proposed oxidation mechanisms of deiodination (A) and decarboxylation (B)... | 95 |
| Figure 4.11. Decomposition of DTZ by simulated sunlight activated PS in the presence of SRFA..... | 97 |
| Figure 4.12. Decomposition of DTZ by simulated sunlight activated PS in the presence of chloride..... | 98 |
| Figure 4.13. Degradation efficiencies of DTZ by simulated sunlight activated PS in the presence of bicarbonate..... | 100 |
| Figure 5.1. LFP of PS and SAL. A: Transient spectra measured at the pulse end (A0) and 20 μ s after (A20). B: Time profile absorbance monitored at 400 nm. C: Time profile absorbance monitored at 450 nm..... | 111 |
| Figure 5.2. Transient absorption spectra of 2-hydroxybenzyl alcohol (2-HBA, A) and 4-hydroxybenzyl alcohol (4-HBA, B) obtained by LFP in water..... | 112 |
| Figure 5.3. Transient absorption spectra of aqueous resorcinol (A), TBL (B) and 3,5-DHBA (C) in the presence of PS produced by LFP (the insert bands represent the phenoxyl radical absorption bands), and the time profiles (20 μ s) of TBL/PS transient species at 410 nm (D1), 425 nm (D2), 440 nm (D3) and 500 nm (D4)..... | 113 |
| Figure 5.4. Vibrational progression of the UV-Vis absorption spectra of the resorcinol phenoxyl radical and the 3,5-DHBA phenoxyl radical obtained by DFT calculations at the B3LYP/6-31+G(d,p) level..... | 114 |
| Figure 5.5. Decay of the sulfate radical monitored at 450 nm as a function of SAL concentration. Transient absorbance were obtained upon LFP (266 nm) for PS at 44 mM (A); Linear plot of the pseudo-first order decay rate constant of $\text{SO}_4^{\cdot-}$ (k , s^{-1}) versus the concentration of SAL (B)..... | 115 |

| | |
|---|-----|
| Figure 5.6. Pseudo-first order rate constants for SAL and TBL for different initial PS concentrations..... | 117 |
| Figure 5.7. Proposed oxidation pathways of TBL (A) and SAL (B) by UV/PS process..... | 123 |
| Figure 5.8. Reactions of the phenoxyl radical from SAL..... | 123 |
| Figure 5.9. Decomposition rate constants of SAL and TBL at various Cl ⁻ concentrations... | 125 |
| Figure 5.10. Effect of Br ⁻ on the oxidation kinetic of SAL and TBL by UV/PS process..... | 127 |
| Figure 5.11. Decay of Br ₂ ^{·-} transient followed at 370 nm in the absence and presence of SAL (A); Linear relationship of the pseudo-first order decay constant of Br ₂ ^{·-} (k, s ⁻¹) versus the concentration of SAL (B)..... | 128 |
| Figure 5.12. Proposed pathways of SAL and TBL in the presence of excess Br ⁻ by UV/PS process..... | 129 |
| Figure 5.13. Degradation rate constants of SAL and TBL at various HCO ₃ ⁻ concentration... | 132 |
| Figure 5.14. Decomposition of SAL (A) and TBL (B) by simulated sunlight activated PS in the presence of different concentration of SRFA..... | 133 |

List of Tables

| | |
|--|-----|
| Table 2.1. Main characteristics of the chemical reagents used in this study..... | 55 |
| Table 2.2. HPLC analysis parameters..... | 60 |
| Table 3.1. Values of k_3 and ϵ'/ϵ for the selected NOMs and carbon organic content corrected for the ash and water content obtained from the IHSS website..... | 74 |
| Table 4.1. Degradation efficiencies of DTZ at different conditions..... | 88 |
| Table 4.2. Proposed structure of DTZ oxidation products by UV activated persulfate..... | 93 |
| Table 5.1. Pseudo first-order degradation rate constants of SAL and TBL in different conditions..... | 116 |
| Table 5.2. Proposed structure of SAL and TBL (120 μ M) degradation products in the presence of PS (12 mM) after irradiation of 60 min (in positive mode)..... | 121 |
| Table 5.3. Reaction rate constants of different reactive species with SAL and TBL..... | 129 |
| Table 5.4. Proposed structure of SAL and TBL (120 μ M) degradation products in the presence of PS (12 mM) and excess Br ⁻ (0.1 M) after irradiation of 60 min (in positive mode)..... | 130 |

General Introduction

Over the last few decades, organic micro-pollutants have been frequently detected in various aquatic environment. The occurrence of these organic micro-pollutants has become a worldwide issue of increasing environmental concern. Traditional wastewater treatment plants (WWTPs) are not designed to completely remove organic micro-pollutants at relative low concentration, which makes them an important route for the release of such chemicals.

The growing concerns over water quality have led to a need for the development of effective treatment technologies as a supplement to WWTPs to remove such micro-pollutants from aquatic systems. Advanced oxidation processes (AOPs) are among the promising alternatives capable of removing these micro-pollutants from WWTPs as well as in natural waters. Most of the AOPs technologies are mainly based on the generation of reactive oxygen species (ROS, e.g. hydroxyl radicals and sulfate radicals).

The using of hydroxyl radicals ($\cdot\text{OH}$) for the elimination of organic micro-pollutants has been proved to be very efficient; while it still has some drawbacks, for instance, the oxidation efficiency of Fenton process would always decline due to the change of solution pH. Sulfate radical-based AOPs (SR-AOPs) are increasingly gaining attention as effective solution to the degradation of recalcitrant organic micro-pollutants in aquatic systems. Sulfate radical has strong oxidation capacity, and also opposes a longer lifetime than $\cdot\text{OH}$. It prefers to react with electron-rich groups *via* electron-transfer reactions, such as aniline and phenolic chemicals. These chemical properties of sulfate radical mentioned above makes SR-AOPs a promising AOPs technology for the removal of organic micro-pollutants.

The main objectives of this work are defined as follows:

- to investigate the oxidation of several selected micro-pollutants by using SR-AOPs, including iodinated X-ray contrast media diatrizoate (DTZ), β 2-adrenoceptor agonists salbutamol (SAL) and terbutaline (TBL);

- to determine the rate constants of selected organic micro-pollutants with sulfate radical;
- to identify the transformation intermediates and oxidation products; and to explore the degradation pathways and mechanisms;
- to evaluate the impacts of natural water constituents (HCO_3^- , Cl^- , Br^- and NOM).

The first part of this thesis, in Chapter 1, gives a brief introduction on the background of relevant research. In this part the occurrence, sources, fates and environmental risks of organic micro-organic pollutants were introduced initially. Since many micro-organic pollutants have been detected in aquatic environment, AOPs technologies are regarded as a supplement to WWTPs for the removal of these micro-pollutants from aquatic systems. AOPs based on hydroxyl radical as well as sulfate radical were also stated in this part, SR-AOPs attract more scientific attention due to its selectivity and adaptability to different conditions. The different activation strategies to generate sulfate radical, degradation of organic micro-pollutants and the effects of natural water constituents on SR-AOPs are all present in this chapter.

The second part, Chapter 2, illustrates the materials and experimental methodologies. In this chapter the chemicals used in this thesis (including their purities and suppliers), the experimental setup, analytical procedures and the calculation methods are all described in details.

Chapter 3 focuses on the kinetic study of the reaction between sulfate radicals and natural organic matter. The objective of this chapter is to determine the absolute rate constants of reactions of $\text{SO}_4^{\bullet-}$ with different NOMs by using the laser flash photolysis (LFP) method. This direct method that allows the monitoring of the $\text{SO}_4^{\bullet-}$ decay also offers the possibility to observe the transient species generated by these reactions, determine their spectroscopic characteristics and measure their decay.

Chapter 4 investigates the degradation of X-ray contrast media diatrizoate by sulfate radicals. In this part, we attempt to elucidate the underlying mechanisms and oxidation pathways of

the reaction between DTZ and $\text{SO}_4^{\cdot-}$, $\text{SO}_4^{\cdot-}$ is generated by simulated sunlight activated PS process. Kinetic studies are conducted for a better understanding of the influence of factors including pH and natural water constituents. The identification of DTZ transformation intermediates and products is also performed by using HPLC-MS method. Based on the HPLC-MS data, the reaction mechanisms and detailed transformation pathways are proposed. Our study provides useful information about using sulfate radical-based technologies for remediation of the groundwater contaminated by DTZ and structurally related X-ray contrast agent.

Chapter 5 studies the degradation kinetic and mechanisms of β 2-adrenoceptor agonists salbutamol (SAL) and terbutaline (TBL) by sulfate radicals. In this chapter, we evaluate the efficacy of simulated sunlight activated PS processes in eliminating SAL and TBL. The main objectives of this part were (1) to identify the main oxidation products of SAL and TBL and propose the oxidation mechanism of them by the reactive species involved in the processes; (2) to investigate the reactivity and predominant reactive species responsible for the degradation of SAL and TBL; (3) to evaluate the effects of natural water constituents such as chloride, bromide, bicarbonate and natural organic matter on the oxidation process of SAL and TBL by UV/PS.

Chapter 6 contains the general conclusions and prospects of this thesis.

Chapter I

Organic micro-pollutants and advanced oxygen process

1.1 Organic micro-pollutants in aquatic environment.

1.1.1. The occurrence of organic micro-pollutants.

Organic micro-pollutants, also termed as emerging contaminants, comprise a large number group anthropogenic as well as natural substances. These chemicals include pharmaceuticals, personal care products (PPCPs), perfluorinated compounds (PFCs), endocrine disrupting chemicals (EDCs), industrial chemicals, pesticides and many other emerging compounds [1]. In natural waters, organic micro-pollutants are commonly present at trace concentrations, ranging from ng L^{-1} to $\mu\text{g L}^{-1}$. The 'low concentration' and diversity of micro-pollutants not only complicate the associated detection and analysis procedures but also create challenges for water and wastewater treatment processes [1].

Over the last few decades, the occurrence of these organic micro-pollutants in the environment has become a worldwide issue of increasing environmental concern. Organic micro-pollutants have been frequently detected in various aquatic environment, such as wastewater treatment plants (WWTPs) effluents [2], surface water [3], drinking water [4] as well as groundwater [5] due to the advance in more sensitive, reliable and cost-effective analytical apparatus. For instance, in the South Wales region of the UK, 56 different PPCPs, endocrine disruptors and illicit drugs were detected in two contrasting rivers: River Taff and River Ely. Most PPCPs found in these two rivers were detected at concentrations reaching single $\mu\text{g L}^{-1}$ and their levels depended mainly on the extent of water dilution resulting from rainfall. The most frequently detected PPCPs were antibacterial drugs (trimethoprim, erythromycin- H_2O and amoxicillin), anti-inflammatories/analgesics (paracetamol, tramadol, codeine, naproxen, ibuprofen and diclofenac) and antiepileptic drugs (carbamazepine and gabapentin) [6]. Yang et al. investigated the occurrence of four perfluorinated sulfonate acids

(PFSAs) and 10 perfluorinated carboxylate acids (PFCAs) in water from Liao River and Taihu Lake, China. They found that in Taihu Lake, perfluorooctanoic acid (PFOA) and perfluorooctanesulfonic acid (PFOS) were the most detected PFCs; and in Liao River, perfluorohexane sulfonate (PFHxS) was the predominant PFCs followed by PFOA, while PFOS was only detected in two of the samples [7]. PFCs have also been detected in North Pacific Ocean with the average concentration at 560 pg L^{-1} , and perfluoroalkyl carboxylates (PFCAs) were the dominant PFCs [8]. Estrogens are often regarded as one of the most important endocrine disrupting chemicals (EDCs), estrogens including estrone (E1), 17β estradiol (E2), estriol (E3) and 17α -ethinylestradiol (EE2), have been found in sewage and surface water in many countries (UK, Germany, France, etc), and their concentrations reached several hundreds of ng L^{-1} [9]. Other EDCs, such as bisphenol A, nonylphenols and octylphenols were also been detected in the treated sewage effluent as well as drinking water sources with concentrations from ng L^{-1} level to several hundreds of $\mu\text{g L}^{-1}$ [9]. The occurrence of some industrial chemicals, such plasticizers and fire retardants has increasingly been subject of research activities over the last decade. Regnery et al. investigated the occurrence of organophosphorus (OPs) flame retardants and plasticizers in urban and remote surface waters in Germany. They found the OPs levels in the rural lakes were considerably lower than in lakes of the urban area Frankfurt and Main. High variability but no significant seasonal trends were observed for all the organophosphorus in urban lake water samples. In addition, they also revealed the rapid degradation of non-chlorinated OPs and the resistance of chlorinated OPs in natural waters upon sunlight irradiation [10]. In USA, pesticides were commonly detected in shallow groundwater, at concentrations generally low since over 95% of the detections were found less than $1 \mu\text{g L}^{-1}$. The most frequently detected pesticides and some of their metabolites were atrazine, deethylatrazine, simazine, metolachlor, and prometon [11]. The occurrence of 22 pesticides in different WWTPs have been studied by Köck-

Schulmeyer et al., their results indicated that total pesticide levels were in most instances below $1 \mu\text{g L}^{-1}$ but removal in the WWTPs was variable and often poor, with concentrations in the effluent sometimes higher than in the corresponding influent [12].

The occurrence of organic micro-pollutants in the aquatic environment is reported in many publications during the last decades and reviewed by many scientists demonstrating an increasing concern about them. Although the reported concentrations of most organic micro-pollutants were relatively low, their environmental risk and potential harm to human beings could still not be ignored.

1.1.2. Sources and fate of organic micro-pollutants in natural waters.

As illustrated in Figure 1.1, several main sources of organic micro-pollutants are summarized including: (a) domestic and hospital effluents; (b) industrial wastewater; (c) landfill leachates; and (d) runoff from agriculture, livestock and aquaculture [1, 13].

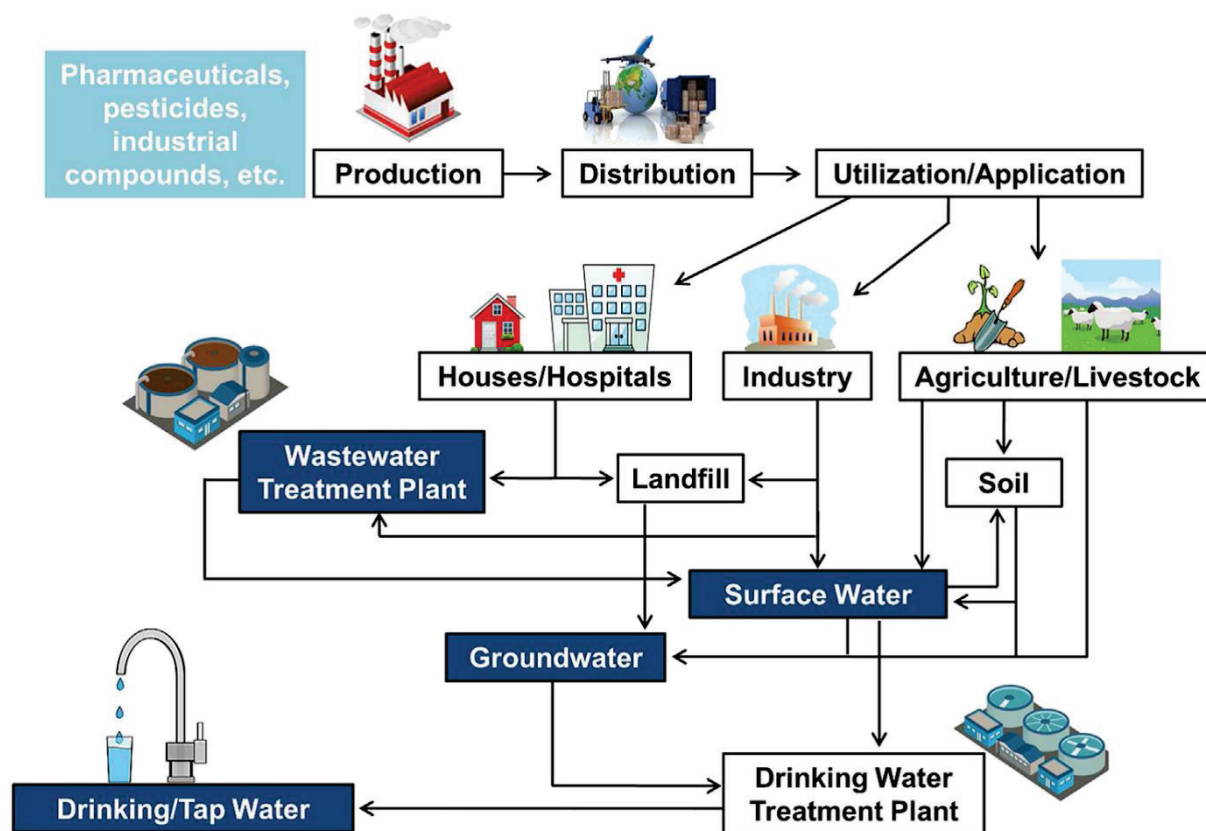


Figure 1.1. Representative sources and routes of micro-pollutants in the environment [20].

The release of effluents from municipal WWTPs is one of the important routes for the appearance of many organic micro-pollutants in the aquatic environment, the wastewater treated in these plants mainly resulting from domestic and industrial activities, as well as from hospitals [14]. Numerous studies are found to support the claim that WWTPs and untreated urban wastewater acted as the major routes through which PPCPs and EDCs get released into various natural waters [14-16]. Many organic micro-pollutants oppose microbial activities such as antibiotics and hormones, most of the conventional WWTPs based on biological process are not designed to effectively remove these organic micro-pollutants [17]. Thus, in this context, a high proportion of the non-degradable or partially removed micro-pollutants would escape and get introduced into the aquatic systems as effluents [18]. For instance, in Germany, it has been reported by Kümmerer that about 70% of the total amount of antibiotics consumed was excreted unchanged from WWTPs [19].

Another source of the introduction of organic micro-pollutants into aquatic environment is the leakage from landfills, manure storage tanks and septic tanks [21]. This kind of pollution source shows great threat to natural waters, especially to groundwater. Eggen et al. have identified the occurrence PFCs, chlorinated alkylphosphates and some PPCPs chemicals in municipal landfill leachates [22], this work has shown that municipal landfill leachates may represent a significant source of concern for legacy, new and emerging chemicals in groundwater. Fawell and Ong also noted that some organic micro-pollutants (i.e. PPCPs and EDCs) would enter into the groundwater through leaching and leaking of poorly designed sewer and landfills [23]. In addition, 10 pharmaceutical compounds were detected by Carrara et al. in groundwater samples released from 3 septic tanks in Canada [24]. Among the contaminants, ibuprofen, gemfibrozil, and naproxen were observed to be transported at the highest concentrations and greatest distances from the infiltration source areas.

The livestock and poultry breeding as well as aquaculture are also important sources for the

inputs of organic micro-pollutants into aquatic systems. As known, direct release of pesticides and pharmaceuticals in environment might occur via application in aquaculture (i.e. fish farming) [13]. These chemicals used in fish farming could enter surface waters directly without undergoing any kind of attenuation process. Poor agricultural practices were also considered as an important origin for the occurrence of pesticides, PPCPs and EDCs in rivers and lakes [25]. Moreover, the application of land-applied bio-solids is regarded as another possible route of the entry for organic micro-pollutants into groundwater. Hale et al. have found high concentrations of brominated diphenyl ethers (BDEs) in bio-solids from four different regions of the United States [26]. Pharmaceuticals (i.e. antibiotics) and EDCs are used in huge amount in livestock and poultry breeding as anti-microbiological agents and promoters, these compounds could release into natural waters mostly via washing off after rain and run-off from manure. Matthiessen et al. concluded that near 92% of the headwater streams in UK were contaminated by EDCs from livestock farms [21], in their study the most frequently detected EDCs are E1 and E2.

Apart from the sources mentioned above, others include recreational activities, transportation or wash-off from roadways and atmospheric deposition [14]. As known, many personal care products could directly enter into aquatic systems via recreational activities such as swimming, bathing or other technological process [27]. For instance, UV filters, one of the most used personal products, have been detected frequently in rivers and lakes [28, 29]. Atmospheric deposition is another route for some micro-pollutants entering the surface waters, it has been reported that high atmospheric depositional inputs would lead to high persistent organic pollutants (POPs) concentrations on surface waters and soils [30, 31].

1.1.3. Environmental fate of organic micro-pollutants in natural waters.

The presence of organic micro-pollutants from the main sources of contaminations (i.e. WWTPs, landfills and agriculture) is firstly attenuated by dilution in surface water up to trace

level. Afterwards, there are multiple processes responsible for the environmental fates of these organic micro-pollutants in aquatic systems, these processes include adsorption, chemical and physico-chemical transformation and biodegradation.

Adsorption onto the surface of suspended solids, colloids and natural dissolved organic matter (DOM) is one of the most important processes that could attenuate micro-pollutants from natural waters [13]. The adsorption of one micro-pollutant depends on its physico-chemical properties as well as geology, soil texture (sand, clay...), sediment and DOM nature [32].

Rogers once proposed to characterize the mobility of organic contaminants by using partition coefficient (K_{ow}), the greater the values are, the more those micro-pollutants sorb upon organic carbons such as suspended soils, non-polar fats, lipids and mineral oil [33]. Specifically, if $\log K_{ow} < 2.5$, it means low adsorption potential; a value between 2.5 and 4.0 represents medium sorption, and $\log K_{ow} > 4.0$ means high sorption ability [33, 34]. Generally, most organic micro-pollutants (i.e. PPCPs and EDCs) are polar and highly hydrophilic with low partition coefficient (K_{ow}) and partially soluble in water [14], leading to low or moderate retention onto sediment and sludge. However, there are still some organic micro-pollutants showing strong sorption potentials with $\log K_{ow} > 4.0$, such as triclosan, fluoxetine and E2 [13]. Zhou et al. have found that activated sludge show adsorption ability for PFOA and PFOS, the removal of PFOS and PFOA decreased with the increase of the solution pH, and some amide groups in protein on the bacterial surface may be involved in the sorption [35]. Hari et al. studied the adsorption of selected pharmaceuticals nalidixic acid and norfloxacin on natural aquifer materials, their results indicated a 1-2 orders of magnitude variation in adsorption affinity with changing pH for these two quinolone pharmaceuticals [36]. Up to date, there are still very few studies concerning the interaction of micro-pollutants with natural aquifer materials.

Once released into aquatic systems, another possible fate of organic micro-pollutants is the

complexation with cationic species, such as Ca^{2+} and Fe^{3+} . Zhou et al. have reported that salbutamol, one of the β 2-agonists, could chelate iron as a bidentate ligand, three molecules of salbutamol could bind one iron to form an octahedral complex, regardless of the pH conditions [37]. A similar phenomena of the complexation of tetracycline with Ca^{2+} was observed by Kemper [38].

As mentioned above, many organic micro-pollutants are found to be recalcitrant to conventional WWTPs that based on biodegradation. However, biodegradation is still another important pathway for the transformation of some organic micro-pollutants in aquatic environment, especially in the secondary stage of treatment in WWTPs. The biodegradation ability may differ significantly from different micro-pollutants. For example, ibuprofen was found to be more readily underwent biodegradation than carbamazepine under most conditions [39]. Aerobic and anaerobic biodegradation are regarded as the most important processes for the decomposition of some organic contaminants. The degradation efficiencies could be affected by many factors, such as operational conditions, micro-pollutant concentration, hydraulic retention time, sludge retention time, temperature and micro-pollutants sorption. For instance, high biodegradation efficiencies of 11 different emerging micro-pollutants (including ibuprofen, naproxen and diclofenac) were achieved by using nitrifying activated sludge [40], and increasing loading rates of micro-pollutants were removed at shorter hydraulic retention times. Researchers also found that activated sludge could also remove EDCs efficiently from WWTPs, Andersen et al. investigated the fate of E1, E2 and EE2 at one German sewage treatment plant. They observed an overall removal efficiency of E1 and E2 of 98%, while EE2 elimination was slightly lower. And they also found that about 90% of E1 and E2 were found to be degraded in the activated sludge system while EE2 primarily was degraded only in the nitrifying tank [41]. Aislabie and Jones summarized that some pesticides are proven to be recalcitrant [42]. Specifically, dichloro-

diphenyl-trichloroethane (DDT) and dieldrin have proven to be recalcitrant by biodegradation, consequently they would remain in the environment for a very long time. In addition, atrazine and simazine, are found to undergo a slow biodegradation rate and might be leached from soil to ground water [42]. The biodegradation of these micro-pollutants would result in the generation of a series of transformation products. For instance, the initial reaction of atrazine by bacteria was the side chain cleavage to form deethylatrazine or deisopropylatrazine [42]. In the biodegradation process of dye remazol orange, the initial pathway was found to be the cleavage of the azo dye remazol orange to form both methyl metanilic acid and 4-aminobenzoic acid after decolorization, and finally to form benzoic acid, alkenes, aldehydes, and alkynes [43]. A similar cleavage process was reported in the biotransformation process of iodinated contrast, iopromide, all the degradation products exhibited the transformation at the side chain containing either carboxylic moieties and the amide moieties [44].

It should be noted that the biodegradation process for organic micro-pollutants in natural waters would be slower than in WWTPs, since the bacterial density and diversity are much lower than the sewage system. Thus, in surface water or ground water, biodegradation process might play a less important role in the depletion of organic micro-pollutants.

Photodegradation is believed to be one of the most important pathways responsible for the depletion of organic micro-pollutants in natural waters [45, 46]. The photodegradation of numerous organic micro-pollutants could be achieved directly by solar absorption or indirectly through various radicals generated from photosensitizers, such as nitrate, iron ion and humic substances [47-49].

Individual organic micro-pollutants could undergo direct photodegradation to varying degrees, depending on their chemical structure. The presence of aromatic rings and conjugated π systems, as well as various functional groups and heteroatoms, facilitate the direct absorption of solar radiation [45]. For instance, Liu and Williams investigated the direct

photolysis of several β -blockers in aquatic system, they found that propranolol could undergo faster direct photodegradation rate than atenolol and metoprolol [50]. Chromophore structures showed great impacts on the direct photolysis kinetics of these micro-pollutants, the naphthalene structure of propranolol was believed to show better solar absorption than the benzyl structure of atenolol and metoprolol. Another important impact factor that could affect the direct photolysis of organic micro-pollutants is the solution pH in natural waters. Many micro-pollutants possess pKa values in the environmentally relevant pH range of 4 -9, meaning that most of them will often exist as a mixture of their protonated/deprotonated species [51]. Speciation can change the electronic environment of the molecule, and in most cases alter the absorption spectra, subsequently altering the quantum yield as well as the direct photolysis kinetics [52, 53]. Chen et al. have observed that under acidic conditions the direct photodegradation rates of E1, E2, E3 and EE2 were lower than that at basic conditions, and high removal efficiencies could be observed above the pKa values of the estrogens [54].

Indirect photolysis mechanisms sometimes play a major role in the overall photochemical fate of organic micro-pollutants, especially for those chemicals that do not appreciably absorb light above 290 nm [51]. For example, cyclophosphamide and ifosfamide, two classical antineoplastics, were not degraded under direct solar irradiation, however, the $\cdot\text{OH}$ -based indirect photolysis process could remove them from aquatic environment [55]. As mentioned, in natural waters, the species studied most in the literature and deemed important to the indirect photolysis of aquatic organic micro-pollutants include dissolved nitrates, iron, and dissolved organic matter. These species were found to promote the degradation, while in some cases inhibit the reaction process. Specifically, it was well documented that the photolysis of nitrate would generate $\cdot\text{OH}$ [56], as shown in following equations:

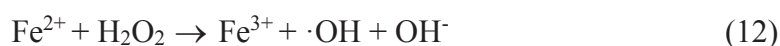
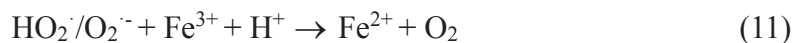
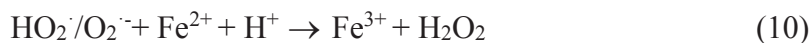
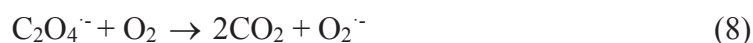
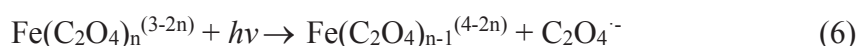




In aqueous solutions, Fe^{3+} and $\text{Fe}(\text{OH})^+$ could also generate $\cdot\text{OH}$ under irradiation [57]:



In addition, iron could be chelated by some organic compounds, such as oxalate, malonate and citrate to form strong complexes, which would undergo rapid photochemical reactions in sunlight [58]. The reaction of iron– oxalato complex to generate $\cdot\text{OH}$ could be explained by excitation into the ligand-to-metal charge transfer band (LMCT) [59], these reaction processes are illustrated as follow.



DOM represents a complex and dynamic species that can have a broad range of effects on the photochemical behavior of organic contaminants. On one hand, the reaction with the reactive species (i.e. excited triplet DOM, $^3\text{DOM}^*$, $^1\text{O}_2$ and $\cdot\text{OH}$) generated via DOM could significantly change the fate and pathway of the micro-pollutants [60]. On the other hand, DOM may also compete with the contaminants for photons [48], and sometimes DOM could also scavenge some intermediates of the reaction [61], these processes were expected to decelerate the photo-transformation of these chemicals. Janssen et al. identified the photodegradation processes of tryptophan in the presence of DOM, they found the reactions with $^3\text{DOM}^*$ and $^1\text{O}_2$ played more important roles than $\cdot\text{OH}$, while, DOM itself was able to reduce the lifetime of

tryptophan radical cation (an important intermediate), and consequently, quenched tryptophan degradation [62]. It should be noted that the origins of DOM e.g. autochthonous (aquatic) or allochthonous (terrestrial), could have significant effects on possible photo-mechanisms of organic contaminants [53]. Guerard et al. demonstrated in the indirect photodegradation process of sulfadimethoxine and triclocarban, aquatic DOM will primarily mediate degradation through $^3\text{DOM}^*$, while terrestrial DOM is more reactive in enhancing the degradation by reactive oxygen species [63].

1.1.4. Environmental risk of organic micro-pollutants.

The presence of organic micro-pollutants has been observed to seriously affect water quality as well as obviously attract attention with regard to drinking water issues. Numerous research works have been conducted to evaluate the potential hazardous effect of the released organic micro-pollutants in aquatic systems [64, 65]. For instance, Kuzmanović et al. carried out the risk assessment based prioritization of 200 organic micro-pollutants in 4 Iberian rivers. In their work, ten contaminants were identified as most important for the studied rivers: pesticides chlorpyrifos, chlorfenvinphos, diazinon, dichlofenthion, prochloraz, ethion, carbofuran and diuron and the industrial organic chemicals nonylphenol and octylphenol [64]. Munoz et al. studied the environmental and human health risk of 11 antibiotics, 10 pesticides, 1 Fungicide and 2 biocides. Their results exhibited that the risk threshold for irgarol concerning seawater organisms is exceeded. While, the risk to predators and especially humans through consumption of fish was found to be very low [65].

Among various organic micro-pollutants in aquatic system, antibiotics and EDCs have attracted many scientific concerns on their environmental effects. Antibiotics are among the most widely used pharmaceuticals in animals as well as in human beings, especially in China in the last decades [66]. Wollenberger et al. have evaluated the toxicity of veterinary antibiotics to *Daphnia magna*, and the reproductive effects for oxytetracycline, sulfadiazine,

tiamulin and tetracycline in the range of 5 to 50 mg L⁻¹, and these antibiotics could also cause mortality in the parent generation during the long-term (3 weeks) exposure [67]. Antibiotics also pose the potential to affect the microbial population in sewage treatment system. For example, it has been reported that mecillinam and ciprofloxacin were highly toxic to the cyanobacterium *Microcystis aeruginosa*, one of the important bacterial in activated sludge [68]. Most of the EDCs, such as estrogens, BPA and subordinate plant metabolites show high toxicity towards aquatic environment as well as human. EDCs have shown adverse effects on a wide range of behaviors of vertebrates, including sexual behaviors, activity, motivation, communication, aggression, dominance and other social behaviors [69]. In human body, they are able to bind to the cell receptor and antagonize the endocrine glands responsible for hormonal secretion. And subsequently, they will block the various mechanistic signals of the endocrine system and hence modify the hormonal receptor cells [64].

In natural waters, it is quite difficult to assess the environmental effect of the thousands of synthetic and natural trace contaminants that may be present in water at low to very low concentrations (pg L⁻¹ to ng L⁻¹) [70]. Therefore, the long-term, subtle and chronic toxic effect should be taken into account rather than acute toxicity.

1.2. Advanced oxidation process in water treatments.

Numerous micro-pollutants in aquatic systems including ground water, surface water, wastewater and even drinking water have raised scientific and public concerns for developing efficient cleaning technologies. As well-known, the release of effluents from conventional Waste Water Treatment Plants (WWTP) is an important route for the appearance of micro-pollutants in the aquatic environment, since they are not designed to completely eliminate organic compounds at low concentrations, which could make the treatment processes vulnerable to such problem of pollution [14]. The efficiency of conventional WWTPs varies depending on the characteristics of the micro-pollutant and also on the treatment process

employed [20]. The main mechanisms applied for micro-pollutants removal during the secondary treatment at WWTPs are biological and/or chemical transformation and sorption [71, 72], and among them the most common employed processes are conventional activated sludge (CAS) and membrane biological reactors (MBRs).

One of the disadvantages of WWTPs is that they are unable to remove the micro-pollutants from wastewater completely. These compounds can be still detected in the effluents after the conventional treatment process, although their concentrations are low [73]. The accumulation of metabolites/by-products might cause a negative removal effect [74]. Due to their excretion as conjugates that are broken in the WWTPs, there are also some micro-pollutants (e.g., pharmaceuticals, hormones, drugs of abuse that are excreted by humans and/or animals) that could be found at higher concentrations in the WWTPs effluents than in the respective influents, especially during biological treatment process. For instance, the concentration of E1 was detected higher in the secondary effluent of a WWTP than that found in the raw influent [72]. Moreover, many of the micro-pollutants are designed to be resistant to metabolism and thus are generally excreted unchanged within 24 h, such as many PPCPs chemicals [75]. Therefore, it is essential to develop effective treatment technologies as a supplement to WWTPs to remove such micro-pollutants from aquatic systems.

Advanced oxidation processes (AOPs) are among the promising alternatives capable of removing these micro-pollutants from WWTPs as well as in natural waters. Most of the AOPs technologies are mainly based on the generation of reactive oxygen species (ROS, e.g. hydroxyl radicals and sulfate radicals) arising from the decomposition of oxidants such as hydrogen peroxide (H_2O_2), persulfate (PS, $\text{S}_2\text{O}_8^{2-}$) or ozone (O_3), involving O_3/UV , $\text{UV}/\text{H}_2\text{O}_2$, UV/PS , Fenton and Fenton-like oxidation, gamma radiolysis and sonolysis, as well as electrochemical oxidation [76, 77].

1.2.1. Hydroxyl radicals ($\cdot\text{OH}$) based AOPs.

Hydroxyl radicals possess a strong oxidation capacity (standard potential = 2.80 V versus standard hydrogen electrode) [79], thus, AOPs based on the *in situ* generation of $\cdot\text{OH}$ have been studied as a promising kind of organic wastewater treatment method [76]. Under treatment by such AOPs, complex organic pollutants can be either oxidized by $\cdot\text{OH}$ to smaller organics or completely mineralized to carbon dioxide (CO_2) and water (H_2O) [80, 81]. OH based AOPs include Fenton processes (including Fenton-like processes)[81, 82], photocatalysis [83, 84], $\text{O}_3/\text{H}_2\text{O}_2$ [85, 86] and plasma oxidation [87] (see Figure 1.2).

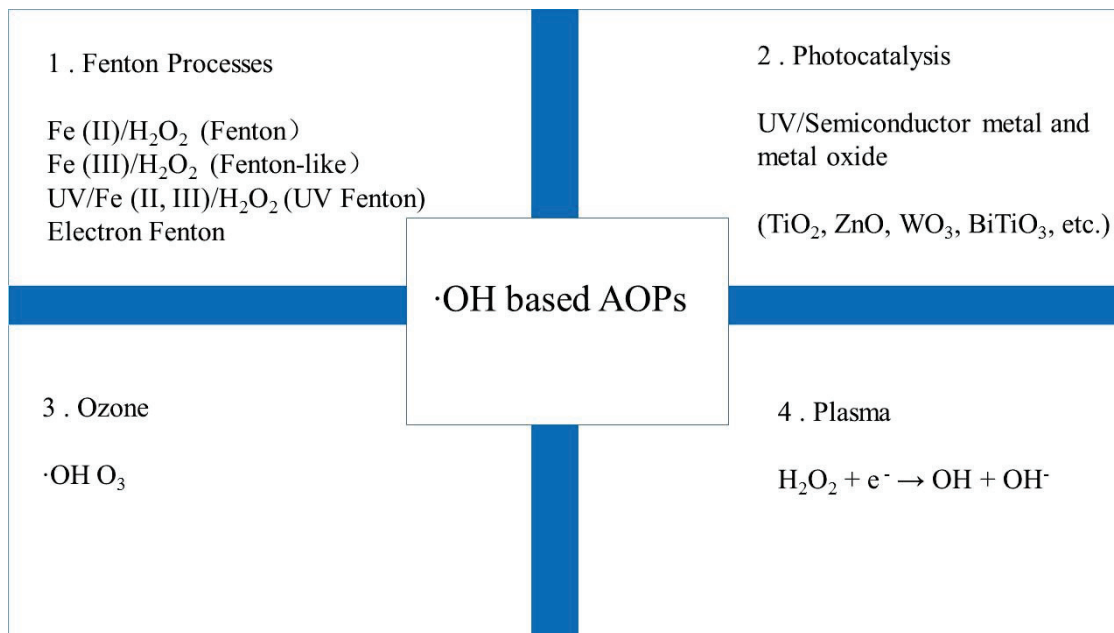


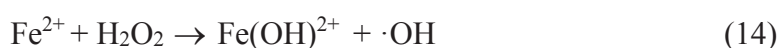
Figure 1.2. Hydroxyl radicals formed according to advanced oxidation technologies [78].

The most frequently used AOPs is the Fenton processes where Fe (II) is used as the catalyst and H_2O_2 as the oxidant (Eq. 12) [88]. Moreover, the newly formed ferric ions (Fe^{3+}) can catalyze H_2O_2 (Eq.13), the reaction of H_2O_2 with Fe^{3+} is known as a Fenton like reaction.



The Fenton (or Fenton-like) processes have shown several advantages such as high performance, simplicity and non-toxicity [89]. Moreover, these processes need no energy input necessary to activate hydrogen peroxide [90]. However, the optimal pH value for

Fenton (or Fenton-like) reaction is around 3, a slight decrease or increase of pH will sharply reduce the oxidation efficiency of the systems [91]. To overcome this limitation, chelating agents of ion species, such as ethylenediaminetetraacetic acid (EDTA), catechol, cyclodextrin and nitrilotriacetic acid are used to extend its range of applicability to neutral condition [92]. Moreover, the oxidation efficiency of Fenton reaction could be enhanced under UV–Vis light irradiation (see Eq 14-16).



As seen, the photolysis of Fe^{3+} complexes ($\text{Fe}(\text{OH})^{2+}$) allows the regeneration Fe^{2+} and the direct photolysis of H_2O_2 can also form $\cdot\text{OH}$ [93]. These process is referred to as the photo-Fenton processes.

The Fenton oxidation process has been employed successfully to treat different industrial wastewaters, including textile [94], pharmaceutical [95], olive oil [96], cork cooking [97], dyes [98] and pesticide wastewaters [99].

Photocatalysis, which makes the use of semiconductor metal oxide as catalyst is another AOPs that have been extensively studied in the last decades [100, 101]. As shown in Figure 1.2, many semiconductors, such as TiO_2 , ZnO , WO_3 and BiTiO_3 , have been tested as photocatalysts [78]. Among these semiconductors, TiO_2 in the anatase form was proved to be the most appropriate one due to its characteristics such as high photo-activity, chemical inertness, non-toxic, low cost and easy to obtain [102]. TiO_2 photo-catalysis have been fully developed in numbers of case studies on water and air purification, and has been recognized as one of the most promising environmental remediation technologies [30]. Plasmas and ozone (O_3) oxidation are also regarded as highly competitive technologies for the removal of organic pollutants from soils. AOPs based on plasmas oxidation was examined as an eco-innovative

method of environmental remediation in recent years [29], and ozone has been shown efficiently degradation for pesticides, hydrocarbons, pharmaceuticals and endocrine disruptors in water treatment process [103, 104].

However, AOPs based on hydroxyl radical generation also have some drawbacks. Specifically, the main disadvantages of Fenton (also Fenton-like) treatment are the reduction pH, and large quantity of the oxidant is needed for the oxidation processes with high content of organic matter or the additional substances (for instance, chelating agents or surfactants). Moreover, the transportation of these oxidants, especially H₂O₂, would increase the cost, since it is unstable and easily to be decomposed by iron oxides and other catalysts. And for photo-catalysis oxidation by TiO₂, the lack of visible light activity also hinders its practical applications, and using UV-lamp would be costly due to the lifetimes of the lamp. The shortage of plasma oxidation is that high amount energy levels are needed to treat waters that are heavily polluted. For ozone oxidation, the ozone generator would be also costly and ozone itself, sometimes is regarded as one of the harmful pollutants.

1.2.2. Sulfate radical (SO₄^{•-}) based AOPs.

Sulfate radical-based advanced oxidation processes (SR-AOPs) are increasingly gaining attention as effective solution to the degradation of recalcitrant organic micro-pollutants in aquatic systems. With a strong oxidation capacity (standard potential = 2.60 V versus standard hydrogen electrode), sulfate radical is able to oxidize organic micro-pollutants to innocuous CO₂ and H₂O [105]. Normally, sulfate radical could react with organic micro-pollutants at rates ranging from 10⁶-10⁹ M⁻¹ s⁻¹ [106]. By comparison with ·OH (t_{1/2} less than 1 μs), SO₄^{•-} opposes a longer lifetime (t_{1/2} = 30–40 μs), this allows excellent mass transfer and contact between sulfate radical with the target micro-pollutant in the heterogeneous system [107]. And the reactivity of sulfate radical is found to be pH independent while the oxidation efficiency of ·OH would decrease at basic conditions [108]. As an electrophilic species, it

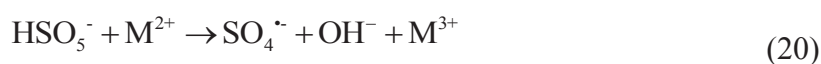
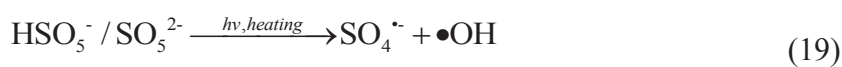
prefers to react with electron-rich groups *via* electron-transfer reactions, such as aniline, phenolic chemicals and other organic compounds that contain unsaturated bonds [109].

It is also believed that SR-AOPs could lead to a better mineralization than $\cdot\text{OH}$ for the degradation of organic contaminants [111]. All these chemical properties of sulfate radical mentioned above makes SR-AOPs an important part in the AOPs for wastewater treatment.

1) Formation of sulfate radicals.

Most commonly, $\text{SO}_4^{\cdot-}$ could be generated via the activation of peroxymonosulfate (PMS, HSO_5^-) or persulfate (PS, $\text{S}_2\text{O}_8^{2-}$). Both PMS (1.82 V) and PS (2.01 V) are strong oxidants that favor two-electron transfer reactions [112], however, in the past decades, many researches focused on the combination of them with catalysts or externally supplied energy to generate the more reactive species, $\text{SO}_4^{\cdot-}$.

Several different strategies have been developed by scientists to activate PS or PMS into sulfate radical, which include heating [113], UV irradiation (Eq 17 and 19) [114, 115], ultrasound [116], adding bases [117], and catalysis with transition metals or carbons (Eq 18 and 20) [105, 118].



Employing energy for PMS or PS activation, the peroxide bond in PMS (or PS) is the target of scission [119]. In such kind of approach, various forms of energy can be utilized such as heat, UV and ultrasound. These methods would not induce new species into the reaction system, while, the inputs of energy might be costly to completely destroy all the organic micro-pollutants. Among all these activation strategies, the activation method by transition metals,

such as Co, Fe, Cu, Zn and Mn, is less complex in reactor/system configuration and more economical compared to the energy-based activation methods [120]. This method could be achieved in both homogeneous and heterogeneous systems. The activation could be achieved by single metal or mixed metal catalysts (e.g, CuFe_2O_4 , CoFe_2O_4 and MnFe_2O_4) [121]. However, the inputs of these metals would cause another environmental problem, some of these metals are considerably toxic and potentially carcinogenic. Some metals, including Zn, Cu, Co and Ni sometimes are regarded as heavy metals that are difficult to be removed. For instance, dissolved Co concentration ranging from 0.002 to 0.107 mg L^{-1} has been detected in drinking water [122]. Nonmetal carbon-based catalysts such as activated carbon [123], graphene oxide [123] and carbon nanotubes [124] provide a potential solution to the metal leaching problem by transition metal catalysts. The carbon-based catalysts show the advantages of high surface areas and abundant catalytic moieties (including carboxyl, carbonyl, quinones, lactones and phenols) [125], and they are relatively cheap and widely used in the water and wastewater treatment, they are regarded as the most promising choice of nonmetal catalyst for practical application for the activation of PMS or PS. Moreover, these materials have already been used as an adsorptive support for metal catalysts to induce synergistic adsorption and oxidation of micro-pollutants by sulfate radicals [126]. While, these nonmetal-based catalysts also show some shortcomings during oxidation processes, after repeated use, as their adsorption capacities decrease the catalytic moieties are susceptible to aggressive oxidation by both PMS (PS) and generated sulfate radicals [125].

II) Degradation efficiency of organic micro-pollutants by sulfate radicals.

There are numerous published papers about the degradation of micro-pollutants by $\text{SO}_4^{\cdot-}$. Most of the research activities focused on the removal efficiency and also the influence factors (operational parameters) such as PMS (PS) concentrations, pH, temperature, catalysts type and dosages and the effect of coexisting water constituents. For instance, Ren et al.

compared the performance of different magnetic ferrosphinel catalysts to activate PMS for the decomposition of di-n-butyl phthalate and found the capacity of catalytic PMS was $\text{CoFe}_2\text{O}_4 > \text{CuFe}_2\text{O}_4 > \text{MnFe}_2\text{O}_4 > \text{ZnFe}_2\text{O}_4$ [127]. Fan et al. studied the degradation of sulfamethazine in heat-activated PS oxidation process. The influence of some key parameters on the removal rates of the target compound was investigated and described in details, such as initial PS concentration, initial pH value and temperature [113]. Liang et al. investigate the effect of solution pH on the oxidation of trichloroethylene (TCE) by heating PS to generate sulfate radicals, the results indicated that maximum TCE degradation occurred at pH 7, and lowering system pH resulted in a greater decrease in TCE degradation rates than increasing system pH [128]. Some researchers also made comparative studies on the oxidation efficiencies by $\cdot\text{OH}$ with $\text{SO}_4^{\cdot-}$ induced degradation. Tan et al. have studied the degradation of antipyrine by UV, UV/ H_2O_2 and UV/PS and they found UV/ H_2O_2 behaved best at pH 2.5–10, while UV/PS behaved best at pH 10.0–11.5 [129]. Moreover, Zhang et al. suggested that the AOPs' performance was higher in the hydrolyzed urine than fresh urine matrix with UV/PS better than UV/ H_2O_2 , and varied significantly depending on pharmaceutical's structure [130]. Another research point is to detect the second-order rate constants for the reaction of sulfate radical with target micro-pollutant. One of the traditional approach is the competition kinetic method by using a chemical probe such as anisole or 4-nitroaniline [130]. In recent years, the direct measurement of this rate constant could be achieved by laser flash photolysis (LFP) method [131].

$\text{SO}_4^{\cdot-}$ reacts more readily with organic micro-pollutants by one electron transfer to form SO_4^{2-} . Some scientists also investigated the underlying mechanisms, the oxidation pathways of the degradation intermediates and products of organic contaminants. For example, in the reaction of sulfate radical with methoxylated benzene, the corresponding radical cations are generated as primary short-lived intermediates, evidencing the electron transfer mechanism [132]. For

the reaction with phenolic compounds, hydroxylation is a classic pathway, resulting in the production of catechol or hydroquinone [133]. The hydroxylation process was also observed during the degradation pathways of trimethoprim by thermo-activated PS [134]. In addition, the cleavage of the side chain could also be found in many literatures, for instance, Ghauch et al. studied the degradation of methylene blue by heating activated PS, the oxidation pathways included demethylation and N-dealkylation [135]. Lutze et al. have proposed the detailed degradation pathway of atrazine by $\text{SO}_4^{\bullet-}$ for the side chain cleavage, the primary radical cation will be formed after the electron transfer reaction, and it would be in equilibrium with the corresponding N-centered radicals, which are expected to undergo a (water catalyzed) 1,2-H shift to form the alkoxyl radicals, thereby forming C-centered radicals. These C-centered ones could react rapidly with dissolved oxygen in the solution. Subsequently, the resulting peroxy radical would lose its O_2^{\bullet} or HO_2^{\bullet} . The final step is the acid and base catalyzed hydrolysis of the imine yields the carbonylic compound and the free amine [136]. For the reaction with halide compounds, the de-halide process could also occur during the reaction with sulfate radical. Xu et al. have found the de-chlorination accompanied by hydroxylation of 2,4,6-trichlorophenol after the reaction with $\text{SO}_4^{\bullet-}$ [137], and a similar pathway was also observed during the decomposition of 4-chlorophenol [138]. It should be noted that the released halide atom could also react with sulfate radicals to form the halide reactive species, which are electrophilic which can be added to unsaturated bonds of organic compounds and produce AOX (adsorbable organic halides) which are persistent to biodegradation [139].

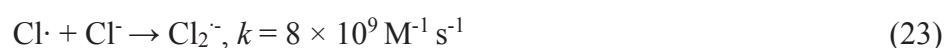
III) Effect of natural water constituents on $\text{SO}_4^{\bullet-}$ based AOPs.

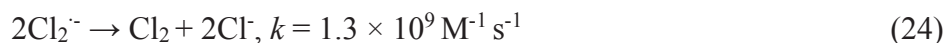
Natural waters or wastewaters contain large amount of non-target water constituents, such as natural organic matters (NOM) and ions. The high redox potentials of $\text{SO}_4^{\bullet-}$ ($E^0 \sim 2.6$ eV) and $\cdot\text{OH}$ ($E^0 \sim 2.7$ eV) make them very reactive to destroy organic contaminants as well as the various constituents in natural waters in AOPs, the competing side reactions with water

constituents other than the target contaminants could also lead to the consumption of these two radicals, resulting in an unpredictable consequence on the oxidation efficiency. Investigating the impacts of them on the oxidation kinetic and mechanism of the target compounds will help to understand its degradation of micro-pollutants in real aquatic systems by AOPs.

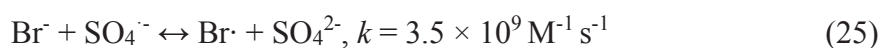
NOM constitutes a large portion of the total organic carbon (TOC) pool in natural environments [140]. They are ubiquitous and are directly involved in numerous important process in environmental aquatic chemistry [141]. In particular, the properties of NOM arising from light absorption are essential as far as the capacity of the environment to degrade organic contaminants is concerned. NOM are brown-colored and show interesting properties under solar irradiation [142]. Some papers have observed a detrimental effect of NOM on the oxidation efficiency of micro-pollutants by SR-AOPs by UV activation [136, 143]. NOM is often regarded as a sink of $\cdot\text{OH}$ and $\text{SO}_4^{\bullet-}$ due to some functional groups, which were prone to react with these two radicals, they would like to compete with the target micro-pollutants [144]. Lutze et al. determined the second order rate constant of sulfate radical with NOM at $6.8 \times 10^3 \text{ L mgC}^{-1} \text{ s}^{-1}$, which was found smaller than that with $\cdot\text{OH}$, indicating that in the presence of NOM, some micro-pollutants could be degraded more efficiently by $\text{SO}_4^{\bullet-}$ than by $\cdot\text{OH}$ [136]. However, up to date, there is still lack of a systematically study on the interaction of $\text{SO}_4^{\bullet-}$ with NOM.

Chloride ion (Cl^-) is one of the major inorganic anions in water resource and almost all natural waters. Cl^- might play a complex role in SR-AOPs due to the scavenging of $\text{SO}_4^{\bullet-}$ to generate less reactive chlorine species such as $\text{Cl}\cdot$, ClOH^- , and $\text{Cl}_2^{\bullet-}$ (Eq 21-24) [145].



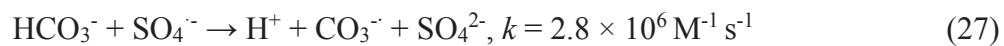


The quenching of $\text{SO}_4^{\cdot-}$ would cause the decrease of oxidation efficiency by SR-AOPs, while the secondary reactions induced by the chlorine species might also react with the target micro-pollutants, leading to an unexpected results. Liang et al. have found that TCE degradation in the presence of chlorides revealed no effect on the degradation rate especially at chloride levels below 0.2 M, however, at chloride levels greater than 0.2 M, the removal rate was seen to reduce [145]. Aniostitakis et al. have observed the formation of chlorophenol (e.g. 2-chlorophenol, 4-chlorophenol and 2,4-dichlorophenol) after the oxidation of phenol by $\text{SO}_4^{\cdot-}$ in the presence of Cl^- [146]. Bromide (Br^-) is another halide ion in some wastewaters, similar to Cl^- , it also shows a scavenging effect on sulfate radicals and forms the corresponding bromine species (Eq 25 and 26) [147].



Ji et al. studied the oxidation of tetrabromobisphenol A by Co activated PMS in the presence of bromide, they found the involvement of reactive bromine species and the formation of brominated disinfection by-products (Br-DBPs) such as bromoform and brominated acetic acids [148]. It should be noted that the presence of NOM would increase the formation potential of halogenated disinfection byproducts (DBPs) in SR-AOPs through reconfiguration of NOM to phenolic intermediates which are susceptible to halogenation [149]. Halogenated DBPs have been shown to cause notable health risks and regulated world widely [150], therefore, the effects of Cl^- and Br^- on SR-AOPs are becoming an attracting filed for environmental scientists.

Moreover, carbonate (or bicarbonate) is another important ion in aquatic system, they also show the quenching effect of sulfate radical to generate carbonate radical ($\text{CO}_3^{\cdot-}$), which is less reactive than $\text{SO}_4^{\cdot-}$ [151].



Fan et al. have found that the degradation rate of sulfamethazine decreased with increase of HCO_3^- concentration [113]. A similar detrimental effect was also obtained by Wu et al. during the oxidation process of 4-tert-butylphenol [131]. However, in another report by Liang et al, the TCE degradation rate did not significantly change with HCO_3^- concentration increased from 0 to 9.2 mM [145]. Such phenomenon was also found by Zhou et al. for the degradation of bisphenol A by $\text{SO}_4^{\cdot-}$, (bi) carbonate exhibited no obvious influence on the removal rate [152]. Thus, the effect of (bi) carbonate must be considered carefully for the treatment of different micro-pollutants. In addition, nitrate (NO_3^-) and phosphate ions have also been reported to show scavenging effect in high concentration for sulfate radical [131, 153]. It was documented that the order of inhibitory effect of some anions followed $\text{S}_2\text{O}_3^{2-} > \text{HCO}_3^- > \text{NO}_2^- > \text{CO}_3^{2-} > \text{HCOO}^- > \text{Cl}^- > \text{HPO}_4^{2-} > \text{NO}_3^- > \text{H}_2\text{PO}_4^- > \text{SO}_4^{2-} > \text{CH}_3\text{COO}^-$ [139]. Indeed, the water constitutes would compete with organic compounds for reaction with sulfate radicals, the reactions of them with sulfate radical was non-selectively, and their effect on the oxidation efficiency might be unpredictable.

Generally, the role of these ubiquitous water constituents might be counterintuitive, and their influence on SR-AOPs must be considered carefully for different kind of micro-pollutants. In addition, the secondary reactions between target micro-pollutants with new formed reactive species need to be further considered before the application of SR-AOPs for the treatment. Because these secondary reactions sometimes would result in higher toxic intermediates of byproducts, such as halogenated disinfection byproducts.

1.3. References.

[1] Y. Luo, W. Guo, H.H. Ngo, L.D. Nghiem, F.I. Hai, J. Zhang, S. Liang, X.C. Wang, A review on the occurrence of micropollutants in the aquatic environment and their fate and removal during wastewater treatment, *Sci Total Environ* 473 (2014) 619-641.

- [2] A. Jelic, M. Gros, A. Ginebreda, R. Cespedes-Sánchez, F. Ventura, M. Petrovic, D. Barcelo, Occurrence, partition and removal of pharmaceuticals in sewage water and sludge during wastewater treatment, *Water Res* 45 (2011) 1165-1176.
- [3] A. Pal, K.Y.-H. Gin, A.Y.-C. Lin, M. Reinhard, Impacts of emerging organic contaminants on freshwater resources: review of recent occurrences, sources, fate and effects, *Sci Total Environ* 408 (2010) 6062-6069.
- [4] C. Wang, H. Shi, C.D. Adams, S. Gamagedara, I. Stayton, T. Timmons, Y. Ma, Investigation of pharmaceuticals in Missouri natural and drinking water using high performance liquid chromatography-tandem mass spectrometry, *Water Res* 45 (2011) 1818-1828.
- [5] G. Teijon, L. Candela, K. Tamoh, A. Molina-Díaz, A. Fernández-Alba, Occurrence of emerging contaminants, priority substances (2008/105/CE) and heavy metals in treated wastewater and groundwater at Depurbaix facility (Barcelona, Spain), *Sci Total Environ* 408 (2010) 3584-3595.
- [6] B. Kasprzyk-Hordern, R.M. Dinsdale, A.J. Guwy, The occurrence of pharmaceuticals, personal care products, endocrine disruptors and illicit drugs in surface water in South Wales, UK, *Water Res* 42 (2008) 3498-3518.
- [7] L. Yang, L. Zhu, Z. Liu, Occurrence and partition of perfluorinated compounds in water and sediment from Liao River and Taihu Lake, China, *Chemosphere* 83 (2011) 806-814.
- [8] M. Cai, Z. Zhao, Z. Yin, L. Ahrens, P. Huang, M. Cai, H. Yang, J. He, R. Sturm, R. Ebinghaus, Occurrence of perfluoroalkyl compounds in surface waters from the North Pacific to the Arctic Ocean, *Environ Sci Technol* 46 (2011) 661-668.
- [9] J.-Q. Jiang, Z. Zhou, V. Sharma, Occurrence, transportation, monitoring and treatment of emerging micro-pollutants in waste water—a review from global views, *Microchem J* 110 (2013) 292-300.

- [10] J. Regnery, W. Püttmann, Occurrence and fate of organophosphorus flame retardants and plasticizers in urban and remote surface waters in Germany, *Water Res* 44 (2010) 4097-4104.
- [11] D.W. Kolpin, J.E. Barbash, R.J. Gilliom, Occurrence of pesticides in shallow groundwater of the United States: Initial results from the National Water-Quality Assessment Program, *Environ Sci Technol* 32 (1998) 558-566.
- [12] M. Köck-Schulmeyer, M. Villagrasa, M. López de Alda, R. Céspedes-Sánchez, F. Ventura, D. Barceló, Occurrence and behavior of pesticides in wastewater treatment plants and their environmental impact, *Sci Total Environ* 458–460 (2013) 466-476.
- [13] S. Mompelat, B. Le Bot, O. Thomas, Occurrence and fate of pharmaceutical products and by-products, from resource to drinking water, *Environ Int* 35 (2009) 803-814.
- [14] J.O. Tijani, O.O. Fatoba, L.F. Petrik, A review of pharmaceuticals and endocrine-disrupting compounds: sources, effects, removal, and detections, *Water, Air, & Soil Pollution* 224 (2013) 1770.
- [15] E.Z. Harrison, S.R. Oakes, M. Hysell, A. Hay, Organic chemicals in sewage sludges, *Sci Total Environ* 367 (2006) 481-497.
- [16] K.K. Barnes, D.W. Kolpin, M.T. Meyer, E.M. Thurman, E.T. Furlong, S.D. Zaugg, L.B. Barber, Water-quality data for pharmaceuticals, hormones, and other organic wastewater contaminants in US streams, 1999-2000, US Geological Survey Open-File Report 2 (2002) 94.
- [17] N.M. Vieno, T. Tuhkanen, L. Kronberg, Seasonal variation in the occurrence of pharmaceuticals in effluents from a sewage treatment plant and in the recipient water, *Environ Sci Technol* 39 (2005) 8220-8226.
- [18] L. Feng, E.D. van Hullebusch, M.A. Rodrigo, G. Esposito, M.A. Oturan, Removal of residual anti-inflammatory and analgesic pharmaceuticals from aqueous systems by electrochemical advanced oxidation processes. A review, *Chem Eng J* 228 (2013) 944-964.

- [19] K. Kümmerer, Antibiotics in the aquatic environment—a review—part I, *Chemosphere* 75 (2009) 417-434.
- [20] M.O. Barbosa, N.F. Moreira, A.R. Ribeiro, M.F. Pereira, A.M. Silva, Occurrence and removal of organic micropollutants: An overview of the watch list of EU Decision 2015/495, *Water Res* 94 (2016) 257-279.
- [21] P. Matthiessen, D. Arnold, A. Johnson, T. Pepper, T. Pottinger, K. Pulman, Contamination of headwater streams in the United Kingdom by oestrogenic hormones from livestock farms, *Sci Total Environ* 367 (2006) 616-630.
- [22] T. Eggen, M. Moeder, A. Arukwe, Municipal landfill leachates: a significant source for new and emerging pollutants, *Sci Total Environ* 408 (2010) 5147-5157.
- [23] J. Fawell, C.N. Ong, Emerging contaminants and the implications for drinking water, *Int J Water Resour D* 28 (2012) 247-263.
- [24] C. Carrara, C.J. Ptacek, W.D. Robertson, D.W. Blowes, M.C. Moncur, E. Sverko, S. Backus, Fate of pharmaceutical and trace organic compounds in three septic system plumes, Ontario, Canada, *Environ Sci Technol* 42 (2008) 2805-2811.
- [25] S. Maletz, T. Floehr, S. Beier, C. Klümper, A. Brouwer, P. Behnisch, E. Higley, J.P. Giesy, M. Hecker, W. Gebhardt, In vitro characterization of the effectiveness of enhanced sewage treatment processes to eliminate endocrine activity of hospital effluents, *Water Res* 47 (2013) 1545-1557.
- [26] R.C. Hale, M.J. La Guardia, E.P. Harvey, M.O. Gaylor, T.M. Mainor, W.H. Duff, Flame retardants: persistent pollutants in land-applied sludges, *Nature* 412 (2001) 140-141.
- [27] M.S. Díaz-Cruz, M. Llorca, D. Barceló, Organic UV filters and their photodegradates, metabolites and disinfection by-products in the aquatic environment, *TrAC Trends in Analytical Chemistry* 27 (2008) 873-887.

- [28] T. Poiger, H.-R. Buser, M.E. Balmer, P.-A. Bergqvist, M.D. Müller, Occurrence of UV filter compounds from sunscreens in surface waters: regional mass balance in two Swiss lakes, *Chemosphere* 55 (2004) 951-963.
- [29] M.E. Balmer, H.-R. Buser, M.D. Müller, T. Poiger, Occurrence of some organic UV filters in wastewater, in surface waters, and in fish from Swiss lakes, *Environ Sci Technol* 39 (2005) 953-962.
- [30] M.S. El-Shahawi, A. Hamza, A.S. Bashammakh, W.T. Al-Saggaf, An overview on the accumulation, distribution, transformations, toxicity and analytical methods for the monitoring of persistent organic pollutants, *Talanta* 80 (2010) 1587-1597.
- [31] J.J. Nam, G.O. Thomas, F.M. Jaward, E. Steinnes, O. Gustafsson, K.C. Jones, PAHs in background soils from Western Europe: Influence of atmospheric deposition and soil organic matter, *Chemosphere* 70 (2008) 1596-1602.
- [32] J. Tolls, Sorption of veterinary pharmaceuticals in soils: a review, *Environ Sci Technol* 35 (2001) 3397-3406.
- [33] H.R. Rogers, Sources, behaviour and fate of organic contaminants during sewage treatment and in sewage sludges, *Sci Total Environ* 185 (1996) 3-26.
- [34] F.A. Caliman, M. Gavrilescu, Pharmaceuticals, personal care products and endocrine disrupting agents in the environment—a review, *CLEAN—Soil, Air, Water* 37 (2009) 277-303.
- [35] Q. Zhou, S. Deng, Q. Zhang, Q. Fan, J. Huang, G. Yu, Sorption of perfluorooctane sulfonate and perfluorooctanoate on activated sludge, *Chemosphere* 81 (2010) 453-458.
- [36] A.C. Hari, R.A. Paruchuri, D.A. Sabatini, T.C. Kibbey, Effects of pH and cationic and nonionic surfactants on the adsorption of pharmaceuticals to a natural aquifer material, *Environ Sci Technol* 39 (2005) 2592-2598.
- [37] L. Zhou, Q. Wang, Y. Zhang, Y. Ji, X. Yang, Aquatic photolysis of β 2-agonist salbutamol: kinetics and mechanism studies, *Environ Sci Pollut R* (2016) 1-10.

- [38] N. Kemper, Veterinary antibiotics in the aquatic and terrestrial environment, *Ecol Indic* 8 (2008) 1-13.
- [39] K.M. Onesios, T.Y. Jim, E.J. Bouwer, Biodegradation and removal of pharmaceuticals and personal care products in treatment systems: a review, *Biodegradation* 20 (2009) 441-466.
- [40] E. Fernandez-Fontaina, F. Omil, J.M. Lema, M. Carballa, Influence of nitrifying conditions on the biodegradation and sorption of emerging micropollutants, *Water Res* 46 (2012) 5434-5444.
- [41] H. Andersen, H. Siegrist, B. Halling-Sørensen, T.A. Ternes, Fate of estrogens in a municipal sewage treatment plant, *Environ Sci Technol* 37 (2003) 4021-4026.
- [42] J. Aislabie, G. Lloyd-Jones, A review of bacterial-degradation of pesticides, *Soil Res* 33 (1995) 925-942.
- [43] K. Sarayu, S. Sandhya, Aerobic biodegradation pathway for Remazol Orange by *Pseudomonas aeruginosa*, *Appl Biochem Biotech* 160 (2010) 1241-1253.
- [44] M. Schulz, D. Löffler, M. Wagner, T.A. Ternes, Transformation of the X-ray contrast medium iopromide in soil and biological wastewater treatment, *Environ Sci Technol* 42 (2008) 7207-7217.
- [45] A.L. Boreen, W.A. Arnold, K. McNeill, Photodegradation of pharmaceuticals in the aquatic environment: a review, *Aquat Sci* 65 (2003) 320-341.
- [46] D. Fatta-Kassinos, M. Vasquez, K. Kümmerer, Transformation products of pharmaceuticals in surface waters and wastewater formed during photolysis and advanced oxidation processes—degradation, elucidation of byproducts and assessment of their biological potency, *Chemosphere* 85 (2011) 693-709.
- [47] Y. Ji, C. Zeng, C. Ferronato, J.-M. Chovelon, X. Yang, Nitrate-induced photodegradation of atenolol in aqueous solution: kinetics, toxicity and degradation pathways, *Chemosphere* 88 (2012) 644-649.

- [48] L. Zhou, Y. Ji, C. Zeng, Y. Zhang, Z. Wang, X. Yang, Aquatic photodegradation of sunscreen agent p-aminobenzoic acid in the presence of dissolved organic matter, *Water Res* 47 (2013) 153-162.
- [49] W. Feng, D. Nansheng, Photochemistry of hydrolytic iron (III) species and photoinduced degradation of organic compounds. A minireview, *Chemosphere* 41 (2000) 1137-1147.
- [50] Q.-T. Liu, H.E. Williams, Kinetics and degradation products for direct photolysis of β -blockers in water, *Environ Sci Technol* 41 (2007) 803-810.
- [51] J.K. Challis, J.C. Carlson, K.J. Friesen, M.L. Hanson, C.S. Wong, Aquatic photochemistry of the sulfonamide antibiotic sulfapyridine, *Journal of Photochemistry and Photobiology A: Chemistry* 262 (2013) 14-21.
- [52] A.L. Boreen, W.A. Arnold, K. McNeill, Photochemical fate of sulfa drugs in the aquatic environment: sulfa drugs containing five-membered heterocyclic groups, *Environ Sci Technol* 38 (2004) 3933-3940.
- [53] J.K. Challis, M.L. Hanson, K.J. Friesen, C.S. Wong, A critical assessment of the photodegradation of pharmaceuticals in aquatic environments: defining our current understanding and identifying knowledge gaps, *Environmental Science: Processes & Impacts* 16 (2014) 672-696.
- [54] Y. Chen, K. Zhang, Y. Zuo, Direct and indirect photodegradation of estriol in the presence of humic acid, nitrate and iron complexes in water solutions, *Sci Total Environ* 463 (2013) 802-809.
- [55] I.J. Buerge, H.-R. Buser, T. Poiger, M.D. Müller, Occurrence and fate of the cytostatic drugs cyclophosphamide and ifosfamide in wastewater and surface waters, *Environ Sci Technol* 40 (2006) 7242-7250.
- [56] P. Boule, *Environmental photochemistry*, Springer Science & Business Media 1999.

- [57] L. Zhou, Y. Zhang, Q. Wang, C. Ferronato, X. Yang, J.-M. Chovelon, Photochemical behavior of carbon nanotubes in natural waters: reactive oxygen species production and effects on \bullet OH generation by Suwannee River fulvic acid, nitrate, and Fe (III), *Environ Sci Pollut R* 23 (2016) 19520-19528.
- [58] Y. Zuo, J. Hoigne, Formation of hydrogen peroxide and depletion of oxalic acid in atmospheric water by photolysis of iron (III)-oxalato complexes, *Environ. Sci. Technol* 26 (1992) 1014-1022.
- [59] B.M. Voelker, F.M. Morel, B. Sulzberger, Iron redox cycling in surface waters: effects of humic substances and light, *Environ Sci Technol* 31 (1997) 1004-1011.
- [60] J. Wenk, U. Von Gunten, S. Canonica, Effect of dissolved organic matter on the transformation of contaminants induced by excited triplet states and the hydroxyl radical, *Environ Sci Technol* 45 (2011) 1334-1340.
- [61] J. Wenk, S.N. Eustis, K. McNeill, S. Canonica, Quenching of excited triplet states by dissolved natural organic matter, *Environ Sci Technol* 47 (2013) 12802-12810.
- [62] E.M.-L. Janssen, P.R. Erickson, K. McNeill, Dual roles of dissolved organic matter as sensitizer and quencher in the photooxidation of tryptophan, *Environ Sci Technol* 48 (2014) 4916-4924.
- [63] J.J. Guerard, P.L. Miller, T.D. Trouts, Y.-P. Chin, The role of fulvic acid composition in the photosensitized degradation of aquatic contaminants, *Aquat Sci* 71 (2009) 160-169.
- [64] M. Kuzmanović, A. Ginebreda, M. Petrović, D. Barceló, Risk assessment based prioritization of 200 organic micropollutants in 4 Iberian rivers, *Sci Total Environ* 503–504 (2015) 289-299.
- [65] I. Muñoz, M.J. Martínez Bueno, A. Agüera, A.R. Fernández-Alba, Environmental and human health risk assessment of organic micro-pollutants occurring in a Spanish marine fish farm, *Environ Pollut* 158 (2010) 1809-1816.

- [66] J. Currie, W. Lin, W. Zhang, Patient knowledge and antibiotic abuse: Evidence from an audit study in China, *J Health Econ* 30 (2011) 933-949.
- [67] L. Wollenberger, B. Halling-Sørensen, K.O. Kusk, Acute and chronic toxicity of veterinary antibiotics to *Daphnia magna*, *Chemosphere* 40 (2000) 723-730.
- [68] B. Halling-Sørensen, H.-C.H. Lützhøft, H.R. Andersen, F. Ingerslev, Environmental risk assessment of antibiotics: comparison of mecillinam, trimethoprim and ciprofloxacin, *J Antimicrob Chemoth* 46 (2000) 53-58.
- [69] S.M. Zala, D.J. Penn, Abnormal behaviours induced by chemical pollution: a review of the evidence and new challenges, *Anim Behav* 68 (2004) 649-664.
- [70] R.P. Schwarzenbach, B.I. Escher, K. Fenner, T.B. Hofstetter, C.A. Johnson, U. Von Gunten, B. Wehrli, The challenge of micropollutants in aquatic systems, *Science* 313 (2006) 1072-1077.
- [71] J. Radjenović, M. Petrović, D. Barceló, Fate and distribution of pharmaceuticals in wastewater and sewage sludge of the conventional activated sludge (CAS) and advanced membrane bioreactor (MBR) treatment, *Water Res* 43 (2009) 831-841.
- [72] P. Verlicchi, M. Al Aukidy, E. Zambello, Occurrence of pharmaceutical compounds in urban wastewater: removal, mass load and environmental risk after a secondary treatment—a review, *Sci Total Environ* 429 (2012) 123-155.
- [73] M.-Q. Cai, R. Wang, L. Feng, L.-Q. Zhang, Determination of selected pharmaceuticals in tap water and drinking water treatment plant by high-performance liquid chromatography-triple quadrupole mass spectrometer in Beijing, China, *Environ Sci Pollut R* 22 (2015) 1854-1867.
- [74] R.L. Oulton, T. Kohn, D.M. Cwiertny, Pharmaceuticals and personal care products in effluent matrices: a survey of transformation and removal during wastewater treatment and

implications for wastewater management, *Journal of Environmental Monitoring* 12 (2010) 1956-1978.

[75] T. Reemtsma, M. Jekel, *Organic pollutants in the water cycle: properties, occurrence, analysis and environmental relevance of polar compounds*, John Wiley & Sons 2006.

[76] J.L. Wang, L.J. Xu, *Advanced oxidation processes for wastewater treatment: formation of hydroxyl radical and application*, *Crit Rev Env Sci Tec* 42 (2012) 251-325.

[77] J. Wang, S. Wang, *Removal of pharmaceuticals and personal care products (PPCPs) from wastewater: a review*, *J Environ Manage* 182 (2016) 620-640.

[78] M. Cheng, G. Zeng, D. Huang, C. Lai, P. Xu, C. Zhang, Y. Liu, *Hydroxyl radicals based advanced oxidation processes (AOPs) for remediation of soils contaminated with organic compounds: a review*, *Chem Eng J* 284 (2016) 582-598.

[79] M.A. Oturan, J.-J. Aaron, *Advanced oxidation processes in water/wastewater treatment: principles and applications. A review*, *Crit Rev Env Sci Tec* 44 (2014) 2577-2641.

[80] J. Feng, X. Hu, P.L. Yue, *Effect of initial solution pH on the degradation of Orange II using clay-based Fe nanocomposites as heterogeneous photo-Fenton catalyst*, *Water Res* 40 (2006) 641-646.

[81] S. Sharma, M. Mukhopadhyay, Z. Murthy, *Treatment of chlorophenols from wastewaters by advanced oxidation processes*, *Separation & Purification Reviews* 42 (2013) 263-295.

[82] J. De Laat, H. Gallard, S. Ancelin, B. Legube, *Comparative study of the oxidation of atrazine and acetone by H₂O₂/UV, Fe (III)/UV, Fe (III)/H₂O₂/UV and Fe (II) or Fe (III)/H₂O₂*, *Chemosphere* 39 (1999) 2693-2706.

[83] H. El Hajjouji, F. Barje, E. Pinelli, J.-R. Bailly, C. Richard, P. Winterton, J.-C. Revel, M. Hafidi, *Photochemical UV/TiO₂ treatment of olive mill wastewater (OMW)*, *Bioresource Technol* 99 (2008) 7264-7269.

- [84] J. Nishio, M. Tokumura, H.T. Znad, Y. Kawase, Photocatalytic decolorization of azo-dye with zinc oxide powder in an external UV light irradiation slurry photoreactor, *J Hazard Mater* 138 (2006) 106-115.
- [85] A. Amat, A. Arques, M. Miranda, F. Lopez, Use of ozone and/or UV in the treatment of effluents from board paper industry, *Chemosphere* 60 (2005) 1111-1117.
- [86] W.R. Chen, C.M. Sharpless, K.G. Linden, I. Suffet, Treatment of volatile organic chemicals on the EPA contaminant candidate list using ozonation and the O₃/H₂O₂ advanced oxidation process, *Environ Sci Technol* 40 (2006) 2734-2739.
- [87] T.C. Wang, G. Qu, J. Li, D. Liang, Evaluation of the potential of soil remediation by direct multi-channel pulsed corona discharge in soil, *J Hazard Mater* 264 (2014) 169-175.
- [88] H. Fenton, LXXIII.—Oxidation of tartaric acid in presence of iron, *Journal of the Chemical Society, Transactions* 65 (1894) 899-910.
- [89] F. Duarte, F. Maldonado-Hódar, L.M. Madeira, Influence of the characteristics of carbon materials on their behaviour as heterogeneous Fenton catalysts for the elimination of the azo dye Orange II from aqueous solutions, *Applied Catalysis B: Environmental* 103 (2011) 109-115.
- [90] F. Lücking, H. Köser, M. Jank, A. Ritter, Iron powder, graphite and activated carbon as catalysts for the oxidation of 4-chlorophenol with hydrogen peroxide in aqueous solution, *Water Res* 32 (1998) 2607-2614.
- [91] S. Gan, H.K. Ng, Inorganic chelated modified-Fenton treatment of polycyclic aromatic hydrocarbon (PAH)-contaminated soils, *Chem Eng J* 180 (2012) 1-8.
- [92] C.L. Yap, S. Gan, H.K. Ng, Fenton based remediation of polycyclic aromatic hydrocarbons-contaminated soils, *Chemosphere* 83 (2011) 1414-1430.

- [93] R.G. Zepp, B.C. Faust, J. Holgne, Hydroxyl radical formation in aqueous reactions (pH 3-8) of iron (II) with hydrogen peroxide: the photo-Fenton reaction, *Environ Sci Technol* 26 (1992) 313-319.
- [94] M. Perez, F. Torrades, X. Domenech, J. Peral, Fenton and photo-Fenton oxidation of textile effluents, *Water Res* 36 (2002) 2703-2710.
- [95] H. Tekin, O. Bilkay, S.S. Ataberk, T.H. Balta, I.H. Ceribasi, F.D. Sanin, F.B. Dilek, U. Yetis, Use of Fenton oxidation to improve the biodegradability of a pharmaceutical wastewater, *J Hazard Mater* 136 (2006) 258-265.
- [96] J. Beltran-Heredia, J. Torregrosa, J. Garcia, J. Domínguez, J. Tierno, Degradation of olive mill wastewater by the combination of Fenton's reagent and ozonation processes with an aerobic biological treatment, *Water science and technology: a journal of the International Association on Water Pollution Research* 44 (2000) 103-108.
- [97] A.M. Pintor, V.J. Vilar, R.A. Boaventura, Decontamination of cork wastewaters by solar-photo-Fenton process using cork bleaching wastewater as H₂O₂ source, *Sol Energy* 85 (2011) 579-587.
- [98] L. Szyrkowicz, C. Juzzolino, S.N. Kaul, A comparative study on oxidation of disperse dyes by electrochemical process, ozone, hypochlorite and Fenton reagent, *Water Res* 35 (2001) 2129-2136.
- [99] M.I. Badawy, M.Y. Ghaly, T.A. Gad-Allah, Advanced oxidation processes for the removal of organophosphorus pesticides from wastewater, *Desalination* 194 (2006) 166-175.
- [100] M. Pelaez, N.T. Nolan, S.C. Pillai, M.K. Seery, P. Falaras, A.G. Kontos, P.S. Dunlop, J.W. Hamilton, J.A. Byrne, K. O'shea, A review on the visible light active titanium dioxide photocatalysts for environmental applications, *Applied Catalysis B: Environmental* 125 (2012) 331-349.

- [101] X. Chen, S.S. Mao, Titanium dioxide nanomaterials: synthesis, properties, modifications, and applications, *Chem Rev* 107 (2007) 2891-2959.
- [102] J.J. Pignatello, E. Oliveros, A. MacKay, Advanced oxidation processes for organic contaminant destruction based on the Fenton reaction and related chemistry, *Crit Rev Env Sci Tec* 36 (2006) 1-84.
- [103] D.-Y. Yu, N. Kang, W. Bae, M.K. Banks, Characteristics in oxidative degradation by ozone for saturated hydrocarbons in soil contaminated with diesel fuel, *Chemosphere* 66 (2007) 799-807.
- [104] R. Broséus, S. Vincent, K. Aboulfadl, A. Daneshvar, S. Sauvé, B. Barbeau, M. Prévost, Ozone oxidation of pharmaceuticals, endocrine disruptors and pesticides during drinking water treatment, *Water Res* 43 (2009) 4707-4717.
- [105] L. Zhou, W. Zheng, Y. Ji, J. Zhang, C. Zeng, Y. Zhang, Q. Wang, X. Yang, Ferrous-activated persulfate oxidation of arsenic (III) and diuron in aquatic system, *J Hazard Mater* 263 (2013) 422-430.
- [106] P. Neta, R.E. Huie, A.B. Ross, Rate constants for reactions of inorganic radicals in aqueous solution, *J Phys Chem Ref Data* 17 (1988) 1027-1284.
- [107] W. Guo, S. Su, C. Yi, Z. Ma, Degradation of antibiotics amoxicillin by Co₃O₄-catalyzed peroxymonosulfate system, *Environ Prog Sustain* 32 (2013) 193-197.
- [108] G. Prieto, S. Beijer, M.L. Smith, M. He, Y. Au, Z. Wang, D.A. Bruce, K.P. De Jong, J.J. Spivey, P.E. De Jongh, Design and synthesis of copper–cobalt catalysts for the selective conversion of synthesis gas to ethanol and higher alcohols, *Angewandte Chemie International Edition* 53 (2014) 6397-6401.
- [109] J. Wenk, S. Canonica, Phenolic antioxidants inhibit the triplet-induced transformation of anilines and sulfonamide antibiotics in aqueous solution, *Environ Sci Technol* 46 (2012) 5455-5462.

- [110] F. Tully, A. Ravishankara, R. Thompson, J. Nicovich, R. Shah, N. Kreutter, Kinetics of the reactions of hydroxyl radical with benzene and toluene, *J. Phys. Chem.:(United States)* 85 (1981).
- [111] M. Sánchez-Polo, R. Ocampo-Pérez, J. Rivera-Utrilla, A.J. Mota, Comparative study of the photodegradation of bisphenol A by HO, SO₄^{•-} and CO₃^{•-}/HCO₃ radicals in aqueous phase, *Sci Total Environ* 463 (2013) 423-431.
- [112] H. Lee, H.-i. Kim, S. Weon, W. Choi, Y.S. Hwang, J. Seo, C. Lee, J.-H. Kim, Activation of Persulfates by Graphitized Nanodiamonds for Removal of Organic Compounds, *Environ Sci Technol* 50 (2016) 10134-10142.
- [113] Y. Fan, Y. Ji, D. Kong, J. Lu, Q. Zhou, Kinetic and mechanistic investigations of the degradation of sulfamethazine in heat-activated persulfate oxidation process, *J Hazard Mater* 300 (2015) 39-47.
- [114] L. Zhou, C. Ferronato, J.-M. Chovelon, M. Sleiman, C. Richard, Investigations of diatrizoate degradation by photo-activated persulfate, *Chem Eng J* 311 (2017) 28-36.
- [115] X. Liu, T. Zhang, Y. Zhou, L. Fang, Y. Shao, Degradation of atenolol by UV/peroxymonosulfate: kinetics, effect of operational parameters and mechanism, *Chemosphere* 93 (2013) 2717-2724.
- [116] C. Cai, H. Zhang, X. Zhong, L. Hou, Ultrasound enhanced heterogeneous activation of peroxymonosulfate by a bimetallic Fe-Co/SBA-15 catalyst for the degradation of Orange II in water, *J Hazard Mater* 283 (2015) 70-79.
- [117] O.S. Furman, A.L. Teel, R.J. Watts, Mechanism of base activation of persulfate, *Environ Sci Technol* 44 (2010) 6423-6428.
- [118] Y.-F. Huang, Y.-H. Huang, Behavioral evidence of the dominant radicals and intermediates involved in bisphenol A degradation using an efficient Co²⁺/PMS oxidation process, *J Hazard Mater* 167 (2009) 418-426.

- [119] B.-T. Zhang, Y. Zhang, Y. Teng, M. Fan, Sulfate radical and its application in decontamination technologies, *Crit Rev Env Sci Tec* 45 (2015) 1756-1800.
- [120] W.-D. Oh, Z. Dong, T.-T. Lim, Generation of sulfate radical through heterogeneous catalysis for organic contaminants removal: Current development, challenges and prospects, *Applied Catalysis B: Environmental* 194 (2016) 169-201.
- [121] Y. Yao, Y. Cai, F. Lu, F. Wei, X. Wang, S. Wang, Magnetic recoverable MnFe₂O₄ and MnFe₂O₄-graphene hybrid as heterogeneous catalysts of peroxymonosulfate activation for efficient degradation of aqueous organic pollutants, *J Hazard Mater* 270 (2014) 61-70.
- [122] L.O. Simonsen, H. Harbak, P. Bennekou, Cobalt metabolism and toxicology—a brief update, *Sci Total Environ* 432 (2012) 210-215.
- [123] C. Moreno-Castilla, M. Fontecha-Cámara, M. Álvarez-Merino, M. López-Ramón, F. Carrasco-Marín, Activated carbon cloth as adsorbent and oxidation catalyst for the removal of amitrole from aqueous solution, *Adsorption* 17 (2011) 413-419.
- [124] H. Liu, P. Sun, M. Feng, H. Liu, S. Yang, L. Wang, Z. Wang, Nitrogen and sulfur co-doped CNT-COOH as an efficient metal-free catalyst for the degradation of UV filter BP-4 based on sulfate radicals, *Applied Catalysis B: Environmental* 187 (2016) 1-10.
- [125] A. Dąbrowski, P. Podkościelny, Z. Hubicki, M. Barczak, Adsorption of phenolic compounds by activated carbon—a critical review, *Chemosphere* 58 (2005) 1049-1070.
- [126] W.-D. Oh, S.-K. Lua, Z. Dong, T.-T. Lim, Performance of magnetic activated carbon composite as peroxymonosulfate activator and regenerable adsorbent via sulfate radical-mediated oxidation processes, *J Hazard Mater* 284 (2015) 1-9.
- [127] Y. Ren, L. Lin, J. Ma, J. Yang, J. Feng, Z. Fan, Sulfate radicals induced from peroxymonosulfate by magnetic ferrosinell MFe₂O₄ (M = Co, Cu, Mn, and Zn) as heterogeneous catalysts in the water, *Applied Catalysis B: Environmental* 165 (2015) 572-578.

- [128] C. Liang, Z.-S. Wang, C.J. Bruell, Influence of pH on persulfate oxidation of TCE at ambient temperatures, *Chemosphere* 66 (2007) 106-113.
- [129] C. Tan, N. Gao, Y. Deng, Y. Zhang, M. Sui, J. Deng, S. Zhou, Degradation of antipyrine by UV, UV/H₂O₂ and UV/PS, *J Hazard Mater* 260 (2013) 1008-1016.
- [130] R. Zhang, P. Sun, T.H. Boyer, L. Zhao, C.-H. Huang, Degradation of pharmaceuticals and metabolite in synthetic human urine by UV, UV/H₂O₂, and UV/PDS, *Environ Sci Technol* 49 (2015) 3056-3066.
- [131] Y. Wu, A. Bianco, M. Brigante, W. Dong, P. de Sainte-Claire, K. Hanna, G. Mailhot, Sulfate Radical Photogeneration Using Fe-EDDS: Influence of Critical Parameters and Naturally Occurring Scavengers, *Environ Sci Technol* (2015).
- [132] P. O'Neill, S. Steenken, D. Schulte-Frohlinde, Formation of radical cations of methoxylated benzenes by reaction with OH radicals, Ti²⁺, Ag²⁺, and SO₄^{•-}-in aqueous solution. An optical and conductometric pulse radiolysis and in situ radiolysis electron spin resonance study, *Journal of Physical Chemistry* 79 (1975) 2773-2779.
- [133] G.P. Anipsitakis, D.D. Dionysiou, Radical generation by the interaction of transition metals with common oxidants, *Environ Sci Technol* 38 (2004) 3705-3712.
- [134] Y. Ji, W. Xie, Y. Fan, Y. Shi, D. Kong, J. Lu, Degradation of trimethoprim by thermo-activated persulfate oxidation: reaction kinetics and transformation mechanisms, *Chem Eng J* 286 (2016) 16-24.
- [135] A. Ghauch, A.M. Tuqan, N. Kibbi, S. Geryes, Methylene blue discoloration by heated persulfate in aqueous solution, *Chem Eng J* 213 (2012) 259-271.
- [136] H.V. Lutze, S. Bircher, I. Rapp, N. Kerlin, R. Bakkour, M. Geisler, C. von Sonntag, T.C. Schmidt, Degradation of chlorotriazine pesticides by sulfate radicals and the influence of organic matter, *Environ Sci Technol* 49 (2015) 1673-1680.

- [137] L. Xu, R. Yuan, Y. Guo, D. Xiao, Y. Cao, Z. Wang, J. Liu, Sulfate radical-induced degradation of 2,4,6-trichlorophenol: A de novo formation of chlorinated compounds, *Chem Eng J* 217 (2013) 169-173.
- [138] J. Zhao, Y. Zhang, X. Quan, S. Chen, Enhanced oxidation of 4-chlorophenol using sulfate radicals generated from zero-valent iron and peroxydisulfate at ambient temperature, *Sep Purif Technol* 71 (2010) 302-307.
- [139] F. Ghanbari, M. Moradi, Application of peroxymonosulfate and its activation methods for degradation of environmental organic pollutants: Review, *Chem Eng J* 310 (2017) 41-62.
- [140] L. Cavani, S. Halladja, A. Ter Halle, G. Guyot, G. Corrado, C. Ciavatta, A. Boulkamh, C. Richard, Relationship between photosensitizing and emission properties of peat humic acid fractions obtained by tangential ultrafiltration, *Environ. Sci. Technol.* 43 (2009) 4348-4354.
- [141] E. Appiani, S.E. Page, K. McNeill, On the use of hydroxyl radical kinetics to assess the number-average molecular weight of dissolved organic matter, *Environ. Sci. Technol.* 48 (2014) 11794-11802.
- [142] M. Schnitzer, S.U. Kahn, *Humic substances in the environment*, (1972).
- [143] Y.-H. Guan, J. Ma, Y.-M. Ren, Y.-L. Liu, J.-Y. Xiao, L.-q. Lin, C. Zhang, Efficient degradation of atrazine by magnetic porous copper ferrite catalyzed peroxymonosulfate oxidation via the formation of hydroxyl and sulfate radicals, *Water Res* 47 (2013) 5431-5438.
- [144] M. Nie, Y. Yang, Z. Zhang, C. Yan, X. Wang, H. Li, W. Dong, Degradation of chloramphenicol by thermally activated persulfate in aqueous solution, *Chem Eng J* 246 (2014) 373-382.
- [145] C. Liang, Z.-S. Wang, N. Mohanty, Influences of carbonate and chloride ions on persulfate oxidation of trichloroethylene at 20 C, *Sci Total Environ* 370 (2006) 271-277.

- [146] G.P. Anipsitakis, D.D. Dionysiou, M.A. Gonzalez, Cobalt-mediated activation of peroxymonosulfate and sulfate radical attack on phenolic compounds. Implications of chloride ions, *Environ Sci Technol* 40 (2006) 1000-1007.
- [147] Y. Wang, J. Le Roux, T. Zhang, J.-P. Croué, Formation of brominated disinfection byproducts from natural organic matter isolates and model compounds in a sulfate radical-based oxidation process, *Environ Sci Technol* 48 (2014) 14534-14542.
- [148] Y. Ji, D. Kong, J. Lu, H. Jin, F. Kang, X. Yin, Q. Zhou, Cobalt catalyzed peroxymonosulfate oxidation of tetrabromobisphenol A: kinetics, reaction pathways, and formation of brominated by-products, *J Hazard Mater* 313 (2016) 229-237.
- [149] J. Lu, W. Dong, Y. Ji, D. Kong, Q. Huang, Natural organic matter exposed to sulfate radicals increases its potential to form halogenated disinfection byproducts, *Environ Sci Technol* 50 (2016) 5060-5067.
- [150] J. Liu, X. Zhang, Comparative toxicity of new halophenolic DBPs in chlorinated saline wastewater effluents against a marine alga: Halophenolic DBPs are generally more toxic than haloaliphatic ones, *Water Res* 65 (2014) 64-72.
- [151] Y. Yang, J.J. Pignatello, J. Ma, W.A. Mitch, Comparison of halide impacts on the efficiency of contaminant degradation by sulfate and hydroxyl radical-based advanced oxidation processes (AOPs), *Environ Sci Technol* 48 (2014) 2344-2351.
- [152] L. Zhao, Y. Ji, D. Kong, J. Lu, Q. Zhou, X. Yin, Simultaneous removal of bisphenol A and phosphate in zero-valent iron activated persulfate oxidation process, *Chem Eng J* 303 (2016) 458-466.
- [153] Y.-H. Huang, Y.-F. Huang, C.-i. Huang, C.-Y. Chen, Efficient decolorization of azo dye Reactive Black B involving aromatic fragment degradation in buffered Co^{2+} /PMS oxidative processes with a ppb level dosage of Co^{2+} -catalyst, *J Hazard Mater* 170 (2009) 1110-1118.

Chapter II

Experiment Section

2.1. Chemicals and Materials.

The chemical reagents used in this study are listed in Table 2.1.

Table 2.1 Main characteristics of the chemical reagents used in this study.

| Name | Formula | Purity | Supplier |
|--|------------------------------------|-----------|------------------------|
| Potassium persulfate (PS) | $K_2S_2O_8$ | 99% | Sigma-Aldrich |
| Sodium diatrizoate hydrate (DTZ) | $C_{11}H_8I_3N_2NaO_4 \cdot xH_2O$ | 98% | Sigma-Aldrich |
| Salbutamol (SAL) | $C_{13}H_{21}NO_3$ | 98% | Sigma-Aldrich |
| Terbutaline (TBL) | $C_{12}H_{19}NO_3$ | 98% | Sigma-Aldrich |
| Nitrobenzene (NB) | $C_6H_5NO_2$ | 99% | Sigma-Aldrich |
| 4-nitroaniline (PNA) | $C_6H_6O_2N_2$ | 99% | Sigma-Aldrich |
| Resorcinol | $C_6H_6O_2$ | 99% | Fluka |
| 2-hydroxybenzyl alcohol (2-HBA) | $C_7H_8O_2$ | 98% | Fluka |
| 4-hydroxybenzyl alcohol (2-HBA) | $C_7H_8O_2$ | 98% | Fluka |
| 3,5-dihydroxybenzyl alcohol (3,5-DHBA) | $C_7H_8O_3$ | 98% | Fluka |
| Hydrogen peroxide | H_2O_2 | 30% (w/w) | Sigma-Aldrich |
| Benzamide | C_7H_7NO | 99% | Sigma-Aldrich |
| Suwannee River Fulvic Acid (SRFA, 2S101F) | | | International Humic |

| | | Substance Society (IHSS) | |
|---|------------------------------------|-----------------------------|-------------------|
| Elliott Soil Fulvic Acid (ESFA, 2S102F) | | | IHSS |
| Suwannee River Aquatic Natural Organic Matter (SRNOM, 1R101N) | | | IHSS |
| Nordic Lake Aquatic Natural Organic Matter (NLNOM, 1R108N) | | | IHSS |
| Aldrich humic acid (sodium salt) | | | Aldrich |
| | | HPLC or | |
| Methanol (MeOH) | CH ₃ OH | LC-MS grade | Fisher Scientific |
| | | HPLC or | |
| Ethanol (EtOH) | CH ₃ CH ₂ OH | LC-MS grade | Fisher Scientific |
| | | HPLC or | |
| Acetonitrile (ACN) | CH ₃ CN | LC-MS grade | Fisher Scientific |
| <i>tert</i> -butanol (TBA) | C ₄ H ₁₀ O | 99.5% | Sigma-Aldrich |
| Sodium bicarbonate | NaHCO ₃ | 99.9% | Sigma-Aldrich |
| Sulfuric acid | H ₂ SO ₄ | 97.5% | Sigma-Aldrich |
| Sodium hydroxide | NaOH | 98% | Sigma-Aldrich |

| | | | |
|---------------------------------|----------------------------------|-----|---------|
| Sodium dihydrogenphosphate | NaH ₂ PO ₄ | 99% | Aldrich |
| Sodium hydrogen phosphate | Na ₂ HPO ₄ | 99% | Aldrich |

Milli-Q water (18 MΩ cm) was prepared from a Millipore Milli-Q System. All experimental solutions were prepared by dissolving the reagents directly in Milli-Q water without further purification. All stock solutions were stored in dark under 4 °C after preparation and used within one month.

2.2 Steady-state photolysis experiments.

For the degradation of DTZ, SAL and TBL, SO₄^{•-} radicals were generated by activation of persulfate under simulated solar irradiation, and the irradiation experiments were conducted in a solar simulator Suntest CPS+, (HERAEUS, Hanau, France) equipped with a 1.5 kW xenon arc and an ultraviolet filter allowing a simulation of the solar spectrum between 290nm and 400 nm. The reaction was carried out in a cylindrical Pyrex reactor (i.d. = 5 cm, H = 15 cm, V = 150 mL) and the temperature was maintained at 20 °C using a circulating water system.

A scheme of the applied reactor and the light intensity are given in Figure 2.1 and 2.2, respectively. Specific aliquot of substrate (DTZ, SAL or TBL) and appropriate volumes of persulfate stock solution were added to achieve 50 mL reaction solution. Control experiments with substrates alone and dark experiments with substrate-persulfate were carried out under identical conditions. Except for buffered solutions (achieved using 10 mM Na₂HPO₄ and 10 mM NaH₂PO₄ in the experiments with bicarbonate), the initial pH of other reaction solutions were adjusted using 0.01 M H₂SO₄ and 0.01 M NaOH. Aliquots of 0.3 mL were withdrawn at selected time intervals and quenched immediately with the same volume of methanol, a scavenger for SO₄^{•-} and ·OH, to stop the chemical oxidation reactions. All experiments were

performed at least in duplicate.

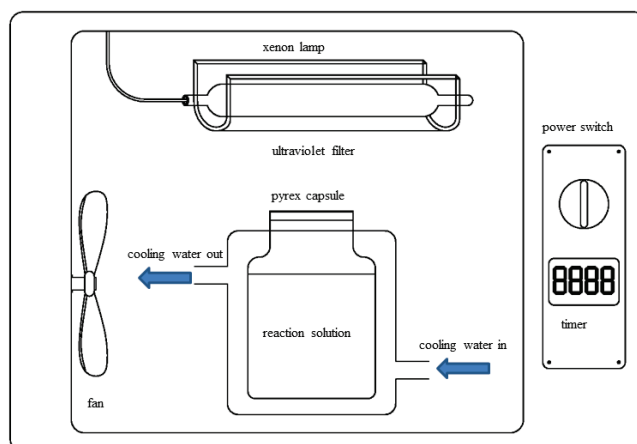


Figure 2.1. The scheme of applied SUNTEST photo-reactor.

The bleaching experiments of DOM by UV activated PS were carried out in a cuvette in parallel beam at 313 nm using a mercury high pressure lamp equipped with a Bausch and Lomb monochromator. The photon fluence rate was 6.81×10^{-5} Einstein $L^{-1} s^{-1}$ in average. The UV–visible spectra of reaction solutions were recorded on a Cary 3 spectrophotometer (Varian) after specific irradiation time.

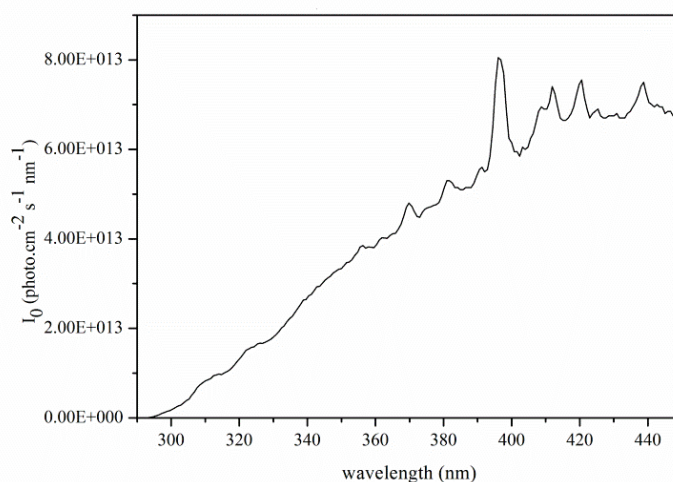


Figure 2.2. Incident light received by the solutions in the SUNTEST.

2.3 Laser Flash Photolysis (LFP) experiments.

Transient absorption experiments were carried out using a nanosecond laser-flash photolysis spectrometer from Applied Photophysics (LKS.60) with laser excitation at 266 nm from a Quanta Ray GCR130-1 Nd:YAG. A 32 bits RISC processor kinetic spectrometer workstation was used to analyze the digitized signal. Appropriate volumes of chemical stock solutions were mixed just before the experiments to obtain the desired mixtures and concentrations. In the cases of SAL and TBL, the excitation energy was set as low as possible to avoid biphotonic photoionization of the phenolic compounds and therefore minimize the generation of the phenoxy radicals through direct their photolysis. LFP photolysis of phenols alone in the same conditions were also conducted, the results confirmed that the generation of the phenoxy radicals was negligible in the case of phenols alone. The decay of the sulfate radical was monitored at 450 nm in the experiments with SAL, DTZ and DOM at maximum absorption of this radical but at 500 nm in the case of TBL because the phenoxy radical of TBL absorbs until ~480 nm. All the experiments were performed at ambient temperature (295 ± 2 K) and in aerated solution, unless otherwise stated.

2.4 Analytical procedures.

2.4.1 High performance liquid chromatography (HPLC).

The concentrations of DTZ, SAL, TBL, NB and PNA were analyzed using a Shimadzu 10A series high performance liquid chromatography (HPLC, Shimadzu) system equipped with a Model 7725i injector with a 20 μ L sample loop and coupled with a LC-10AT binary pump and a SPD-M10ADAD. Samples were separated using an Yperspher BDS C₁₈ column (5 μ m, 125 mm*4.0 mm, i.d.) (Interchim, France) at 40 °C. The mobile phase was a mixture of acetonitrile and acidified-water (3 % formic acid by volume, pH 3.0). An overview of the HPLC parameters is given together in Table 2.2.

Table 2.2. HPLC analysis parameters.

| Compound | Flow rate (mL/min) | Mobile phase composition | | Injection volume (μ L) | Detection wavelength (nm) |
|----------|-----------------------|-----------------------------|--------------|-----------------------------------|---------------------------------|
| | | water | acetonitrile | | |
| DTZ | 0.8 | 99% | 1% | 20 | 237 |
| SAL | 0.8 | 50% | 50% | 20 | 224 |
| TBL | 0.8 | 40% | 60% | 20 | 230 |
| PNA | 0.8 | 40% | 60% | 20 | 380 |
| NB | 0.8 | 40% | 60% | 20 | 275 |

2.4.2. Liquid chromatography-mass spectrometry (LC-MS).

High resolution mass spectrometry (HR-MS) analyses were performed to identify the oxidation products of DTZ, SAL and TBL, a Waters Q-TOF mass spectrometer in positive ion (ES^+) ionization mode was used, which was coupled to an HPLC Waters Alliance system consisting of a 2695 module for compounds separation and a 2998 photodiode array detector. An Yperspher BDS C18 column was also used, and the flow rate was set at 0.2 mL min^{-1} .

All information of HR-MS data including retention times, exact m/z , and ion intensities was analyzed with Xcalibur (Thermo Scientific, U.S.) in the Qual Browser. The formula of the potential products could be obtained from the exact mass with a mass accuracy of $<5 \text{ ppm}$. Based on the formula, the possible structures of the oxidation products were proposed.

2.4.3. TOC measurement.

Concentrations of SRFA and Aldrich humic acid were expressed as total organic carbon (TOC, mgC L^{-1}) and determined using a Shimadzu 5000A analyzer (Japan). Calibration was achieved by injecting standards of succinic acid solution.

2.4.4. UV-Vis absorption spectra.

The UV-Vis spectra of the selected chemicals were recorded using a Lambda 950 UV-Vis spectrophotometer (PerkinElmer, USA) and quartz cuvettes.

2.4.5. pH measurement.

The pH of the solutions was measured using a combined glass electrode connected to a PHM 210 Standard pH meter (Radiometer, Copenhagen).

2.5. Rate constants measurements.

2.5.1. Measurement of the second-order rate constants with $\cdot\text{OH}$.

The second-order rate constants of reaction of DTZ, SAL and TBL with hydroxyl radical ($\cdot\text{OH}$) were determined by completion kinetics method according to the following equation. H_2O_2 was used as sensitizer of $\cdot\text{OH}$ under the irradiation of Suntest. Nitrobenzene (NB), with a known rate constant with $\cdot\text{OH}$ ($3 \times 10^9 \text{ M}^{-1} \text{ s}^{-1}$) was used as a reference chemical in this study [1]. The reaction between NB and $\cdot\text{OH}$ is nearly diffusion controlled with 1:1 stoichiometry. The reaction solutions contained H_2O_2 (10 mg L^{-1}), NB ($120 \text{ }\mu\text{M}$) and our target compounds were irradiated under SUNTEST. During the irradiation, the loss of the target compounds was monitored along with the loss of NB.

$$k_{OH,P} = \frac{\ln([P]_t/\ln[P]_0)}{\ln([NB]_t/\ln[NB]_0)} k_{OH,NB} \quad (1)$$

where P refers to the selected chemicals (DTZ, SAL or TBL), the second order rate constants of reaction of hydroxyl radical with these chemicals can be calculated from the slope of the plot $\ln([P]/[P]_0)$ versus $\ln([NB]/[NB]_0)$.

2.5.2. Measurement of the second-order rate constants with $\text{SO}_4^{\cdot-}$.

The rate constant of DTZ, SAL and TBL with $\text{SO}_4^{\cdot-}$ was measured by laser flash photolysis method. Transient absorption experiments were carried out on a nanosecond laser-flash photolysis spectrometer from Applied Photophysics (LKS.60) with laser excitation at 266 nm from Quanta Ray GCR130-1 Nd:YAG, and the excitation energy was set at 10 mJ/pulse. The

decay of sulfate radical was followed at 450 nm for DTZ and SAL, while 500 nm for TBL. $\text{SO}_4^{\bullet-}$ was observed with a decay rate at $(1.7 \pm 0.4) \times 10^5 \text{ s}^{-1}$ in the absence of target chemicals. After the addition of them, the rate of sulfate radical decay began to increase. By using a linear regression of the decay rate of sulfate radical versus target compounds concentration, we could estimate the second order rate constant of DTZ with $\text{SO}_4^{\bullet-}$.

2.5.3. Measurement of the second-order rate constants with $\text{CO}_3^{\bullet-}$.

The method for determining the rate constants of DTZ (or SAL, TBL) with carbonate radical was similar to that with hydroxyl radical method only the competitor was replaced by 4-nitroaniline (PNA) ($k_{\text{CO}_3^{\bullet-}/\text{PNA}} = 7.3 \times 10^7 \text{ M}^{-1} \text{ s}^{-1}$) [2]. Carbonate radical was generated by adding excess bicarbonate (0.1 M) in UV/ H_2O_2 process with 600 μM H_2O_2 .

The irradiation experiments were conducted in a home-made photochemical reactor equipped with a 125 W high pressure mercury lamp (Cathodeon, Cambridge, UK) housed in a borosilicate immersion well ($\lambda > 290 \text{ nm}$). The lamp was turned on preliminarily for 20 min for stabilization, then 50 mL reaction solutions were pipetted into a Pyrex reactor (i.d. = 5 cm, $H = 15 \text{ cm}$) and irradiated during different time intervals. The reactor was placed in a metal photo-reactor for irradiation, opened to air and maintained at $24 \pm 1 \text{ }^\circ\text{C}$ by a cooling water circulation system. The light intensity (300-400 nm) in the center of the reaction solutions was measured at approximately 3.3 mW cm^{-2} by actinometer, comparable to the midday sunlight in June, Lyon (France; $45 \text{ }^\circ\text{N}$ latitude).

$$k_{\text{CO}_3^{\bullet-}, \text{DTZ}} = \frac{\ln([\text{DTZ}]_t / \ln[\text{DTZ}]_0)}{\ln([\text{PNA}]_t / \ln[\text{PNA}]_0)} k_{\text{CO}_3^{\bullet-}, \text{PNA}} \quad (2)$$

Under this condition, the steady-state concentration of $\cdot\text{OH}$ ($\approx 10^{-15} \text{ M}$) was much lower than $\text{CO}_3^{\bullet-}$ ($\approx 10^{-10} \text{ M}$). In this case, the influence of $\cdot\text{OH}$ could be neglected [3].

2.6. Calculations.

2.6.1. DFT Calculations.

The Density Functional Theory (DFT) calculations were performed using the Gaussian 09

software package [4]. The ground state geometries of the investigated species were optimized using the hybrid density functional B3LYP method with the 6-31+ G(d,p) basis set. The absorption spectra were calculated with the time-dependent DFT method (TD-DFT) at the B3LYP/6-31+G(d,p) level. The vibrational progression in the absorption spectra was obtained from analysis of electronic excitations between vibrational levels of the ground and excited states. This basis set was shown to give accurate results for the phenoxyl radical (the 6-31+G(d,p) or cc-pVTZ basis sets yielded similar absorption energies) [5]. In an attempt to check whether the solvent affected our results, we completed B3LYP/6-31+G(d,p) calculations by simulating the solvent explicitly. Two water molecules were added in the model in the vicinity of the phenoxyl substituent. However, the maximum wavelength of absorption changed by less than 3 nm. It was thus decided to perform calculations without the solvent.

2.6.2. Lighting screening factors.

To calculate the lighting screening factor for a single wavelength we used the formula introduced by Wenk et al [6].

$$S_{\lambda} = \frac{1 - 10^{-\alpha_{\lambda}l}}{2.303\alpha_{\lambda}l} \quad (3)$$

Where S_{λ} is the screening factor, α_{λ} (cm^{-1}) is the wavelength specific attenuation coefficient; l (cm) is the optical path length of the tubes used in photochemical experiments. And, the integrated screening factor could be estimated as follows,

$$S = \frac{\sum_{\lambda} S_{\lambda} \times I_{\lambda}}{\sum_{\lambda} I_{\lambda}} \quad (4)$$

Where I_{λ} is the light intensity of the lamp used in the experiments.

2.6.3. Determination of PS concentration.

PS could react with iodide in accordance with Eq 5. This reaction can be accelerated and

completed in a reasonable time (e.g., 15 min) at room temperatures in the presence of an excess of iodide [7]. Thus, a UV spectrophotometric method is proposed for measurement of a yellow iodine color formed from the reaction of PS with I⁻.

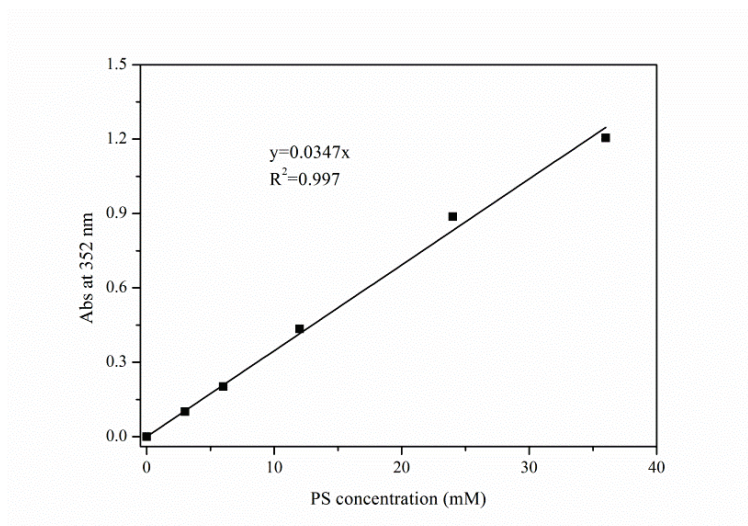
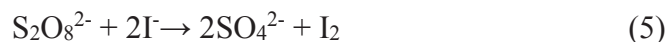


Figure 2.3. Standard curve for PS concentration determination (x-axis represents the initial concentration of PS solution added to the mixture solution).

Calibration was conducted firstly by preparing a series of standard solutions, 10 μL PS solution, 3 mL DI water, 1 mL NaI solution (3M) and 3 mL NaHCO_3 solution (10 g L^{-1}) was added to a 10 mL EPA glass vial. The resulting solutions were hand shaken and allowed to equilibrate for 15 min. The mixture solution was detected by the UV-Vis spectrophotometer for the absorbance at 352 nm. The calibration curve is presented in Figure 2.3.

2.6.4. Calculation of PS consumption in the reaction with DTZ.

By using UV spectrophotometric method, we found that during the reaction time of 60 min, PS concentration was not changed. This result could also be supported by the calculation.

In the absence of DTZ, the light intensity absorbed by PS, I_{PS} , was calculated as follow:

$$I_{PS} = \sum_{290}^{340} I_0^\lambda (1 - 10^{-\epsilon^\lambda cb}) \quad (6)$$

Where I_0^λ is the light intensity of the lamp at a specific wavelength, ϵ^λ is molar extinction

coefficient of PS at the same wavelength ($M^{-1}cm^{-1}$), c is the PS concentration (M), and b is the path length of the light through the reaction solution (in our reactor, $b = 3.5$ cm). And in the presence of DTZ, I^{PS} was equal to:

$$I_{PS} = \sum_{290}^{340} I_0^\lambda \frac{\varepsilon_{PS}^\lambda c_{PS}}{\varepsilon_{PS}^\lambda c_{PS} + \varepsilon_{DTZ}^\lambda c_{DTZ}} (1 - 10^{-(\varepsilon_{PS}^\lambda c_{PS} + \varepsilon_{DTZ}^\lambda c_{DTZ})b}) \quad (7)$$

Thus, based on the UV-Vis absorbance spectrum of PS and the intensity of the light source, in the absence of DTZ, the I^{PS} value (12 mM) could be calculated as 4.0×10^{-8} Einstein $L^{-1} s^{-1}$.

Thus, the decay of PS under irradiation could be written as:

$$-\frac{d[PS]}{dt} = k[PS] = \frac{1}{2} \Phi I_{PS} \quad (8)$$

Where Φ represents the quantum yield of sulfate radical formation under UV irradiation, here we use the value of 1.4 from the literature [8].

The decay rate of PS was calculated as 2.7×10^{-8} M s^{-1} , if we assume the rate remains constant, the half-life time of 12 mM PS would be around 2.6 days.

And in the presence of DTZ, due to the competition of PS with DTZ for photons, the decay of PS would be much slower, which is consistent with our result that within 60 min the PS concentration hardly changed.

2.6.5. Calculation of I_{PS} in the reaction with DTZ.

During the reaction process, I_{PS} was calculated as follows:

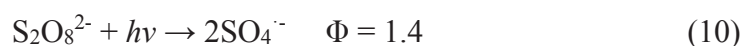
$$I_{PS} = \sum_{290}^{340} I_0^\lambda \frac{\varepsilon_{PS}^\lambda c_{PS}}{\varepsilon_{PS}^\lambda c_{PS} + \varepsilon_{DTZ}^\lambda c_{DTZ} + \sum_1^i \varepsilon_{P_i}^\lambda c_{P_i}} (1 - 10^{-(\varepsilon_{PS}^\lambda c_{PS} + \varepsilon_{DTZ}^\lambda c_{DTZ} + \sum_1^i \varepsilon_{P_i}^\lambda c_{P_i})b}) \quad (9)$$

Where P_i are the oxidation products and ε_i are their molar absorption coefficients. Based on the data from UV-Vis spectra of the reaction solutions, the I_{PS} values ($[PS]_0 = 12$ mM, $[DTZ]_0 = 30$ mg/L) could be calculated, after 1 h reaction time, the light intensity absorbed by PS

decreased between 20 and 25%.

2.6.6. Calculation of sulfate radical concentration in the reaction process with DTZ.

The concentration of $\text{SO}_4^{\bullet-}$ could not remain constant during the reaction process. Here we tried to calculate the concentration at the initial step of the reaction. We assume that DTZ was the only substrate that reacted with $\text{SO}_4^{\bullet-}$ at the beginning of the oxidation (the reaction with water could be negligible).



Assuming the hypothesis of the steady-state concentration, the rate of $\text{SO}_4^{\bullet-}$ generation from PS equals to the rate of its consumption by DTZ), we can deduce:

$$I_{PS}\Phi = k_a[\text{DTZ}][\text{SO}_4^{\bullet-}] \quad (12)$$

Where I_{PS} is the light intensity absorbed by PS in the presence of DTZ, which could be calculated by Eq 7.

2.7. References.

- [1] R.G. Zepp, J. Hoigne, H. Bader, Nitrate-induced photooxidation of trace organic chemicals in water, *Environ. Sci. Technol.* 21 (1987) 443-450.
- [2] J. Huang, S.A. Mabury, A new method for measuring carbonate radical reactivity toward pesticides, *Environ. Toxicol. Chem.* 19 (2000) 1501-1507.
- [3] R. Zhang, P. Sun, T.H. Boyer, L. Zhao, C.H. Huang, Degradation of Pharmaceuticals and Metabolite in Synthetic Human Urine by UV, UV/H₂O₂, and UV/PDS, *Environ. Sci. Technol.* 49 (2015) 3056-3066.

- [4] M. Frisch, G. Trucks, H. Schlegel, G. Scuseria, M. Robb, J. Cheeseman, G. Scalmani, V. Barone, B. Mennucci, G. Petersson, Gaussian 09, revision D. 01, Gaussian, Inc., Wallingford CT, 2009.
- [5] F. Santoro, C. Cappelli, V. Barone, Effective Time-Independent Calculations of Vibrational Resonance Raman Spectra of Isolated and Solvated Molecules Including Duschinsky and Herzberg–Teller Effects, *J. Chem. Theory Comput.* 7 (2011) 1824-1839.
- [6] J. Wenk, U. Von Gunten, S. Canonica, Effect of dissolved organic matter on the transformation of contaminants induced by excited triplet states and the hydroxyl radical, *Environ. Sci. Technol.* 45 (2011) 1334-1340.
- [7] C. Liang, C.F. Huang, N. Mohanty, R.M. Kurakalva, A rapid spectrophotometric determination of persulfate anion in ISCO, *Chemosphere* 73 (2008) 1540-1543.
- [8] J.-Y. Fang, C. Shang, Bromate formation from bromide oxidation by the UV/persulfate process, *Environ. Sci. Technol.* 46 (2012) 8976-8983.

Chapter III

Reactivity of sulfate radicals with natural organic matters

Sulfate radicals ($\text{SO}_4^{\bullet-}$) have attracted increasing scientific and technological interests in the recent years, owing to their relatively high standard oxidation potential (2.5-3.1 eV) [1]. In general, $\text{SO}_4^{\bullet-}$ can react with the organic contaminants with a second order rate constant in the range of 10^6 - $10^9 \text{ M}^{-1} \text{ s}^{-1}$ [1]. Advanced oxidation processes based on $\text{SO}_4^{\bullet-}$ (SR-AOPs) could be applied as an alternative to those based on hydroxyl radical ($\bullet\text{OH}$) for the remediation of the organic pollutants in surface, groundwater or wastewater [2, 3]. $\text{SO}_4^{\bullet-}$ is generated via the activation of peroxymonosulfate (SO_5^{2-} , PMS) or persulfate ($\text{S}_2\text{O}_8^{2-}$, PS) by UV, heat or transition metals [4-6]. SR-AOPs possess several advantages including the stability of the precursors (PMS or PS), favoring storage and transportation, high water solubility, the versatile activation strategies and the wide operating pH range [7, 8]. However, being a strong one-electron oxidant, sulfate radicals may inevitably react with the natural water constituents resulting in unpredictable consequences on the oxidation efficiency.

Natural organic matter (NOM) is ubiquitously present in surface, ground, drinking, and waste waters. NOM is a complex mixture of aliphatic and aromatic molecules containing a variety of functionalities [9-11]. It has been reported repeatedly that the presence of NOM decreases the degradation efficiency of numerous contaminants in SR-AOPs, such as roxarsone, atrazine and chloramphenicol [12-14]. To quantify the potential effect of NOM on SR-AOPs, it is necessary to acquire kinetic data on the reaction of sulfate radical with NOM. However, up to now, limited research has focused on this topic. By using an indirect kinetic competition method, Lutze et al have determined the second order rate constant of a commercial humic acid (Depur from Carl Roth) with $\text{SO}_4^{\bullet-}$. They got $6.8 \times 10^3 \text{ L mgC}^{-1} \text{ s}^{-1}$ [13]. The accuracy of the rate constants obtained by indirect methods depends on the “reference compound” used,

reactivity of which towards $\text{SO}_4^{\bullet-}$ must be already known.

The objective of this study was to determine the absolute rate constants of reactions of $\text{SO}_4^{\bullet-}$ with different NOMs by using the laser flash photolysis (LFP) method. This direct method that allows the monitoring of the $\text{SO}_4^{\bullet-}$ decay also offers the possibility to observe the transient species generated by these reactions, determine their spectroscopic characteristics and measure their decay. To our knowledge, the only experiments reported in the literature were performed at very low NOM concentration (0-400 $\mu\text{g/L}$) and had as a main goal to study the interaction between NOM and PS [15].

3.1. Results and discussion.

3.1.1 Formation and identification of transient species

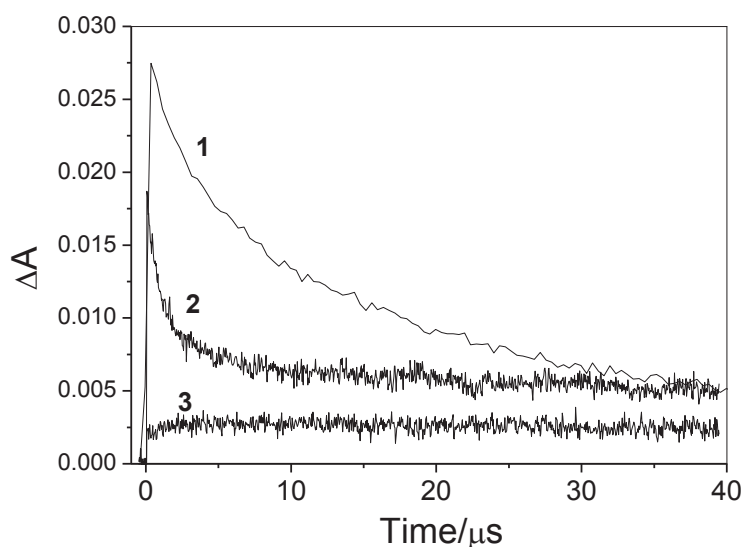


Figure 3.1. Time profile absorbance monitored for PS (1) and PS + NLNOM (2) at 450 nm; time profile absorbance monitored at 600 nm for PS + NLNOM (3). Excitation at 266 nm, [PS] = 40 mM, [NLNOM] = 250 mg L⁻¹.

The transient absorption spectrum of the sulfate radical formed after 266 nm laser excitation of PS (40 mM) (Eq 1) shows a maximum at 450 nm and decays in about 160 μs (Figure 3.1), which is in accordance with the reported literature data [16, 17]. When PS was irradiated in the presence of NOMs, the decay of $\text{SO}_4^{\bullet-}$ was drastically accelerated as observed in Figure 1.

The concomitant formation of new transients could be detected at 600 nm, wavelength at which $\text{SO}_4^{\bullet-}$ does not absorb (Figure 3.1).

The new species showed a very broad band with maximum around 450 nm (Figure 3.2A). The decay of these species was satisfactorily fitted by a double exponential with $k_{d1} = 9200 \pm 400 \text{ s}^{-1}$ and $k_{d2} = 1000 \pm 400 \text{ s}^{-1}$ (Figure 3.2B). As a strong electrophile, $\text{SO}_4^{\bullet-}$ is able to react with electron-rich compounds, such as phenolic compounds and anilines, and electron transfer reaction is the preferred reaction pathway [13, 18]). The new generated transient species could be assigned to the phenoxyl radicals as it has been reported that the phenoxyl radicals of NOM show a broad absorption band (maxima at 470-480 nm) with a lifetime of 600-700 μs corresponding to $k_2 = 1430\text{-}1700 \text{ s}^{-1}$ [19]. This lifetime is consistent with k_{d2} .

For each of the 4 selected NOMs, experiments were conducted to record the decay curves of $\text{SO}_4^{\bullet-}$ for NOMs concentrations varying from 100 to 400 mg L^{-1} . The detection wavelength was set at 450 nm and the decay was recorded until 50 μs , this time interval being enough to get the full loss of $\text{SO}_4^{\bullet-}$.

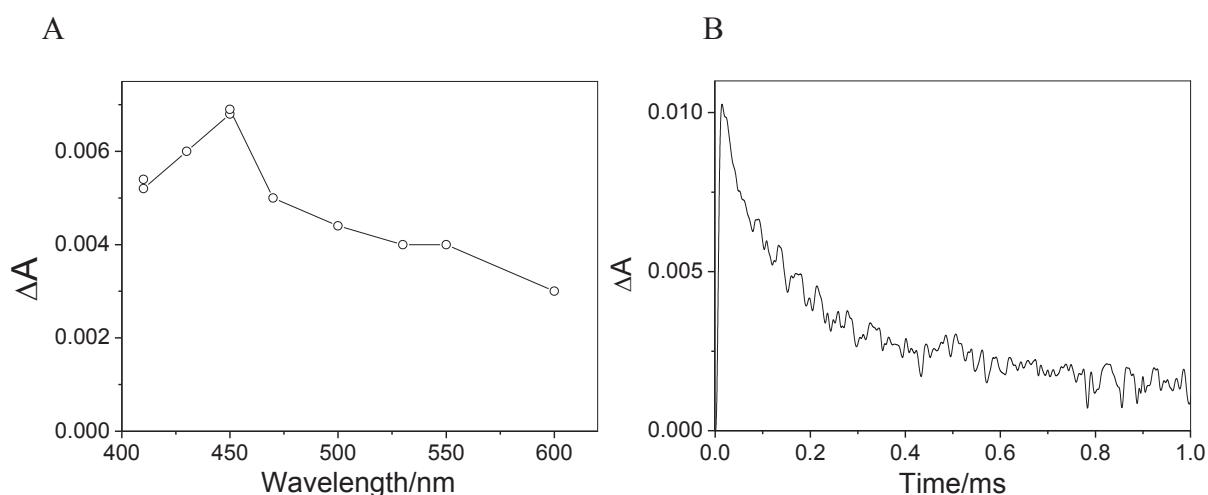
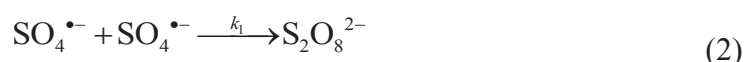


Figure 3.2. Excitation of a solution containing PS and NLNOM. Transient spectrum measured 50 μs after the pulse end (A) and absorbance decay measured at 450 nm (B).

3.1.2 Reactivity of $\text{SO}_4^{\bullet-}$ towards selected NOM.

The decay kinetic of $\text{SO}_4^{\bullet-}$ in pure water was already reported in the literature [11, 20]. The decay is mainly governed by the bimolecular recombination of $\text{SO}_4^{\bullet-}$ (Eq 2). The reaction rate constant k_1 was demonstrated to vary with the ionic force of the medium according to $\log 2k_1 = 8.94 + 0.92 \text{ I}^{0.5}$ [20]. The reaction of $\text{SO}_4^{\bullet-}$ with $\text{S}_2\text{O}_8^{2-}$ is also possible (Eq 3) but of minor importance ($k_2 < 1500 \text{ M}^{-1}\text{s}^{-1}$) in the concentration of $\text{S}_2\text{O}_8^{2-}$ generally used.



In the presence of NOM, Eq 4 must be also considered.



The rate of $\text{SO}_4^{\bullet-}$ disappearance is equal to:

$$- dc/dt = c_0 - [2k_1c^2 + k_3 [\text{NOM}]c] \quad (5)$$

where c is the concentration of $\text{SO}_4^{\bullet-}$. Expressed in absorbance, Eq 5 becomes equation 6, where A^S is the absorbance of $\text{SO}_4^{\bullet-}$, ε is the extinction coefficient of $\text{SO}_4^{\bullet-}$, and l , the width of the laser spot in our device (0.4 cm):

$$- dA^S/dt = A_0^S - \left(\frac{2k_1A^S{}^2}{\varepsilon l} + k_3 [\text{NOM}]A^S \right) \quad (6)$$

At 450 nm, ε is equal to $1600 \pm 100 \text{ M}^{-1}\text{cm}^{-1}$ (McElroy and Waygood, 1990). The transient species generated in the reaction of $\text{SO}_4^{\bullet-}$ with NOM also absorb at 450 nm. The rate of formation of these radicals can be written:

$$dc'/dt = k_3 [\text{NOM}]c \quad (7)$$

where c' is the concentration of the generated species. Their rate of formation expressed in absorbance (A^R) is equal to:

$$dA^R/dt = k_3 [\text{NOM}]A^S\varepsilon'/\varepsilon \quad (8)$$

where ε' is the weighted average of the extinction coefficient of the generated transients. The absorbance variation of the mixture is equal to:

$$- dA / dt = A_0^S \cdot \left(\frac{2k_1 A^S}{\varepsilon l} + k_3 [\text{NOM}] A^S \right) + k_3 [\text{NOM}] A^S \varepsilon' / \varepsilon \quad (9)$$

The differential Eq 9 was exploited through a numerical method, the time increment being set at 10^{-8} s. The parameters k_1 , k_3 and ε' were adjusted to get the best fit of the experimental time profile absorbances at 450 nm.

In a first step, we got the k_1 value using the decay kinetics of $\text{SO}_4^{\bullet-}$ when PS is excited alone, taking $[\text{NOM}]=0$ in Eq 9. The decay curve modelisation gave $k_1=1.2 \times 10^9 \text{ M}^{-1}\text{s}^{-1}$, in excellent agreement with the value of Ivanova et al (2000). Our result is also in a good accordance with the value of $9.1 \times 10^8 \text{ M}^{-1}\text{s}^{-1}$, obtained from the relationship of McEloy and Waygood (1990) taking $I=0.12$ deduced from $[\text{K}_2\text{S}_2\text{O}_8]=0.04\text{M}$. In a second step, we used the decay kinetics of $\text{SO}_4^{\bullet-}$ in the presence of the different NOMs to determine the k_3 and ε' values. Numerical calculations gave the product $k_3[\text{NOM}]$ for each NOM concentration. Plotting this product against $[\text{NOM}]$ led to k_3 (see Table 3.1). Values of k_3 lay within the range 690-910 $\text{s}^{-1}\text{mg}^{-1}\text{L}$ and vary in the order: NLNOM > ESFA, SRFA > SRNOM (Table 1). k_3 can be also calculated on the basis of the organic carbon: $44 \pm 1\%$ for ESFA, SRFA and SRNOM, and 26% only for NLNOM due to a high ash content. In this latter case, k_3 is about twice higher for NLNOM than for the other NOMs.

The reaction rate constant of NOM with hydroxyl radical ($\bullet\text{OH}$) measured with NOM was reported at $2.7 \times 10^4 \text{ s}^{-1}\text{mgC}^{-1} \text{ L}$ (Brezonik and Fulkerson-Brekken, 1998), which is much higher than that with $\text{SO}_4^{\bullet-}$ detected in this study. Sulfate and hydroxyl radicals differ considerably in their reaction rates, thus, the inhibiting effect of NOM, on the degradation of organic contaminants will be lower in $\text{SO}_4^{\bullet-}$ AOPs than in $\bullet\text{OH}$ AOPs.

Table 3.1. Values of k_3 and ϵ'/ϵ for the selected NOMs and carbon organic content corrected for the ash and water content obtained from the IHSS website.

| NOM | $k_3 \text{ s}^{-1}\text{mg}^{-1}\text{L}$ | $k_3 \text{ s}^{-1}\text{mgC}^{-1}\text{L}$ | ϵ'/ϵ | $C^b \%$ |
|-------|--|---|----------------------|----------|
| ESFA | 835±24 | 1900±55 | 0.25 | 44 |
| SRFA | 800±115 | 1860±260 | 0.50 | 43 |
| SRNOM | 690±26 | 1530±58 | 0.33 | 45 |
| NLNOM | 910±100 | 3500±385 | 0.29 | 26 |

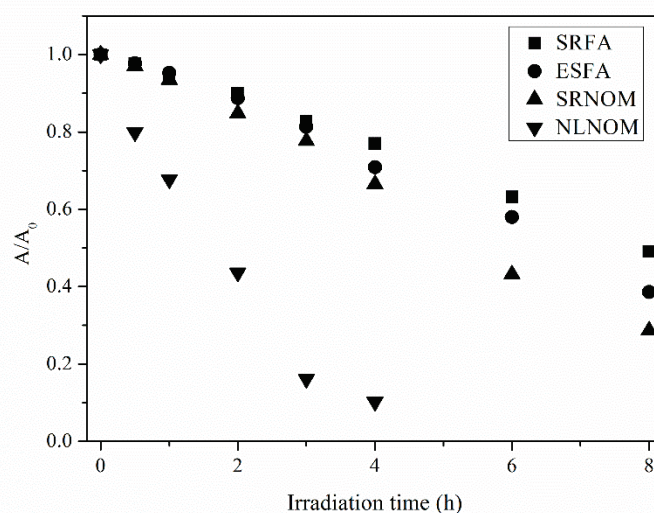


Figure 3.3. Bleaching of the four selected NOMs by photo-activation of PS at 330 nm (control experiments indicated that the bleaching by direct photodegradation was negligible). [NOM] = 50 mg.L⁻¹, [PS] = 10 mM.

The ϵ'/ϵ value varied within the range 0.25-0.5 (see Table 3.1) giving ϵ' values comprised between 400 and 800 M⁻¹cm⁻¹ at 450 nm. As different types of radicals are most probably generated, these ϵ' values represent a weighted average of the extinction coefficients. For comparison, the unsubstituted phenoxyl radical ($\lambda_{\text{max}}=400 \text{ nm}$) shows an ϵ equal to 3000 M⁻¹cm⁻¹.

3.1.3 Bleaching.

Bleaching (or fading) of NOM is an important process that leads to increased light penetration into the water column. In our work, $\text{SO}_4^{\bullet-}$ was found to be capable of bleaching the 4 selected DOM, as shown in Figure 3.3. The bleaching rates vary in the order $\text{NLNOM} > \text{SRNOM}$, ESFA , SRFA , which is fully consistent with the LFP measured second-order rate constants.

3.2 Conclusion.

NOM is one of the most important constituents in natural water and wastewater, it would react inevitably with $\text{SO}_4^{\bullet-}$ in the application of SR-AOPs. The present study estimated the reaction rate constants of $\text{SO}_4^{\bullet-}$ with four selected NOM by recording the decay of $\text{SO}_4^{\bullet-}$ and the formation of new species by means of LFP. The presence of NOM was found to accelerate the decay rate of $\text{SO}_4^{\bullet-}$, and the new generated species were assigned to phenoxyl radicals of NOM. By using a numerical method, the rate constants for $\text{SO}_4^{\bullet-}$ scavenging were calculated at 1.5, 1.8, 1.9 and $3.5 \times 10^3 \text{ s}^{-1} \text{ mgC}^{-1} \text{ L}$ for SRNOM, SRFA, ESFA and NLNOM, respectively. The bleaching rates of these NOM were consistent with LFP measured rate constants.

The rate constants of $\bullet\text{OH}$ reaction with different NOMs were reported at $2.7 \times 10^4 \text{ s}^{-1} \text{ mgC}^{-1} \text{ L}$, which is much higher than those with $\text{SO}_4^{\bullet-}$. Thus, due to the scavenging by NOM, AOPs based on $\text{SO}_4^{\bullet-}$ seems more efficient than those based on $\bullet\text{OH}$ in natural water and wastewater (containing NOM), depending on the reaction conditions and the target contaminant.

3.3 References.

[1] P. Neta, R.E. Huie, A.B. Ross, Rate constants for reactions of inorganic radicals in aqueous solution, *J. Phys. Chem. Ref. Data* 17 (1988) 1027-1284.

[2] H. Hori, A. Yamamoto, E. Hayakawa, S. Taniyasu, N. Yamashita, S. Kutsuna, H. Kiatagawa, R. Arakawa, Efficient decomposition of environmentally persistent

perfluorocarboxylic acids by use of persulfate as a photochemical oxidant, *Environmental Science & Technology* 39 (2005) 2383-2388.

[3] Y. Yang, J.J. Pignatello, J. Ma, W.A. Mitch, Comparison of halide impacts on the efficiency of contaminant degradation by sulfate and hydroxyl radical-based advanced oxidation processes (AOPs), *Environmental science & technology* 48 (2014) 2344-2351.

[4] L. Zhou, W. Zheng, Y. Ji, J. Zhang, C. Zeng, Y. Zhang, Q. Wang, X. Yang, Ferrous-activated persulfate oxidation of arsenic (III) and diuron in aquatic system, *J. Hazard. Mater.* 263 (2013) 422-430.

[5] R. Zhang, P. Sun, T.H. Boyer, L. Zhao, C.-H. Huang, Degradation of pharmaceuticals and metabolite in synthetic human urine by UV, UV/H₂O₂, and UV/PDS, *Environmental science & technology* 49 (2015) 3056-3066.

[6] Y. Ji, Y. Shi, W. Dong, X. Wen, M. Jiang, J. Lu, Thermo-activated persulfate oxidation system for tetracycline antibiotics degradation in aqueous solution, *Chem. Eng. J.* 298 (2016) 225-233.

[7] T.K. Lau, W. Chu, N.J. Graham, The aqueous degradation of butylated hydroxyanisole by UV/S₂O₈²⁻: study of reaction mechanisms via dimerization and mineralization, *Environmental science & technology* 41 (2007) 613-619.

[8] G.P. Anipsitakis, D.D. Dionysiou, Radical generation by the interaction of transition metals with common oxidants, *Environ Sci Technol* 38 (2004) 3705-3712.

[9] P. Westerhoff, S.P. Mezyk, W.J. Cooper, D. Minakata, Electron pulse radiolysis determination of hydroxyl radical rate constants with Suwannee River fulvic acid and other dissolved organic matter isolates, *Environmental science & technology* 41 (2007) 4640-4646.

- [10] W. Chen, P. Westerhoff, J.A. Leenheer, K. Booksh, Fluorescence excitation-emission matrix regional integration to quantify spectra for dissolved organic matter, *Environmental science & technology* 37 (2003) 5701-5710.
- [11] C. Richard, G. Guyot, A. Rivaton, O. Trubetskaya, O. Trubetskoj, L. Cavani, C. Ciavatta, Spectroscopic approach for elucidation of structural peculiarities of Andisol soil humic acid fractionated by SEC-PAGE setup, *Geoderma* 142 (2007) 210-216.
- [12] Y. Ji, Y. Shi, D. Kong, J. Lu, Degradation of roxarsone in a sulfate radical mediated oxidation process and formation of polynitrated by-products, *RSC Advances* 6 (2016) 82040-82048.
- [13] H.V. Lutze, S. Bircher, I. Rapp, N. Kerlin, R. Bakkour, M. Geisler, C. von Sonntag, T.C. Schmidt, Degradation of chlorotriazine pesticides by sulfate radicals and the influence of organic matter, *Environmental science & technology* 49 (2015) 1673-1680.
- [14] M. Nie, Y. Yang, Z. Zhang, C. Yan, X. Wang, H. Li, W. Dong, Degradation of chloramphenicol by thermally activated persulfate in aqueous solution, *Chem. Eng. J.* 246 (2014) 373-382.
- [15] P.M.D. Gara, G.N. Bosio, M.C. Gonzalez, N. Russo, M. del Carmen Michelini, R.P. Diez, D.O. Mártire, A combined theoretical and experimental study on the oxidation of fulvic acid by the sulfate radical anion, *Photochemical & Photobiological Sciences* 8 (2009) 992-997.
- [16] Y. Wu, A. Bianco, M. Brigante, W. Dong, P. de Sainte-Claire, K. Hanna, G. Mailhot, Sulfate radical photogeneration using Fe-EDDS: influence of critical parameters and naturally occurring scavengers, *Environmental science & technology* 49 (2015) 14343-14349.

- [17] C. George, J.-M. Chovelon, A laser flash photolysis study of the decay of SO_4^- and Cl_2^- radical anions in the presence of Cl^- in aqueous solutions, *Chemosphere* 47 (2002) 385-393.
- [18] T. Zhang, Y. Chen, T. Leiknes, Oxidation of Refractory Benzothiazoles with PMS/ CuFe_2O_4 : Kinetics and Transformation Intermediates, *Environmental science & technology* (2016).
- [19] M.V. Martin, R.A. Mignone, J.A. Rosso, P. David Gara, R. Pis Diez, C.D. Borsarelli, D.O. Mártire, Transient spectroscopic characterization and theoretical modeling of fulvic acid radicals formed by UV-A radiation, *Journal of Photochemistry and Photobiology A: Chemistry* 332 (2017) 571-579.
- [20] W. McElroy, S. Waygood, Kinetics of the reactions of the SO_4^- radical with SO_4 , $\text{S}_2\text{O}_8^{2-}$, H_2O and Fe^{2+} , *Journal of the Chemical Society, Faraday Transactions* 86 (1990) 2557-2564.

Chapter IV

Degradation of Diatrizoate by Photo-activated Persulfate

In recent decades, a growing number of studies have documented the widespread occurrence of pharmaceuticals in aquatic environment, raising serious concerns about their influence on aquatic ecosystems and human health [1-4]. Many pharmaceuticals were found to be recalcitrant to conventional drinking water and wastewater treatment processes (WWTPs) [5, 6]. As a consequence, pharmaceuticals are frequently detected in natural waters, and in drinking waters and constitute a potential risk for human health [7-11].

Iodinated X-ray contrast media (ICMs), a class of medical diagnostic agents routinely prescribed for imaging tissues and internal, are among the most recalcitrant and highly persistent pharmaceuticals [5]. Large quantities of ICM are administered to individual patients undergoing tests ($> 100 \text{ g dose}^{-1}$), and the annual worldwide consumption of ICMs was reported as approximately $3.5 \times 10^6 \text{ kg}$ [12]. ICMs are designed to be resistant to metabolism and thus are generally excreted unchanged within 24 h [13]. Conventional WWTPs could not remove ICMs effectively, leading to their occurrence in surface water and ground water at concentration ranging from ng L^{-1} to $\mu\text{g L}^{-1}$ [14-17]. The ICMs contribute substantially to the organic halogen levels in municipal and hospital effluents, which has raised additional concerns [18]. The published information about the environmental risk of ICMs is not abundant, however, some research has shown that DTZ may have nephrotoxic effects in animals and humans [19, 20]. Although there is lack of information about their impact on health, drinking water should be free of ICMs to minimize the potential risk of long-term adverse health effects. Therefore, it is essential to develop an effective treatment technology to remove these compounds from waters.

Advanced oxidation processes (AOPs) are promising alternatives capable of removing these

pharmaceuticals from WWTPs. The AOPs technology is mainly based on the generation of reactive species arising from the decomposition of oxidants such as hydrogen peroxide (H_2O_2) and persulfate (PS, $\text{S}_2\text{O}_8^{2-}$). Among the commonly used oxidants, PS received wide attention due to its high redox potential ($E^0 \sim 2.1 \text{ V}$) [21, 22]. PS is a relatively stable oxidant in water, however, it can be activated by UV, heat, base, or transition metals to generate a stronger oxidant, sulfate radical ($\text{SO}_4^{\bullet-}$, $E^0 \sim 2.6 \text{ V}$) [23-27]. It has been demonstrated that, $\text{SO}_4^{\bullet-}$, in general, could react with organic compounds with a second-order rate constant in the range $10^6 - 10^9 \text{ M}^{-1} \text{ s}^{-1}$ [28]. Unlike the well-known hydroxyl radical ($\cdot\text{OH}$), $\text{SO}_4^{\bullet-}$ is believed to react with organic compounds mainly via electron transfer mechanism, which makes it more selective [29]. Moreover, by comparison with $\cdot\text{OH}$, $\text{SO}_4^{\bullet-}$ is less likely scavenged by dissolved organic matter (DOM), such as humic and fulvic acids, that are ubiquitously present in natural waters [30]. Therefore, $\text{SO}_4^{\bullet-}$ -based oxidation processes show advantageous relative to conventional $\text{HO}\cdot$ -based AOPs in certain water treatment and remediation scenarios [31].

Various AOPs processes have been utilized to degrade ICMs, such as UV/ H_2O_2 , UV/ TiO_2 , O_3 [32-34]. While treatment feasibility of ICMs was examined, previous studies did not provide mechanistic details and did not explore the effects of naturally occurring substances (e.g., DOM, bicarbonate), which are essential for optimizing the treatment process. Moreover, studies reporting the treatment of ICMs by $\text{SO}_4^{\bullet-}$ -based oxidation process, especially ionic ICM like diatrizoate (DTZ) that was remarkably resistant to biodegradation, are scarce [35, 36]. Velo-Gala *et.al* undertook a comparative study on different AOPs processes for the degradation of DTZ, and found that $\text{SO}_4^{\bullet-}$ -based oxidation process could be an effective choice [37]. However, a detailed kinetic and mechanistic map describing the degradation of DTZ by $\text{SO}_4^{\bullet-}$ is still lacking.

In this part, we attempted to elucidate the underlying mechanisms and oxidation pathways of the reaction between DTZ and $\text{SO}_4^{\bullet-}$. $\text{SO}_4^{\bullet-}$ was generated by simulated sunlight activated PS

process. Kinetic studies were conducted for a better understanding of the influence of factors including pH and natural water constituents. The identification of DTZ transformation intermediates and products was also performed by using HPLC-MS method. Based on the HPLC-MS data, the reaction mechanisms and detailed transformation pathways were proposed. Our study provides useful information about using sulfate radical-based technologies for remediation of the groundwater contaminated by DTZ and structurally related X-ray contrast agent.

4.1 Results and discussion.

Preliminary dark control experiments with DTZ and PS were conducted (in Figure 4.1). No loss of DTZ was observed, indicating that no reaction occurs in the absence of light activation.

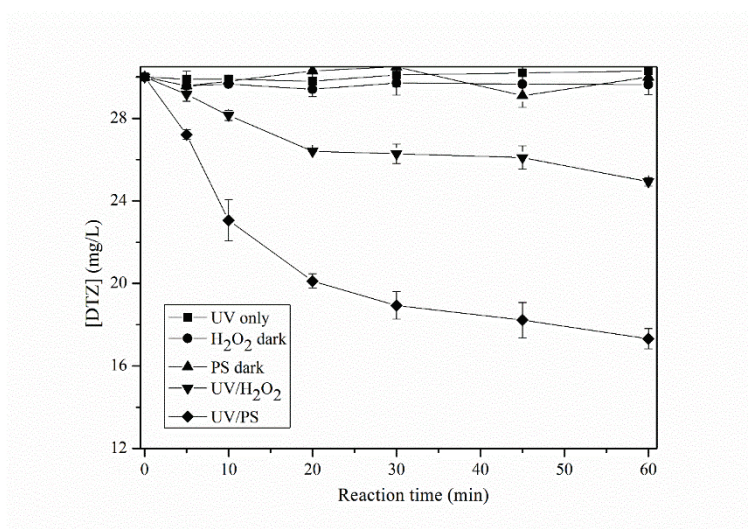


Figure 4.1. Degradation of DTZ by UV, H₂O₂ in dark, PS in dark, UV/H₂O₂ and UV/PS. ([DTZ]₀ = 30 mg L⁻¹, [H₂O₂]₀ = [PS]₀ = 12 mM, initial pH = 6.5).

4.1.1 Reaction kinetics.

Before investigating the AOPs process, we studied the photolysis of DTZ alone in the solar simulator. As shown in Fig 4.1, the decay of DTZ was negligible, in accordance with the work by Sugihara *et al.* who showed that DTZ did not undergo photolysis under UVA

irradiation [38]. From this point on, the discussion will focus on the indirect photolysis for a more straightforward comparison on reactive species' contributions under different conditions.

I) Comparison of UV/H₂O₂ and UV/PS oxidation.

Fig 4.1 exhibits the degradation of DTZ treated by UV/H₂O₂ and UV/PS, respectively. In both cases, the degradation of DTZ was significant in the first 20 min, afterwards the rate of DTZ disappearance slowed down. Such an auto-inhibition of the reaction has been reported for many compounds during oxidation processes by sulfate radical, such as diuron [23], polychlorinated biphenyls [42], atrazine [50], methylene blue [61] and tetrabromobisphenol A [62].

The presence of H₂O₂ led to the removal of 17% of DTZ after 1 h of irradiation. The degradation could be attributed to the generation of highly oxidizing radical species, ·OH. Indeed, when excess methanol (100 mM, as ·OH scavenger) was added in the solution, the oxidation of DTZ was inhibited by more than 95%.

On the other hand, 42 % of DTZ was degraded when using UV/PS after 1 h of irradiation. The degradation of DTZ was mostly due to the formation of sulfate radical (SO₄^{·-}) (Eq 1 and 2), where P represents the oxidation products.



The second order rate constant for DTZ with SO₄^{·-} was determined as $(1.9 \pm 0.2) \times 10^9 \text{ M}^{-1} \text{ s}^{-1}$ by means of laser flash photolysis (see Figure 4.2). For the reaction with ·OH, the value of $(6.1 \pm 0.1) \times 10^8 \text{ M}^{-1} \text{ s}^{-1}$ was calculated, which was in accordance with literature data (ranging from 5.40 to $9.58 \times 10^8 \text{ M}^{-1} \text{ s}^{-1}$) [33, 39]. The rate constant is slower than that with SO₄^{·-}, demonstrating that using activated persulfate to generate SO₄^{·-} could be a much more

effective way to remove DTZ. PS was much effective than H₂O₂ for the removal of DTZ under solar irradiation under neutral conditions. Similar results were also found in a previous study, the degradation rate of DTZ by UV/PS is 30% faster than that by UV/H₂O₂ [37]. The higher performance of PS can be attributed to its higher light absorption in the wavelength range of simulated solar light emission spectra (Figure 4.3). For instance, the molar extinction coefficient of PS, ϵ , is equal to 0.68 M⁻¹cm⁻¹ at 310 nm, against 0.42 M⁻¹cm⁻¹ for H₂O₂.

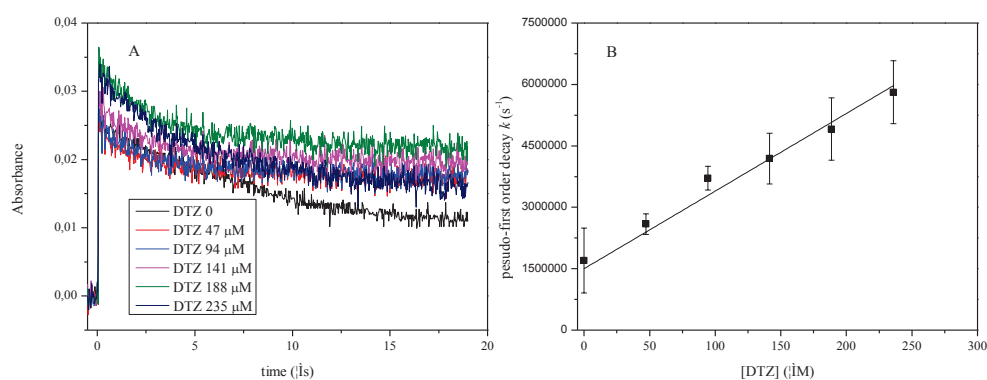


Figure 4.2. Decay of sulfate radical transient followed at 450 nm in the absence and presence of DTZ (A); the linear relationship of the pseudo-first order decay constant of SO₄^{•-} (k , s⁻¹) versus the concentration of DTZ (B) ([PS] =88 mM).

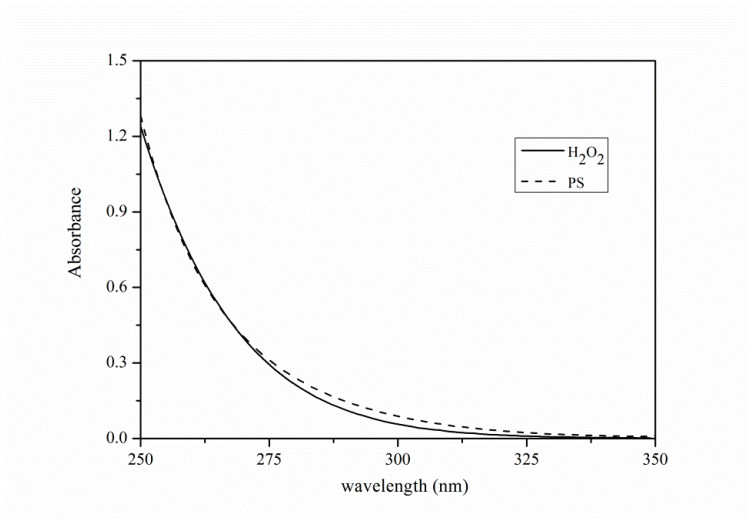
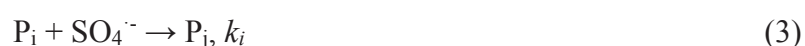


Figure 4.3. Absorption spectrum of H₂O₂ and PS at 50 mM from 250 to 350 nm.

In our study, the deceleration of DTZ degradation can be attributed to the formation of oxidation products, which could affect the reaction through two different ways. Firstly, the light-absorbing products would compete with PS for light flux, thereby reducing the yield of SO₄^{•-}. Secondly, oxidation products could also compete with DTZ for the reaction with SO₄^{•-}. These competitive reactions should slow down the decomposition rate of DTZ.



In the first stages of the reaction, if we assume that sulfate radicals only react with DTZ, the rate of DTZ degradation could be written:

$$-\frac{d[DTZ]}{dt} = I_{PS}^0 \Phi \quad (4)$$

Where I_{PS} is the light intensity absorbed by PS and Φ , is the quantum yield of sulfate radical formation. In the course of the reaction, when oxidation products compete with DTZ for sulfate radical, the rate law becomes:

$$-\frac{d[\text{DTZ}]}{dt} = I_{PS} \Phi \frac{k_0[\text{DTZ}]}{\sum_1^i k_i[\text{P}_i] + k_0[\text{DTZ}]} \quad (5)$$

Where P_i are the oxidation products and k_i are their reaction rate constants with $\text{SO}_4^{\cdot-}$.

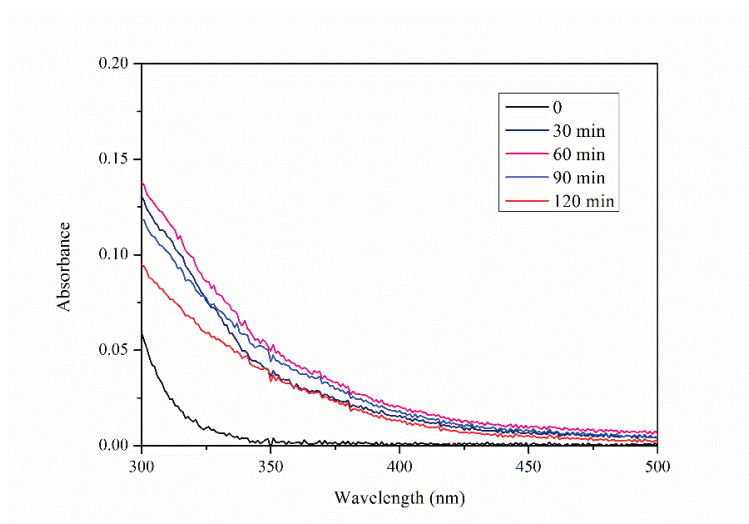


Figure 4.4. The UV-Vis spectrum of DTZ reaction solutions oxidized by UV/PS ($[\text{DTZ}]_0 = 30 \text{ mg/L}$, $[\text{PS}]_0 = 12 \text{ mM}$, initial $\text{pH} = 6.5$) in a cell of pathlength 1 cm. Note that in the reactor the pathlength is equal to 3.5 cm.

The decay of I_{PS} has been calculated based on the UV-Vis spectra of the reaction solution (Figure 4.4). The result indicated that after 1 h of irradiation, I_{PS} was reduced by 20-25%, as shown in Figure 4.5. From Figure 4.9 we could know that several phenolic products were generated in the reaction. As electron-rich compounds, phenolic compounds could react with sulfate radical at rates higher than that of the mother compound, DTZ [59]. Considering Eq 4 and 5, the rate of DTZ degradation should decrease when products accumulate in the medium.

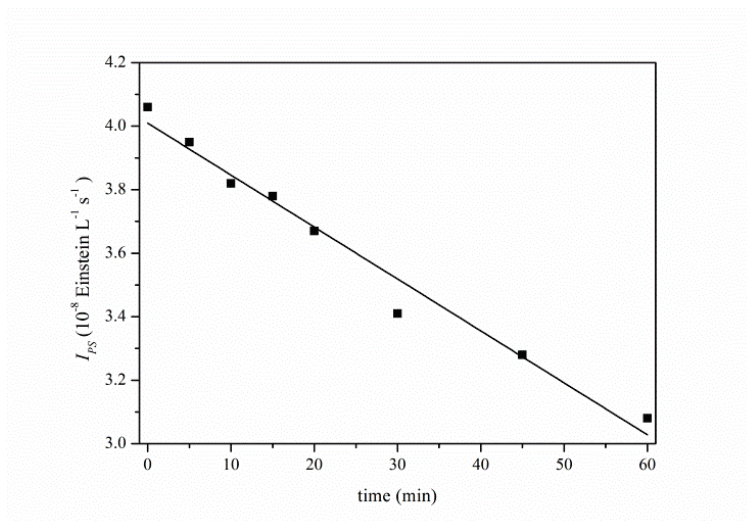


Figure 4.5. Light intensity absorbed by PS during the reaction process ([PS] = 12 mM, [DTZ]₀ = 30 mg/L, initial pH = 6.5).

II) Effects of initial solution pH and initial PS concentrations.

In real-world applications, pH conditions are expected to be variable, a fixed pH is not realistic. Therefore, we assessed the kinetic of DTZ degradation under different initial pH values (4.5 - 10.5). Summarized results are presented in Figure 4.6 and Table 4.1. Overall, the increase of pH from 4.5 to 8.5 did not affect the removal efficiency of DTZ, which remained in the range 61-63 %. However, the oxidation was found to decline at pH 10.5, as only 49 % of DTZ was removed. This result is consistent with previous report where high pH values (pH 12) slowed the degradation of DTZ by UV/PS compared with neutral and acidic conditions[37]. In addition, it is worthy to note that the solution pH in all experiments decreased during the reaction process, mostly due to the decomposition of PS and the formation of acidic species.

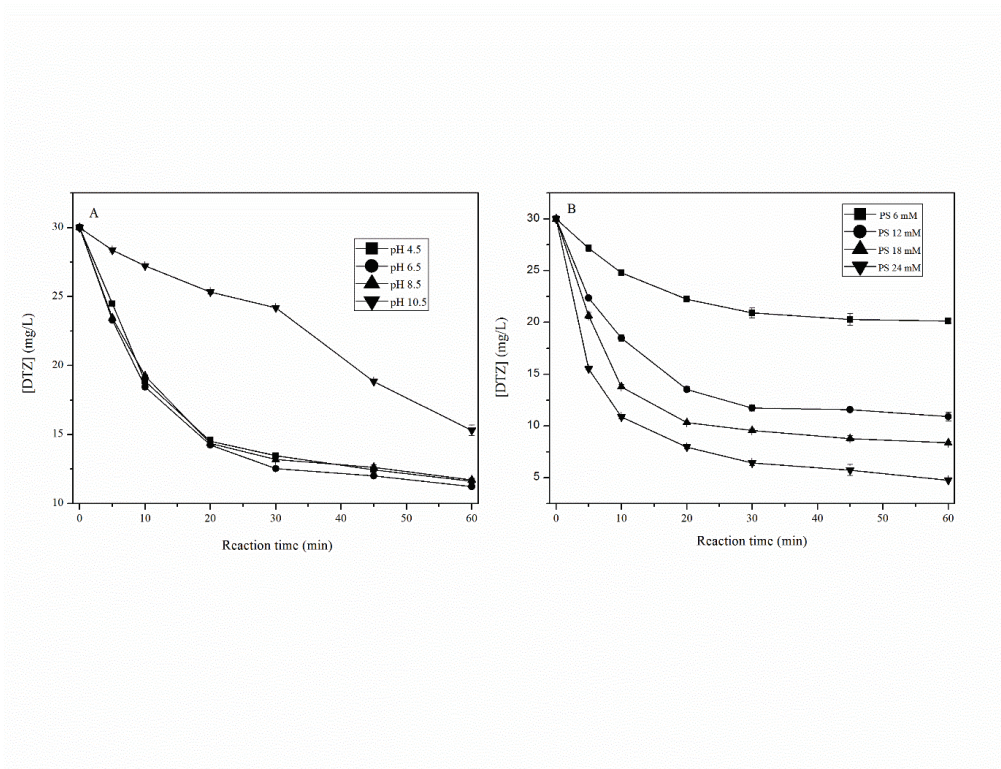


Figure 4.6. Degradation of DTZ by UV/PS (A) for various pH, ($[DTZ]_0 = 30 \text{ mg L}^{-1}$, $[PS]_0 = 12 \text{ mM}$); (B) for different initial PS doses ($[DTZ]_0 = 30 \text{ mg L}^{-1}$, initial pH = 6.5).

Solution pH might play a complex role in sulfate radical based oxidation process on organic contaminants since it could affect the ionization state of organic compounds as well as the formation of reactive species (i.e. $\text{SO}_4^{\cdot -}$ and $\cdot\text{OH}$) [40]. Depending on the pH, DTZ can exist in up to six different acid-base forms (Figure 4.7). When the solution pH is higher than 6, the form in which three H^+ are removed (No 6 in Figure 4.7) is the dominant species with a contribution larger than 90 %. Although all the samples (pH ranging from 4.5 to 10.5) underwent acidification during the reaction, for the last 3 groups (pH 6.5, 8.5 and 10.5), the reaction solutions experienced a similar change of DTZ species during the reaction. We could conclude that the speciation of DTZ was not responsible for the inhibition of oxidation at pH 10.5.

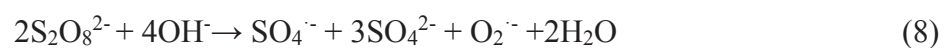
Table 4.1. Degradation efficiencies of DTZ at different conditions ([DTZ]₀ =30 mg/L, reaction time 1 h).

| object | Initial pH | PS concentration (mM) | DTZ | |
|------------------|---------------|-----------------------|------------|----------|
| | | | % degraded | Final pH |
| pH effect | 4.5 | 12.0 | 61.3 ± 0.1 | 3.6 |
| | 6.5 | 12.0 | 62.6 ± 0.2 | 3.8 |
| | 8.5 | 12.0 | 61.0 ± 0.4 | 3.9 |
| | 10.5 | 12.0 | 49.0 ± 1.2 | 4.4 |
| PS effect | 6.5 | 6.0 | 32.9 ± 0.7 | 4.0 |
| | 6.5 | 12.0 | 62.6 ± 0.2 | 3.8 |
| | 6.5 | 18.0 | 72.1 ± 0.3 | 3.5 |
| | 6.5 | 24.0 | 84.1 ± 0.1 | 3.4 |

Since the decline of DTZ removal rate could not be attributed to the effect of pH on oxidation efficiency, the evolution of reactive species during the reaction was taken into consideration. It has been demonstrated that SO₄^{•-} can yield ·OH under neutral or basic conditions (Eq 6-7) [41, 42].



The formation of ·OH in basic conditions could partly explain the decline of DTZ degradation, since the second order rate constant of DTZ with ·OH was smaller ($6.1 \times 10^8 \text{ M}^{-1} \text{ s}^{-1}$) than that with SO₄^{•-} ($1.9 \times 10^9 \text{ M}^{-1} \text{ s}^{-1}$) [33,39,43]. Another possible explanation of the pH effect is the base-activated PS decomposition described by Eq 8 [24].



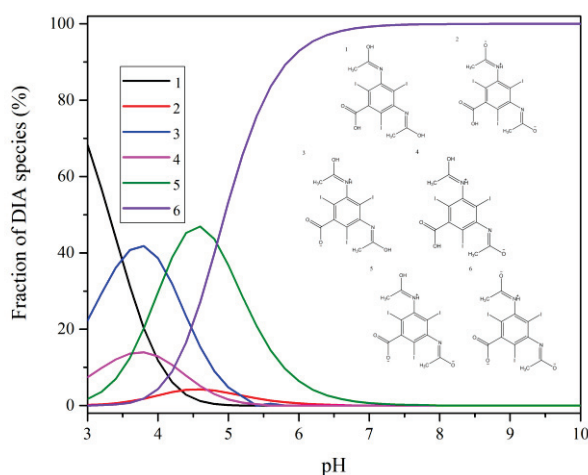


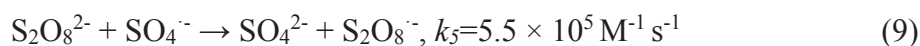
Figure 4.7. Speciation of DTZ at different pH values.

The yield of $\text{SO}_4^{\cdot-}$ via base-activated persulfate is much lower than that from UV-activated persulfate (Eq 3) as only one $\text{SO}_4^{\cdot-}$ radical is generated per 2 PS molecules. The competition of these two reactions inevitably decreased the concentration of $\text{SO}_4^{\cdot-}$, as well as that of $\cdot\text{OH}$. Zhang *et al.* confirmed this reduction by determining the steady-state concentrations of $\text{SO}_4^{\cdot-}$ and $\cdot\text{OH}$ ($[\text{SO}_4^{\cdot-}]_{\text{ss}}$ and $[\cdot\text{OH}]_{\text{ss}}$) by UV/PS under different pH values [44]. They found that both $[\text{SO}_4^{\cdot-}]_{\text{ss}}$ and $[\cdot\text{OH}]_{\text{ss}}$ values were lower in basic than neutral conditions. At pH 8.5, due to the relatively low concentration of OH^- ($\approx 4.2 \times 10^{-6}$ M in the beginning, and would continue to decrease during the reaction), the effect of these two reactions was indistinctive, which made the removal efficiency of DTZ among the range of pH 4.5 - 8.5 was nearly identical.

III) Effects of solution PS dose.

Table 4.1 also lists the degradation efficiencies of 30 mg L^{-1} DTZ by UV activated PS for different PS concentrations. Increasing the initial PS concentration significantly enhanced the degradation efficiency of DTZ. This result suggests that higher PS concentration yielded higher level of $\text{SO}_4^{\cdot-}$ by UV activation, promoting the oxidation of DTZ.

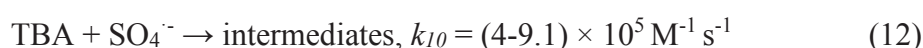
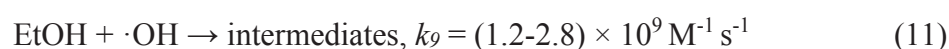
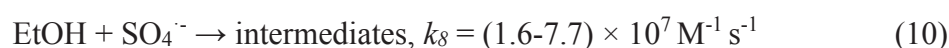
Some previous studies have reported that an increase of the initial PS concentration could not continuously ensure an increase of the decomposition efficiency due to the scavenging of $\text{SO}_4^{\cdot-}$ by $\text{S}_2\text{O}_8^{2-}$ (Eq 9), especially under acidic conditions [45-47].



However, this inhibiting effect of PS was not observed in the present work. Laser flash photolysis experiments were conducted (in the absence of DTZ) to better elucidate the scavenging effect of persulfate anions. The decay rates of $\text{SO}_4^{\cdot-}$ decay were found to be 1.7, 2.0, 1.7, 1.8, 1.7 and $1.8 \times 10^5 \text{ s}^{-1}$ at PS concentration of 6, 12, 24, 30, 36 and 44 mM, respectively. If the scavenging effect of PS played a role in the reaction process, the decay rate should increase with the increasing of PS concentrations. The highest PS initial concentration used in our work did not reach the critical level to slow down the degradation rate constant of DTZ.

4.1.2 Identification of oxidizing species ($\text{SO}_4^{\cdot-}$ and $\cdot\text{OH}$).

The DTZ loss mentioned above suggests that reactive species were produced by PS under simulated sunlight irradiation. $\text{SO}_4^{\cdot-}$ and $\cdot\text{OH}$ can be considered as the main oxidizing species involved in the decomposition process of DTZ. A better understanding of the contribution of each of these radicals in the reaction was evaluated by using specific scavengers like ethanol (EtOH) and tert-butyl alcohol (TBA) [48, 49]. The bimolecular rate constants of reaction of these two scavengers with the radicals are given in Eq 10-13. EtOH is a more efficient quencher than TBA, and both alcohols quench $\cdot\text{OH}$ more easily than $\text{SO}_4^{\cdot-}$.



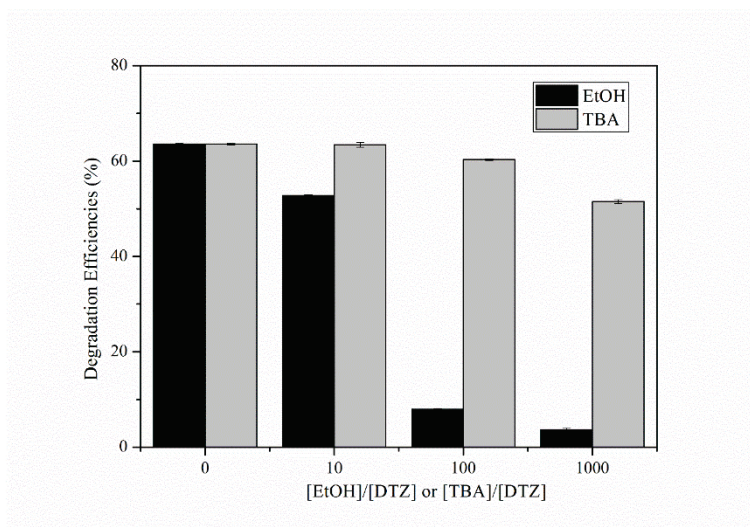
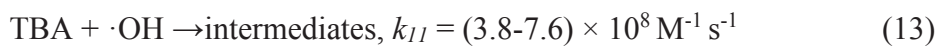


Figure 4.8. Degradation efficiencies of DTZ by UV/PS in the presence of different scavengers (EtOH and TBA) molar ratios. ([DTZ]₀ = 30 mg L⁻¹, [PS]₀ = 12 mM, initial pH = 6.5, reaction time = 60 min).

Their inhibiting effect was measured for various [EtOH]/[DTZ] and [TBA]/[DTZ] ratios.

Figure 4.8 displays the results. Comparing the degradation efficiencies in the absence and in the presence of the scavengers allows us to determine the contribution of SO₄^{-•} and ·OH in the reaction. Postulating the quasi-stationary state for SO₄^{-•} and ·OH gives Eq 14 and 15 in the case where TBA was added.

$$r_{\text{OH}} = k_{\text{OH,DTZ}}[\cdot\text{OH}][\text{DTZ}] + k_{14}[\cdot\text{OH}][\text{TBA}] \quad (14)$$

$$r_{\text{SO}_4^-} = k_{\text{SO}_4^-,\text{DTZ}}[\text{SO}_4^{\cdot-}][\text{DTZ}] + k_{13}[\text{SO}_4^{\cdot-}][\text{TBA}] \quad (15)$$

This allows the determination of [SO₄^{-•}] and [·OH] and the degradation rate of DTZ can be written as:

$$r_{(DTZ)TBA} = k_{\cdot OH,DTZ}[\cdot OH][DTZ] + k_{SO_4^{\cdot-},DTZ}[SO_4^{\cdot-}][DTZ] = \frac{k_{\cdot OH,DTZ}[DTZ]}{k_{\cdot OH,DTZ}[DTZ] + k_{\cdot OH,TBA}[TBA]} r_{\cdot OH} + \frac{k_{SO_4^{\cdot-},DTZ}[DTZ]}{k_{SO_4^{\cdot-},DTZ}[DTZ] + k_{SO_4^{\cdot-},TBA}[TBA]} r_{SO_4^{\cdot-}} \quad (16)$$

Here, we used the mean values of k_{I3} and k_{I4} from Eq 12 and 13 to calculate the contribution of $SO_4^{\cdot-}$ and $\cdot OH$. For instance, when $[TBA]/[DTZ] = 100$, $r_{(DTZ)TBA}$ is equal to:

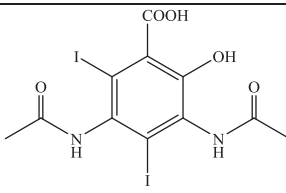
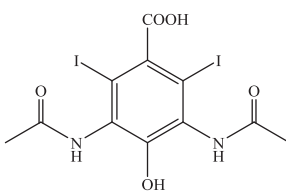
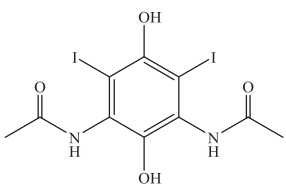
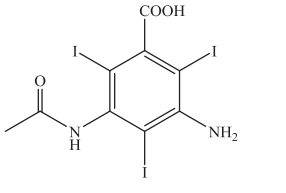
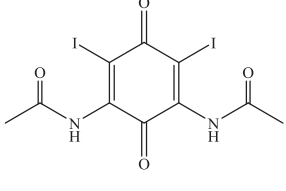
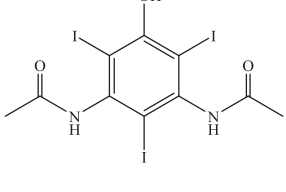
$$r_{(DTZ)TBA} = 0.01r_{\cdot OH} + 0.97r_{SO_4^{\cdot-}} \quad (17)$$

At this condition ($[TBA]/[DTZ] = 100$), the contribution of $\cdot OH$ was negligible. By comparison the degradation efficiency in the absence of TBA with that in the presence of TBA ($[TBA]/[DTZ] = 100$), we could calculate that $SO_4^{\cdot-}$ plays a dominant role in the oxidation process.

4.1.3 Degradation products and reaction pathways.

Reaction products generated during UV-activated PS oxidation of DTZ were identified by HPLC-MS. The identification was based on the analysis of the total ion chromatograms (TIC) and the corresponding mass spectra obtained by the positive ion electrospray HPLC-MS. Data are provided in Table 4.2, and the proposed degradation pathways is illustrated in Figure 4.9. As seen, three pathways take place: pathway a) is the side chain cleavage with formation of an NH_2 group, pathway b) is the deiodination-hydroxylation, and pathway c) is the decarboxylation- hydroxylation.

Table 4.2. Proposed structure of DTZ oxidation products by UV activated persulfate.

| No. | Retention Time (min) | [M+H] ⁺ | Proposed formula | Proposed structure |
|-----|----------------------|--------------------|--|---|
| 1 | 0.87 and 1.65 | 504.8735 | C ₁₁ H ₁₁ O ₅ N ₂ I ₂ |  or  |
| 2 | 1.88 | 476.8788 | C ₁₀ H ₁₁ O ₄ N ₂ I ₂ |  |
| 3 | 2.12 | 572.7644 | C ₉ H ₈ O ₃ N ₂ I ₃ |  |
| 4 | 2.74 | 474.8628 | C ₁₀ H ₉ O ₄ N ₂ I ₂ |  |
| 5 | 3.49 | 586.7799 | C ₁₀ H ₁₀ O ₃ N ₂ I ₃ |  |

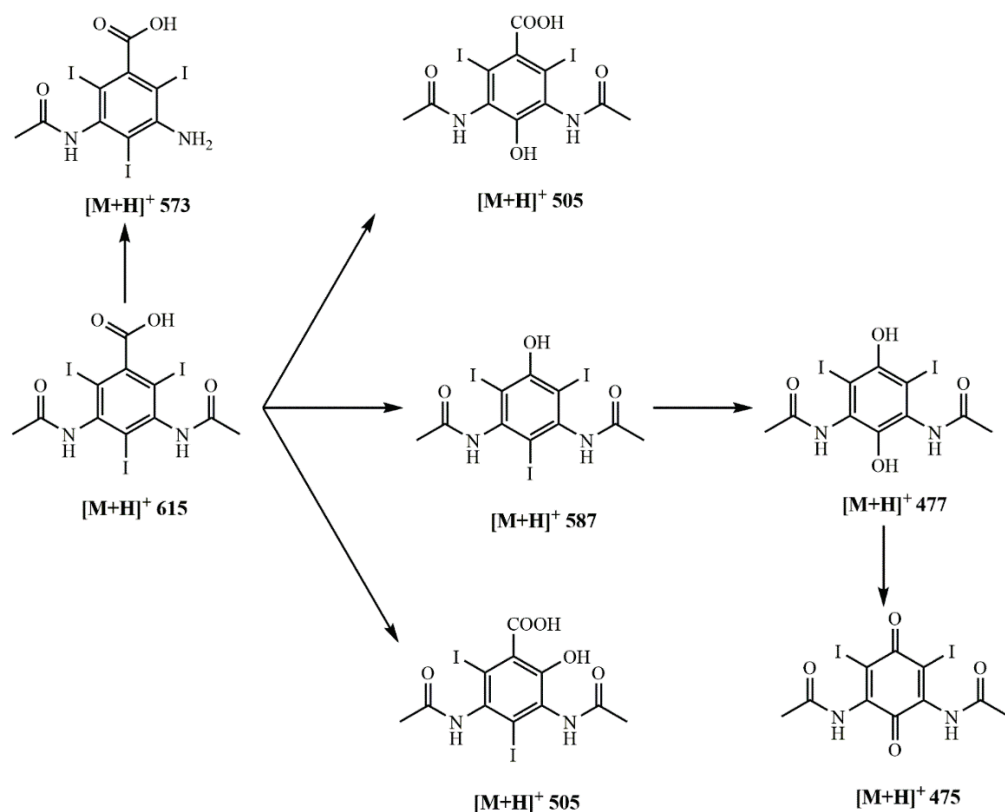


Figure 4.9. Proposed oxidation pathways of DTZ by simulated sunlight activated PS. ([DTZ]₀ = 30 mg L⁻¹, [PS]₀ = 12 mM, pH = 6.5, reaction time = 60 min).

As a strong oxidant, SO₄^{•-} tends to attack electron rich sites of the compound. For the reaction with DTZ, the initial step is expected to be an electron-transfer from DTZ to SO₄^{•-}, leading to the generation of SO₄²⁻ and the DTZ radical cation. The hydrolysis of the radical cation produces the corresponding HO-adducts. The ipso addition of -OH at the iodo site would result in the loss of iodine atom, producing the phenolic products with m/z = 505 in ES⁺ corresponding to [M+H]⁺ (Figure 4.10A). Two peaks at m/z = 505 were identified in the TIC spectra, showing that the substitution of I by OH can take place at two different iodo positions. On the other hand, the ipso addition of -OH at the carbon site bearing the carboxylic acid function could generate decarboxylation-hydroxylation, as confirmed by the detection of the peak at m/z = 587 in ES⁺ (Figure 4.10B). These products were also formed by the attack of ·OH on DTZ, which has been reported in previous work of Jeong *et.al* [39]. Afterwards,

the further decarboxylation-hydroxylation of the phenol or the deiodination-hydroxylation process of the decarboxylated photoproduct can occur, producing the hydroquinonic product ($m/z=477$ in ES^+) and the corresponding quinonic product ($m/z = 475$ in ES^+) through further oxidation.

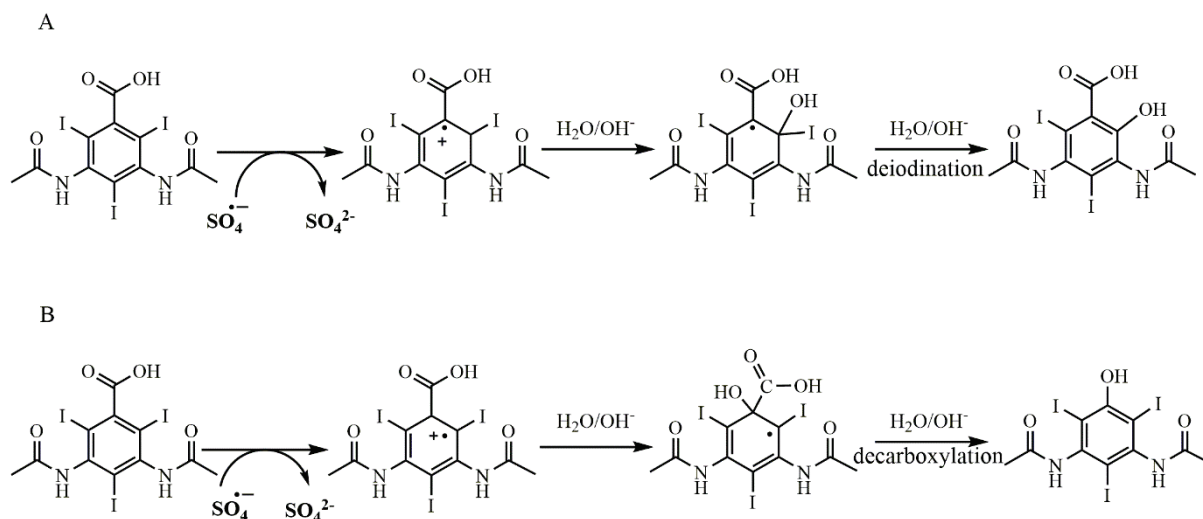


Figure 4.10. Proposed oxidation mechanisms of deiodination (A) and decarboxylation (B).

Moreover, the product $m/z = 573$ in ES^+ was also characterized, corresponding to the loss of 42 mass units from the parent chemical, which was labeled as the aniline product after the cleavage of the side chain.

The UV-Vis spectrum change of DTZ solution in the course of the oxidation was also recorded (Figure 4.4). As can be seen, DTZ does not absorb radiations > 350 nm. Yet, the absorbance increased during the reaction between 300 and 500 nm, indicating the formation of highly conjugated molecules. The absorbance reached a maximum after around 60 min of reaction, afterwards, it begun to decrease. Even though PS is still present in the solution, the evolution of the reactional mixture could be at least in part attributed to the absorption of the photoproducts absorbing above 350 nm. This absorption can potentially induce the phototransformation of long-wavelength absorbing photoproducts that visibly disappear in

Figure 4.6, but might also induce or sensitized the degradation of other photoproducts. Thus, the reaction of DTZ with sulfate radical might be the initial step of the total reaction, and the generation of solar light-absorbing compounds being the driven force for an extended photochemical degradation. For instance, the transformation of hydroquinone product ($m/z=477$) to the quinone product ($m/z=475$) seems more like a photodegradation pathway than a oxidation process by sulfate radical.

4.1.4 Impacts of natural water constituents.

DOM, chloride (Cl^-) and bicarbonate (HCO_3^-) are ubiquitous natural water constituents. The high redox potentials of $\text{SO}_4^{\cdot-}$ ($E^0 \sim 2.6 \text{ eV}$) and $\cdot\text{OH}$ ($E^0 \sim 2.7 \text{ eV}$) make them very reactive to destroy organic contaminants as well as the various constituents in natural waters, the competing side reactions with water constituents other than the target contaminants could also lead to the consumption of these two radicals, resulting in an unpredictable consequence on the oxidation efficiency. Investigating the impacts of these natural water constituents on target compound will help to understand its degradation in natural waters by AOPs.

I) Effect of DOM.

The simulated sunlight activated PS induced DTZ degradation was investigated in the presence of SRFA, a reference DOM used in aquatic photochemistry, results are illustrated in Figure 4.11. As seen, the degradation of DTZ was almost drastically inhibited by the addition of SRFA, and the oxidation efficiency was still reduced by an increase in SRFA concentration, indicating a concentration-dependent detrimental effect of SRFA on DTZ degradation. The inhibiting effect of DOM on sulfate radical-based oxidation had also been reported in previous studies [30, 50]. DOM is known to be a sink of $\cdot\text{OH}$ and $\text{SO}_4^{\cdot-}$ due to some functional groups, which were prone to react with these two radicals [50-52]. Thus, the inhibiting effect could be explained by the competitive scavenging of these two radicals by

DOM. Another possibility is the light screening effect of DOM, which could strongly weaken the radiant flux necessary for persulfate degradation.

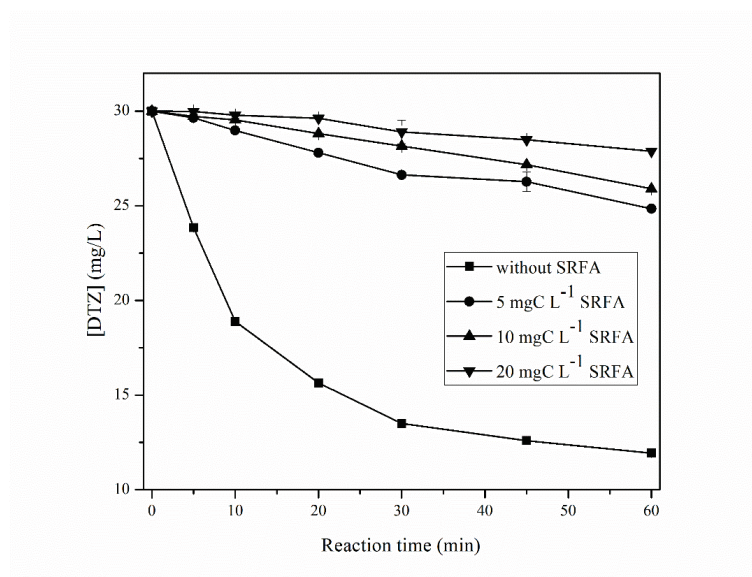
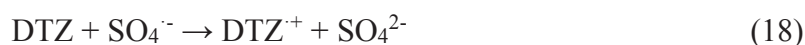


Figure 4.11. Decomposition of DTZ by simulated sunlight activated PS in the presence of SRFA. ($[\text{DTZ}]_0 = 30 \text{ mg L}^{-1}$, $[\text{PS}]_0 = 12 \text{ mM}$, initial pH = 6.5, reaction time = 60 min).

In addition, the second-order reaction rate constant of SRFA with $\cdot\text{OH}$ was reported as $2.7 \times 10^4 \text{ L mgC}^{-1} \text{ s}^{-1}$ [53], which is comparable to those observed for DOM in natural water samples (the average value was $2.5 \times 10^4 \text{ L mgC}^{-1} \text{ s}^{-1}$ [54]). On the other hand, the second-order reaction rate constant of SRFA with $\text{SO}_4^{\cdot-}$ was reported as $6.8 \times 10^3 \text{ L mgC}^{-1} \text{ s}^{-1}$ [30]. The lower reactivity of SRFA towards $\text{SO}_4^{\cdot-}$ compared with $\cdot\text{OH}$ was explained by the slow H-abstraction reactions by $\text{SO}_4^{\cdot-}$ [30]. Consequently, in the presence of DOM, DTZ could be degraded more efficiently by $\text{SO}_4^{\cdot-}$ than by $\cdot\text{OH}$.

DOM has been reported to be able to quench the cation radicals of some organic contaminants, such as amino acids, anilines and sulfonamide compounds [55, 56]. In the same way, with an aniline structure, cation radical DTZ^+ , could be reduced by DOM according Eq 18 and 19.





Thus, DOM could inhibit the oxidation of DTZ by UV/PS via 3 different mechanisms, including scavenging sulfate radical, light screening effect, and reduction of the intermediates. Among them the light screening effect was dominant, which made the decrease of removal efficiency of DTZ not proportional to the concentrations of SRFA.

II) Effect of Chloride.

Chloride ion might play a complex role in $\text{SO}_4^{\cdot-}$ based oxidation process due to the scavenging of $\text{SO}_4^{\cdot-}$ and $\cdot\text{OH}$ to generate less reactive chlorine species such as $\text{Cl}\cdot$, $\text{ClOH}^{\cdot-}$, and $\text{Cl}_2^{\cdot-}$ [29,57,58]. As shown in Figure 4.12, the effect of chloride ions on the degradation of DTZ at chloride concentrations ranging from 0 to 100 mM was very poor. However, when 500 mM Cl^- was added in, DTZ degradation was inhibited.

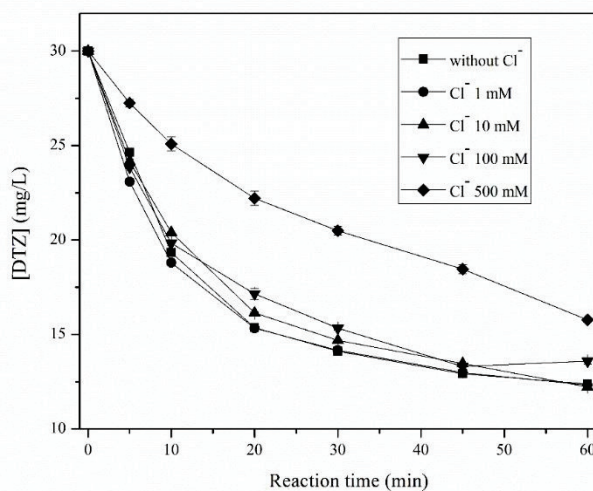
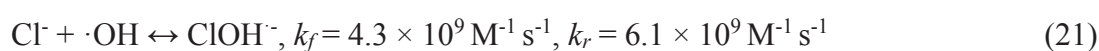


Figure 4.12. Decomposition of DTZ by simulated sunlight activated PS in the presence of chloride. ($[\text{DTZ}]_0 = 30 \text{ mg L}^{-1}$, $[\text{PS}]_0 = 12 \text{ mM}$, initial pH = 6.5, reaction time = 60 min).

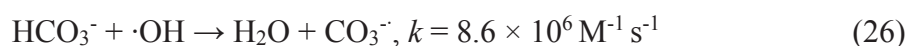
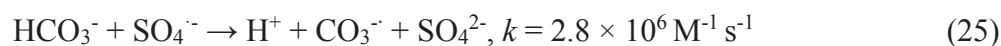
Eq 20 and 21 show the possible sinks for $\text{SO}_4^{\cdot-}$ and $\cdot\text{OH}$, although the reaction rate of $\text{SO}_4^{\cdot-}$ and $\cdot\text{OH}$ are very high, there are also fast backward reactions. At low chloride concentration

(1-100 mM), the scavenging effect of $\text{SO}_4^{\cdot-}$ by Cl^- was weak, mainly due to the backward reaction. However, high concentration of Cl^- (e.g., > 300 mM) could favour the forward reaction of Eq 20, leading to the consumption of sulfate radicals [56]. Thus, the inhibiting effect at 500 mM chloride concentration could be attributed to the scavenging of sulfate radicals by Cl^- to generate the less reactive species. The scavenging of $\text{SO}_4^{\cdot-}$ by Cl^- has already been studied by our laboratory, $\text{Cl}_2^{\cdot-}$ was found to be the main secondary radical [60].



III) Effect of Bicarbonate.

The impact of bicarbonate (concentration ranging from 0 to 40 mM) was also investigated in the present study at pH 8.2 (corresponding to 98% in the form HCO_3^-), and the results are displayed in Figure 4.13. The presence of HCO_3^- induced promoting effect on simulated sunlight activated PS oxidation of DTZ, while the continuous increase of bicarbonate concentration did not lead to a rising trend of DTZ degradation efficiency. This result was unexpected and interesting, since bicarbonate generally played a negative role in AOPs due to the quenching ability of $\text{SO}_4^{\cdot-}$ and $\cdot\text{OH}$ to form less reactive carbonate radicals ($\text{HCO}_3^{\cdot-}$ and $\text{CO}_3^{\cdot-}$) [57]. Actually $\text{CO}_3^{\cdot-}$ could react with electron-rich compounds such as phenols and anilines at a fairly high rate [59].



In this study, the promoting effect of bicarbonate might be explained by the reaction between carbonate radical and DTZ. The second order rate constant of this reaction was detected as $5.4 \times 10^7 \text{ M}^{-1} \text{ s}^{-1}$, which was less than that with $\text{SO}_4^{\cdot-}$ and $\cdot\text{OH}$. Since the concentration of bicarbonate was higher and $\text{CO}_3^{\cdot-}$ less reactive, a higher steady-state concentration of $\text{CO}_3^{\cdot-}$ was expected [44]. This counterbalanced the decrease level of $\text{SO}_4^{\cdot-}$ and $\cdot\text{OH}$ due to carbonate scavenging and manifested a promoting effect on DTZ oxidation.

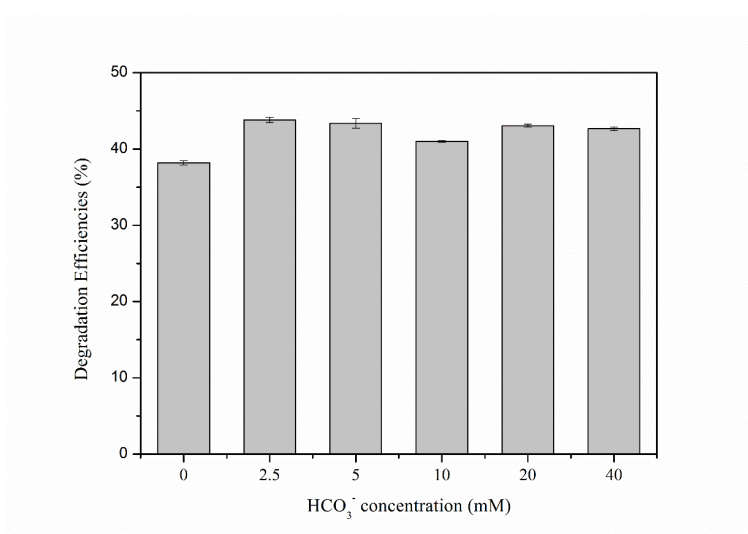


Figure .13. Degradation efficiencies of DTZ by simulated sunlight activated PS in the presence of bicarbonate. ([DTZ]₀ =30 mg L⁻¹, [PS]₀ = 12 mM, pH = 8.2, reaction time = 60 min, 10 mM Na₂HPO₄ and NaH₂PO₄ solutions were used to buffer the solutions).

4.2 Conclusions.

The present work shows that simulated sunlight could activate persulfate to produce $\text{SO}_4^{\cdot-}$ and induce the effective degradation of DTZ across a wide range of pH conditions (i.e. 4.5 to 8.5). Photo-activated PS was found to be more efficient as oxidant than H_2O_2 . Sulfate radicals ($\text{SO}_4^{\cdot-}$) was found to be the dominant reactive species in the oxidation process, while, $\cdot\text{OH}$, was of less importance. The degradation was enhanced by the increasing of PS levels. The oxidation pathways included deiodination-hydroxylation, decarboxylation- hydroxylation and

side chain cleavage. The initial step of DTZ degradation is the attack of $\text{SO}_4^{\bullet-}$, while the light-absorbing intermediates generated could take over. These observations highlight the formation of light-absorbing intermediate products and their involvement in the fate of ICMs in AOPs process.

In addition, DOM showed a detrimental effect on DTZ degradation while, a slight increase of DTZ decomposition was obtained in the presence of bicarbonate. Moreover, high concentration chloride inhibited the removal of DTZ. Our findings have potential environmental implications. For example, sulfate radical could react with naturally occurring constituents, such as bicarbonate and chloride and dissolved organic matter to form other types of reactive species. DOM is known as a sink of $\cdot\text{OH}$ and $\text{SO}_4^{\bullet-}$, however, $\cdot\text{OH}$ and $\text{SO}_4^{\bullet-}$ differ considerably in their reaction rates with DOM, $\cdot\text{OH}$ reacts more quickly with DOM than $\text{SO}_4^{\bullet-}$. Thus, in natural waters (contained DOM), AOPs based on sulfate radicals seems more efficient than those based on hydroxyl radicals. However, this depends on the structure of target substrates. DOM could reduce the cation radicals of some contaminants to inhibit the oxidation, like anilines. Further studies should better consider the role of secondary reactive species (including light-absorbing intermediates) and the influence of naturally occurring constituents in natural waters.

4.3. References.

- [1] K. Kümmerer, Antibiotics in the aquatic environment—a review—part I, *Chemosphere* 75 (2009) 417-434.
- [2] T. Heberer, Occurrence, fate, and removal of pharmaceutical residues in the aquatic environment: a review of recent research data, *Toxicol. Lett.* 131 (2002) 5-17.
- [3] C.G. Daughton, T.A. Ternes, Pharmaceuticals and personal care products in the environment: agents of subtle change? *Environ. Health Perspect.* 107 (1999) 907.

- [4] T.A. Ternes, A. Joss, H. Siegrist, Peer reviewed: scrutinizing pharmaceuticals and personal care products in wastewater treatment, *Environ. Sci. Technol.* 38 (2004) 392A-399A.
- [5] T.A. Ternes, R. Hirsch, Occurrence and behavior of X-ray contrast media in sewage facilities and the aquatic environment, *Environ. Sci. Technol.* 34 (2000) 2741-2748.
- [6] E. Mohle, C. Kempter, A. Kern, J. Metzger, Examination of the degradation of drugs in municipal sewage plants using liquid chromatography-electrospray mass spectrometry, *Acta Hydroch. Hydrob.* 27 (1999) 430-436.
- [7] A.J. Watkinson, E.J. Murby, D.W. Kolpin, S.D. Costanzo, The occurrence of antibiotics in an urban watershed: From wastewater to drinking water, *Sci. Total Environ.* 407 (2009) 2711-2723.
- [8] S. Ding, J. Niu, Y. Bao, L. Hu, Evidence of superoxide radical contribution to demineralization of sulfamethoxazole by visible-light-driven Bi₂O₃/Bi₂O₂CO₃/Sr₆Bi₂O₉ photocatalyst, *J. Hazard. Mater.* 262 (2013) 812-818.
- [9] M. Klavarioti, D. Mantzavinos, D. Kassinos, Removal of residual pharmaceuticals from aqueous systems by advanced oxidation processes, *Environ. Int.* 35 (2009) 402-417.
- [10] W. Xu, G. Zhang, S. Zou, X. Li, Y.. Liu, Determination of selected antibiotics in the Victoria Harbour and the Pearl River, South China using high-performance liquid chromatography-electrospray ionization tandem mass spectrometry, *Environ. Pollut.* 145 (2007) 672-679.
- [11] M.J. García-Galán, M.S. Díaz-Cruz, D. Barceló, Occurrence of sulfonamide residues along the Ebro river basin: Removal in wastewater treatment plants and environmental impact assessment, *Environ. Int.* 37 (2011) 462-473.
- [12] S. Pérez, D. Barceló, Fate and occurrence of X-ray contrast media in the environment, *Anal. Bioanal. Chem.* 387 (2007) 1235-1246.

- [13] T. Reemtsma, M. Jekel, Organic pollutants in the water cycle: properties, occurrence, analysis and environmental relevance of polar compounds, John Wiley and Sons Ltd.2006.
- [14] F. Sacher, F.T. Lange, H.J. Brauch, I. Blankenhorn, Pharmaceuticals in groundwaters: analytical methods and results of a monitoring program in Baden-Württemberg, Germany, J. Chromatogr. A 938 (2001) 199-210.
- [15] C. Abegglen, A. Joss, C.S. McArdell, G. Fink, M.P. Schlüsener, T.A. Ternes, H. Siegrist, The fate of selected micropollutants in a single-house MBR, Water Res. 43 (2009) 2036-2046.
- [16] W. Seitz, W.H. Weber, J.-Q. Jiang, B.J. Lloyd, M. Maier, D. Maier, W. Schulz, Monitoring of iodinated X-ray contrast media in surface water, Chemosphere 64 (2006) 1318-1324.
- [17] A. Putschew, S. Wischnack, M. Jekel, Occurrence of triiodinated X-ray contrast agents in the aquatic environment, Sci. Total Environ. 255 (2000) 129-134.
- [18] K. Kümmerer, T. Erbe, S. Gartiser, L. Brinker, AOX—Emissions from hospitals into municipal waste water, Chemosphere 36 (1998) 2437-2445.
- [19] H.D. Humes, D.A. Hunt, M.D. White, Direct toxic effect of the radiocontrast agent diatrizoate on renal proximal tubule cells, Am. J. Physiol-Renal. 252 (1987) F246-F255.
- [20] M.E. Gale, A.H. Robbins, R.J. Hamburger, W. Widrich, Renal toxicity of contrast agents: iopamidol, iothalamate, and diatrizoate, Am. J. Roentgenol. 142 (1984) 333-335.
- [21] K.C. Huang, R.A. Couttenye, G.E. Hoag, Kinetics of heat-assisted persulfate oxidation of methyl tert-butyl ether (MTBE), Chemosphere 49 (2002) 413-420.
- [22] M. Ahmad, A.L. Teel, R.J. Watts, Persulfate activation by subsurface minerals, J. Contam. Hydrol. 115 (2010) 34-45.
- [23] L. Zhou, W. Zheng, Y. Ji, J. Zhang, C. Zeng, Y. Zhang, Q. Wang, X. Yang, Ferrous-activated persulfate oxidation of arsenic (III) and diuron in aquatic system, J. Hazard. Mater. 263 (2013) 422-430

- [24] O.S. Furman, A.L. Teel, R.J. Watts, Mechanism of base activation of persulfate, *Environ. Sci. Technol.* 44 (2010) 6423-6428.
- [25] C.C. Lin, L.T. Lee, L.J. Hsu, Performance of UV/S₂O₈²⁻ process in degrading polyvinyl alcohol in aqueous solutions, *J. Photoch. Photobio.A.* 252 (2013) 1-7.
- [26] Y. Wu, A. Bianco, M. Brigante, W. Dong, P. de Sainte-Claire, K. Hanna, G. Mailhot, Sulfate Radical Photogeneration Using Fe-EDDS: Influence of Critical Parameters and Naturally Occurring Scavengers, *Environ. Sci. Technol.* 49 (2015) 14343-14349.
- [27] J. Lu, J. Wu, Y. Ji, D. Kong, Transformation of bromide in thermo activated persulfate oxidation processes, *Water Res.* 78 (2015) 1-8.
- [28] P. Neta, R.E. Huie, A.B. Ross, Rate constants for reactions of inorganic radicals in aqueous solution, *J. Phys. Chem. Ref. Data.* 17 (1988) 1027-1284.
- [29] R.E. Huie, C.L. Clifton, P. Neta, Electron transfer reaction rates and equilibria of the carbonate and sulfate radical anions, *Radiat. Phys. Chem.* 38 (1991) 477-481.
- [30] H.V. Lutze, S. Bircher, I. Rapp, N. Kerlin, R. Bakkour, M. Geisler, C. von Sonntag, T.C. Schmidt, Degradation of Chlorotriazine Pesticides by Sulfate Radicals and the Influence of Organic Matter, *Environ. Sci. Technol.* 49 (2015) 1673-1680.
- [31] Y. Ji, C. Dong, D. Kong, J. Lu, New insights into atrazine degradation by cobalt catalyzed peroxymonosulfate oxidation: Kinetics, reaction products and transformation mechanisms, *J. Hazard. Mater.* 285 (2015) 491-500.
- [32] M.M. Huber, S. Canonica, G.-Y. Park, U. Von Gunten, Oxidation of pharmaceuticals during ozonation and advanced oxidation processes, *Environ. Sci. Technol.* 37 (2003) 1016-1024.
- [33] F.J. Real, F.J. Benitez, J.L. Acero, J.J. Sagasti, F. Casas, Kinetics of the chemical oxidation of the pharmaceuticals primidone, ketoprofen, and diatrizoate in ultrapure and natural waters, *Ind. Eng. Chem. Res.* 48 (2009) 3380-3388.

- [34] T.E. Doll, F.H. Frimmel, Kinetic study of photocatalytic degradation of carbamazepine, clofibric acid, iomeprol and iopromide assisted by different TiO₂ materials—determination of intermediates and reaction pathways, *Water Res.* 38 (2004) 955-964.
- [35] W. Kalsch, Biodegradation of the iodinated X-ray contrast media diatrizoate and iopromide, *Sci. Total Environ.* 225 (1999) 143-153.
- [36] A. Haiß, K. Kümmerer, Biodegradability of the X-ray contrast compound diatrizoic acid, identification of aerobic degradation products and effects against sewage sludge microorganisms, *Chemosphere* 62 (2006) 294-302.
- [37] I. Velo-Gala, J.J. López-Peñalver, M. Sánchez-Polo, J. Rivera-Utrilla, Comparative study of oxidative degradation of sodium diatrizoate in aqueous solution by H₂O₂/Fe²⁺, H₂O₂/Fe³⁺, Fe(VI) and UV, H₂O₂/UV, K₂S₂O₈/UV, *Chem. Eng. J.* 241 (2014) 504-512.
- [38] M.N. Sugihara, D. Moeller, T. Paul, T.J. Strathmann, TiO₂-photocatalyzed transformation of the recalcitrant X-ray contrast agent diatrizoate, *Appl. Catal. B-Environ.* 129 (2013) 114-122.
- [39] J. Jeong, J. Jung, W.J. Cooper, W. Song, Degradation mechanisms and kinetic studies for the treatment of X-ray contrast media compounds by advanced oxidation/reduction processes, *Water Res.* 44 (2010) 4391-4398.
- [40] Y. Ji, Y. Fan, K. Liu, D. Kong, J. Lu, Thermo activated persulfate oxidation of antibiotic sulfamethoxazole and structurally related compounds, *Water Res.* 87 (2015) 1-9
- [41] C. Liang, Z.-S. Wang, C.J. Bruell, Influence of pH on persulfate oxidation of TCE at ambient temperatures, *Chemosphere* 66 (2007) 106-113.
- [42] G.D. Fang, D.D. Dionysiou, D.M. Zhou, Y. Wang, X.D. Zhu, J.X. Fan, L. Cang, Y.J. Wang, Transformation of polychlorinated biphenyls by persulfate at ambient temperature, *Chemosphere* 90 (2013) 1573-1580

- [43] M. Quintiliani, P. Betto, J. Davies, M. Ebert, Radiation studies of iodinated benzoic acids, *Radiat. Biolol. Chem.* 1979.
- [44] R. Zhang, P. Sun, T.H. Boyer, L. Zhao, C.H. Huang, Degradation of Pharmaceuticals and Metabolite in Synthetic Human Urine by UV, UV/H₂O₂, and UV/PDS, *Environ. Sci. Technol.* 49 (2015) 3056-3066.
- [45] H. Hori, A. Yamamoto, E. Hayakawa, S. Taniyasu, N. Yamashita, S. Kutsuna, H. Kiatagawa, R. Arakawa, Efficient decomposition of environmentally persistent perfluorocarboxylic acids by use of persulfate as a photochemical oxidant, *Environ. Sci. Technol.* 39 (2005) 2383-2388.
- [46] D. Salari, A. Niaei, S. Aber, M.H. Rasoulifard, The photooxidative destruction of CI Basic Yellow 2 using UV/S₂O₈²⁻ process in a rectangular continuous photoreactor, *J. Hazard. Mater.* 166 (2009) 61-66.
- [47] Y. Gao, N. Gao, Y. Deng, Y. Yang, Y. Ma, Ultraviolet (UV) light-activated persulfate oxidation of sulfamethazine in water, *Chem. Eng. J.* 195 (2012) 248-253.
- [48] G.P. Anipsitakis, D.D. Dionysiou, Radical generation by the interaction of transition metals with common oxidants, *Environ. Sci. Technol.* 38 (2004) 3705-3712
- [49] M.G. Antoniou, A. Armah, D.D. Dionysiou, Degradation of microcystin-LR using sulfate radicals generated through photolysis, thermolysis and e⁻ transfer mechanisms, *Appl. Catal. B-Environ.* 96 (2010) 290-298.
- [50] Y.H. Guan, J. Ma, Y.M. Ren, Y.L. Liu, J.Y. Xiao, L. Lin, C. Zhang, Efficient degradation of atrazine by magnetic porous copper ferrite catalyzed peroxymonosulfate oxidation via the formation of hydroxyl and sulfate radicals, *Water Res.* 47 (2013) 5431-5438.
- [51] J.J. Pignatello, E. Oliveros, A. MacKay, Advanced oxidation processes for organic contaminant destruction based on the Fenton reaction and related chemistry, *Crit. Rev. Env. Sci. Tec.* 36 (2006) 1-84.

- [52] M. Nie, Y. Yang, Z. Zhang, C. Yan, X. Wang, H. Li, W. Dong, Degradation of chloramphenicol by thermally activated persulfate in aqueous solution, *Chem. Eng. J.* 246 (2014) 373-382.
- [53] J. Goldstone, M. Pullin, S. Bertilsson, B. Voelker, Reactions of hydroxyl radical with humic substances: Bleaching, mineralization, and production of bioavailable carbon substrates, *Environ. Sci. Technol.* 36 (2002) 364-372.
- [54] R.P. Schwarzenbach, P.M. Gschwend, D.M. Imboden, *Environmental organic chemistry*, John Wiley and Sons Ltd. 2005.
- [55] E.M.L. Janssen, P.R. Erickson, K. McNeill, Dual roles of dissolved organic matter as sensitizer and quencher in the photooxidation of tryptophan, *Environ. Sci. Technol.* 48 (2014) 4916-4924.
- [56] J. Wenk, S. Canonica, Phenolic antioxidants inhibit the triplet-induced transformation of anilines and sulfonamide antibiotics in aqueous solution, *Environ. Sci. Technol.* 46 (2012) 5455-5462.
- [57] Y. Yang, J.J. Pignatello, J. Ma, W.A. Mitch, Comparison of halide impacts on the efficiency of contaminant degradation by sulfate and hydroxyl radical-based advanced oxidation processes (AOPs), *Environ. Sci. Technol.* 48 (2014) 2344-2351.
- [58] C. Liang, Z.S. Wang, N. Mohanty, Influences of carbonate and chloride ions on persulfate oxidation of trichloroethylene at 20 °C, *Sci. Total Environ.* 370 (2006) 271-277.
- [59] J. Huang, S.A. Mabury, A new method for measuring carbonate radical reactivity toward pesticides, *Environ. Toxicol. Chem.* 19 (2000) 1501-1507.
- [60] C. George, J-M. Chovelon, A laser flash photolysis study of the decay of SO₄⁻ and Cl₂⁻ radical anions in the presence of Cl⁻ in aqueous solutions, *Chemosphere* 47 (2002) 385-393.
- [61] A. Ghauch, A.M. Tuqan, N. Kibbi, S. Geryes, Methylene blue discoloration by heated persulfate in aqueous solution, *Chem. Eng. J.* 213 (2012) 259-271.

[62] Y. Guo, J. Zhou, X. Lou, R. Liu, D. Xiao, C. Fang, Z. Wang, J. Liu, Enhanced degradation of Tetrabromobisphenol A in water by a UV/base/persulfate system: Kinetics and intermediates, *Chem. Eng. J.* 254 (2014) 538-544.

Chapter V

Degradation of β_2 -adrenoceptor Agonists Salbutamol and Terbutaline by Photo-activated Persulfate

Pharmaceuticals and personal care products (PPCPs) are emerging contaminants that have drawn extensive attention recently due to their potential hazardous effect on ecological system and human beings, even at trace concentrations [1]. In the last few years, β_2 -adrenergic receptor agonists have been increasingly used for human beings as well as for livestock [2]. Salbutamol (SAL, also known as albuterol) and terbutaline (TBL) are selected as the target subjects of this study due to their widely uses. SAL is clinically the most widely used in treatment of bronchial asthma, it has been detected in several European countries, and the concentration ranges from 1.14 to 471 ng/L [3-5]. TBL is considered as one of the major feed additive medicines to increase the proportion of lean meat of livestock [2], it is also used as many as 1 million pregnancies annually to arrest preterm labor [6]. β_2 -adrenergic receptor agonists possess a common β -phenyl- β -ethanol amine group, the structure makes them hydrophilic and not easily biodegradable [7]. Conventional sewage treatment plants are not able to degrade residues of these chemicals completely from waste streams [7], thus, developing effective treatment technology for elimination of these chemicals in waters is of great interest.

Advanced oxidation process (AOPs) based on the generation of reactive species are becoming increasingly popular as a technology for the degradation of contaminants with the final goal of wastewater decontamination [8, 9]. Among the AOPs, hydrogen peroxide (H_2O_2) and persulfate ($\text{S}_2\text{O}_8^{2-}$, PS) are among the most popular oxidants [10]. The AOPs based on PS for the remediation of contaminated soils, groundwater and sediments has received considerable attention in recent years [11, 12]. PS can be activated by UV, heat, base or transition metals to

generate sulfate radical ($\text{SO}_4^{\cdot-}$), a strong one-electron oxidant ($E^0 \approx 2.6 \text{ V}$)[13]. $\text{SO}_4^{\cdot-}$ is capable of oxidizing a large number of contaminants such as polychlorinated biphenyls (PCBs), polycyclic aromatic hydrocarbons (PAHs), perfluoroalkyl compounds (PFCs) and azo dyes [14-17]. Mechanisms of $\text{SO}_4^{\cdot-}$ reactions differ somewhat from those of hydroxyl radical ($\cdot\text{OH}$) reactions. $\text{SO}_4^{\cdot-}$ reacts more readily by one-electron transfer than $\cdot\text{OH}$ but slower by H-abstraction and addition [18, 19]. Additionally, $\text{SO}_4^{\cdot-}$ is less impacted by soluble microbial products and natural organic matter which are ubiquitously present in waters than $\cdot\text{OH}$ [20, 21]. Thus, $\text{SO}_4^{\cdot-}$ -based oxidation could complement the more common $\cdot\text{OH}$ -based one in AOPs technologies. $\text{SO}_4^{\cdot-}$ has been shown effective in treating pharmaceuticals in waters [22-24], many pharmaceuticals can react with $\text{SO}_4^{\cdot-}$ at comparable rates as with $\cdot\text{OH}$ [25, 26]. However, the reaction rates and pathways of $\text{SO}_4^{\cdot-}$ with numerous pharmaceuticals including SAL and TBL have not been studied.

Sulfate radical is a strong electrophile, and in the reaction with electron-rich compounds, such as phenolic compounds (ArOH), electron transfer reaction is a preferred reaction pathway[19, 27]. For electron transfer reactions in the case of ArOH, intermediate radical cations are proposed to be generated (Eq 2 and 3). They would deprotonate subsequently to form phenoxy radicals[28, 29]. Both of SAL and TBL are substituted phenols, the formation of phenoxy radicals in the reaction process as well as their transformation pathways need further investigation.



In the present study, we evaluated the efficacy of simulated sunlight activated PS processes in eliminating SAL and TBL. The main objectives of this part are (1) to identify the main oxidation products of SAL and TBL and propose the oxidation mechanism of them by the

reactive species involved in the processes; (2) to investigate the reactivity and predominant reactive species responsible for the degradation of SAL and TBL.

5.1 Results and discussion.

5.1.1 Formation and identification of transient species.

The transient absorption spectrum of the sulfate radical formed after 266 nm laser excitation of PS (44 mM) (Eq 1) shows a maximum at 450 nm (Figure 5.1A) and decay in about 100 μ s. To investigate the reaction mechanisms of SAL/TBL with the sulfate radical, LFP experiments were carried out to identify the new generated transient species involved in the oxidation processes and to measure the reaction kinetics.

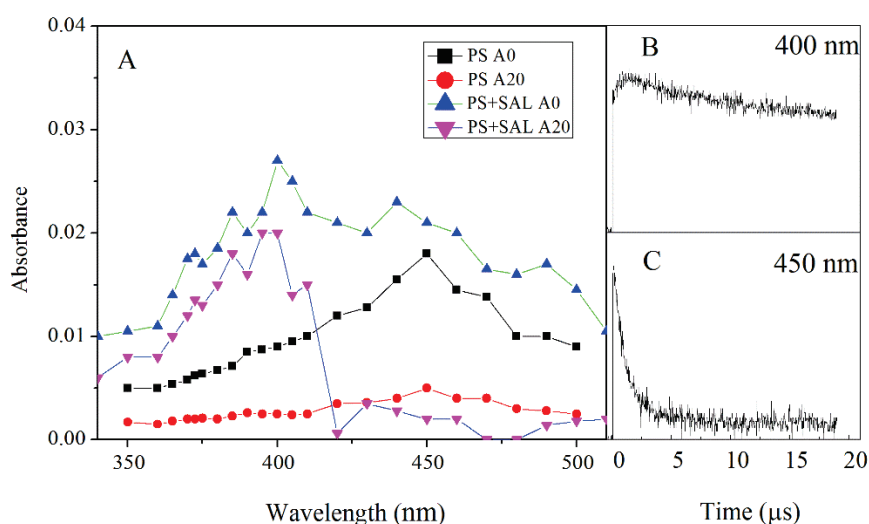


Figure 5.1. LFP of PS and SAL. A: Transient spectra measured at the pulse end (A0) and 20 μ s after (A20). B: Time profile absorbance monitored at 400 nm. C: Time profile absorbance monitored at 450 nm (266 nm, [SAL] =250 μ M, [PS] = 44 mM, pH = 6).

D) Transient signals from SAL and assignment of its absorption bands.

Figure 1 also shows the transient species generated when PS is photolyzed in the presence of SAL (250 μ M). At the end of the pulse, a broad absorption band extending from 350 to more than 500 nm is observed (Figure 5.1A). The decay of the transient absorbance between 410 to 500 nm is fully achieved within 10 μ s after the pulse (Figure 5.1C), while the absorbance between 350 and 410 nm decay much more slowly (Figure 5.1B). This indicates the presence

of at least two species. The short-lived species is assigned to the sulfate radical and the long-lived one to the phenoxyl radical generated from SAL, in accordance with the consecutive peak structure between 360 and 420 nm of the absorption spectrum [30-32]. This series of equally spaced peaks is mainly due to the vibrational progressions, the peak at the longer wavelength corresponding to the 0-0 transition. Very similar spectra were found in the irradiated solutions of SAL structural analogs 2-hydroxybenzyl alcohol (2-HBA) and 4-hydroxybenzyl alcohol (4-HBA) with PS (Figure 5.2).

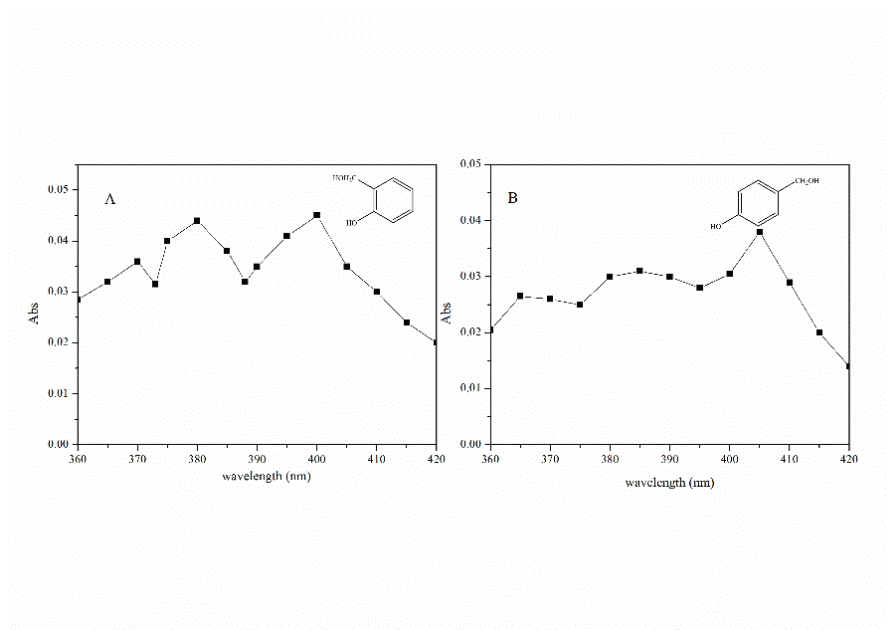


Figure 5.2. Transient absorption spectra of 2-hydroxybenzyl alcohol (2-HBA, A) and 4-hydroxybenzyl alcohol (4-HBA, B) obtained by LFP in water (266 nm, [2-HBA] = [4-HBA] = 250 μ M, [PS] = 44 mM).

II) Transient signals from TBL and assignment of its absorption bands.

LFP experiments were also carried out for TBL and its structural analogs, resorcinol and 3,5-dihydroxybenzyl alcohol (3,5-DHBA). Again, the decay of the sulfate radical at 450 nm is fast, while long-lived transients are detected between 350 and 480 nm. In the case of resorcinol (Figure 5.3A), the transient spectrum shows two bands at 405 and 425 nm (band 1 and 2) similar to those assigned to the phenoxyl radical [29, 33]. For both TBL (Figure 5.3B)

and 3,5-DHBA (Figure 5.3C) a third absorption band with a maximum at 440 nm (band 3) is observed. As this additional band shows the same decay rate as the two others (Figure 5.3D1 to 5.3D3), we concluded that it belonged to the same species. Based on the DFT calculation results, the new band was also assigned to the feature of the phenoxyl radical. As seen in Figure 5.4, the calculation indicated that the maximum absorption of resorcinol phenoxyl radical appeared at 395 nm, while it was located at 440 nm for 3,5-DHBA. Therefore, the CH₂OH substituent on the ring induces a significant red-shift of the absorption spectrum of the phenoxyl radical.

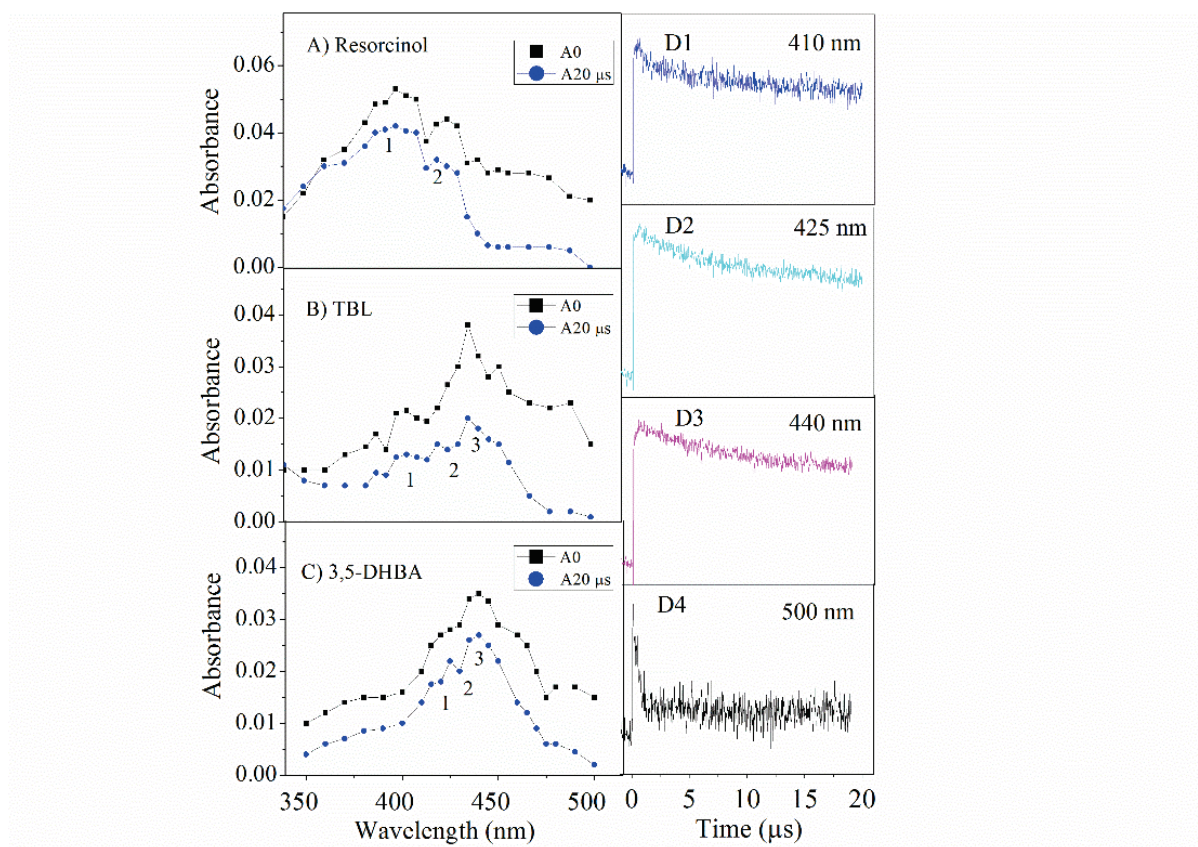


Figure 5.3. Transient absorption spectra of aqueous resorcinol (A), TBL (B) and 3,5-DHBA (C) in the presence of PS produced by LFP (the insert bands represent the phenoxyl radical absorption bands), and the time profiles (20 μs) of TBL/PS transient species at 410 nm (D1), 425 nm (D2), 440 nm (D3) and 500 nm (D4) (266 nm, [TBL] = [3,5-DHBA] = [resorcinol] = 250 μM, [PS] = 44 mM, pH = 6).

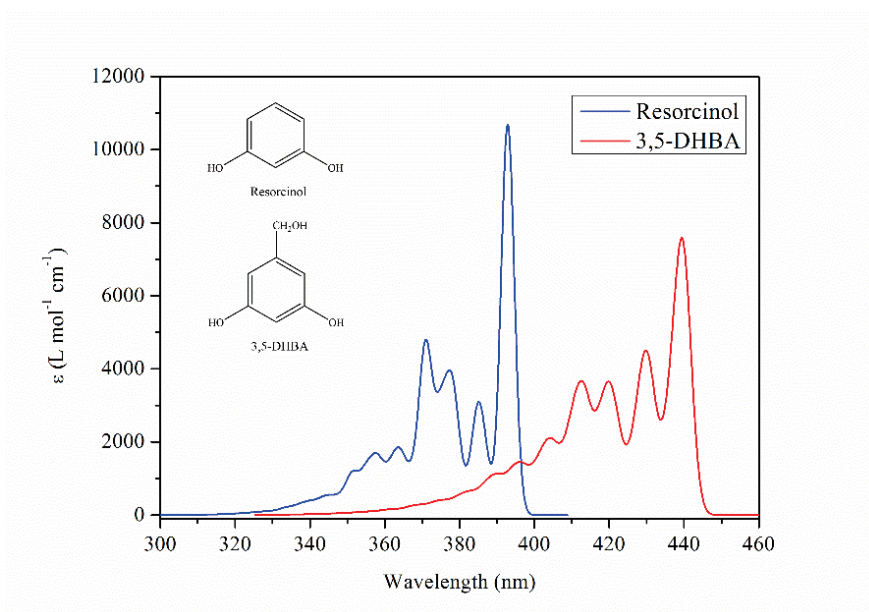


Figure 5.4. Vibrational progression of the UV-Vis absorption spectra of the resorcinol phenoxyl radical and the 3,5-DHBA phenoxyl radical obtained by DFT calculations at the B3LYP/6-31+G(d,p) level.

5.1.2 Reactivity of sulfate radical towards SAL and TBL.

To measure the rate constant of reaction between the sulfate radical and SAL, we monitored the transient absorbance decay at 450 nm for SAL concentrations ranging from 0 to 250 μM . The decay rate constant increased from 1.5×10^5 to 10^6 s^{-1} , evidencing the high reactivity of the sulfate radical towards SAL (Figure 5.5A). Using a linear regression, the second order rate constant could be estimated at $(3.7 \pm 0.3) \times 10^9 \text{ M}^{-1} \text{ s}^{-1}$ (Figure 5.5B). The same procedure was used for TBL and the reaction rate constant of $\text{SO}_4^{\cdot-}$ with TBL was estimated at $(4.2 \pm 0.3) \times 10^9 \text{ M}^{-1} \text{ s}^{-1}$. The rate constants of reaction of $\cdot\text{OH}$ with SAL and TBL were also determined by the competition kinetic methods, using nitrobenzene as the molecular probe. Values of $(5.3 \pm 0.7) \times 10^9 \text{ M}^{-1} \text{ s}^{-1}$ and $(5.9 \pm 0.8) \times 10^9 \text{ M}^{-1} \text{ s}^{-1}$, respectively, were found. For both SAL and TBL, the reaction rate constants with $\text{SO}_4^{\cdot-}$ were comparable to those with $\cdot\text{OH}$, demonstrating that photo-activated persulfate to generate $\text{SO}_4^{\cdot-}$ could be an effective way to remove SAL and TBL from water solutions.

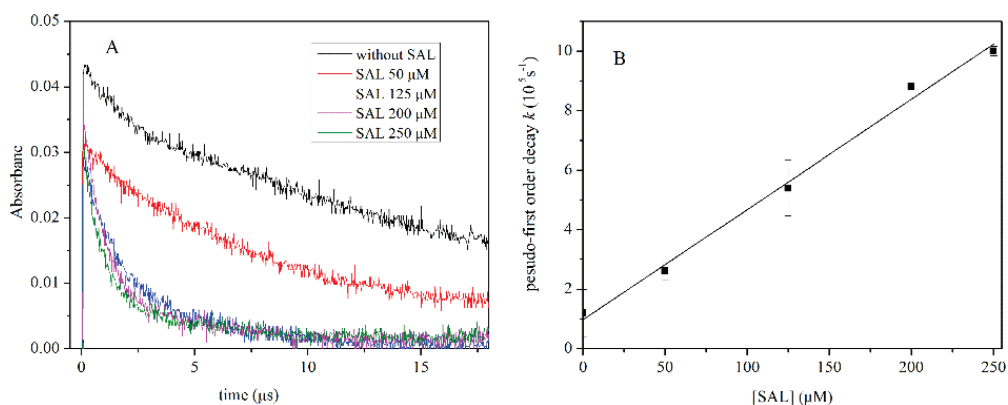


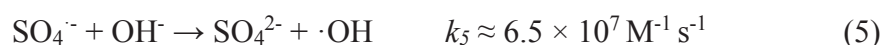
Figure 5.5. Decay of the sulfate radical monitored at 450 nm as a function of SAL concentration. Transient absorbance were obtained upon LFP (266 nm) for PS at 44 mM (A); Linear plot of the pseudo-first order decay rate constant of $\text{SO}_4^{\cdot-}$ (k , s^{-1}) versus the concentration of SAL (B).

5.1.3 UV/PS oxidation under simulated solar light.

In simulated solar light, irradiations for 2h of SAL and TBL in the presence of PS (6 mM) led to a removal of SAL and TBL of more than 94%, showing that using activated persulfate to generate $\text{SO}_4^{\cdot-}$ is an effective way to remove SAL and TBL under experimental conditions.

I) Effect of pH.

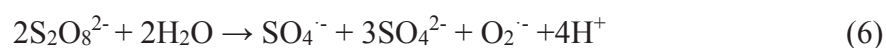
Solution pH might play a complex role in the simulated sunlight activated PS process. Indeed, it had been demonstrated that $\text{SO}_4^{\cdot-}$ is transformed to $\cdot\text{OH}$ under neutral or basic conditions (Eq 4-5) [34, 35]. In real world applications, solutions to be treated can show a very large pH range, it is therefore important to investigate the effect of solution pH. Thus, in the present work, the effect of initial pH (from 5.0 to 9.0) on the degradation efficiencies of SAL and TBL was evaluated.



The observed rate constants (k_{obs}) under various initial pH values are presented in Table 5.1. The rates of SAL and TBL degradation increased as pH declined, acidic conditions being

favorable for the oxidations. In addition, the pH values in all these experiments decreased during the reaction process, mostly due to the decomposition of persulfate and the formation of acidic by-products.

The possible explanation of the pH effect is the base-activated PS decomposition. Sulfate radical can be generated at high pH values [36] (Eq 6), however, the yield of this decomposition reaction is much lower than that at acidic conditions from photon activated PS.



Zhang et al., have determined the steady-state concentrations of $\text{SO}_4^{\cdot-}$ and $\cdot\text{OH}$ ($[\text{SO}_4^{\cdot-}]_{\text{ss}}$ and $[\cdot\text{OH}]_{\text{ss}}$) by UV/PS under different pH values [37]. Both $[\text{SO}_4^{\cdot-}]_{\text{ss}}$ and $[\cdot\text{OH}]_{\text{ss}}$ values were lower at basic (pH 9) than that at acidic condition (pH 6).

Table 5.1. Pseudo first-order degradation rate constants of SAL and TBL in different conditions ($[\text{SAL}]_0 = [\text{TBL}]_0 = 120 \mu\text{M}$, $[\text{PS}]_0 = 6 \text{ mM}$).

| | Initial | Scavenger | SAL | TBL |
|------------------|---------|--------------------|------------------------------------|------------------------------------|
| | pH | concentration (mM) | $k_{obs} (10^{-4} \text{ s}^{-1})$ | $k_{obs} (10^{-4} \text{ s}^{-1})$ |
| Scavenger effect | 7.0 | 0 | 2.18 ± 0.13 | 2.51 ± 0.08 |
| | 7.0 | EtOH 12 | 1.02 ± 0.06 | 2.14 ± 0.03 |
| | 7.0 | EtOH 120 | 0.33 ± 0.02 | 0.71 ± 0.02 |
| | 7.0 | TBA 12 | 1.92 ± 0.06 | 2.27 ± 0.07 |
| | 7.0 | TBA 120 | 1.57 ± 0.05 | 2.10 ± 0.02 |
| pH effect | 5.0 | - | 2.30 ± 0.09 | 2.68 ± 0.06 |
| | 6.0 | - | 2.27 ± 0.05 | 2.61 ± 0.05 |
| | 7.0 | - | 2.18 ± 0.13 | 2.51 ± 0.08 |
| | 8.0 | - | 2.11 ± 0.09 | 2.36 ± 0.06 |
| | 9.0 | - | 1.80 ± 0.10 | 1.86 ± 0.11 |

pKa for the phenol group of SAL and TBL are 10.12 and 10.64, respectively.

II) Effect of PS dose.

The rate constants of SAL and TBL (k_{obs}) degradation under different PS concentrations are illustrated in Figure 5.6. As reported in many articles, increasing the initial PS concentration significantly enhances the degradation rates of SAL and TBL [38, 39]. This result suggests that higher PS concentrations yield higher level of reactive species by UV activation. Moreover, a linear relationship between k_{obs} and PS concentration can be clearly observed, indicating that degradation rates are closely related with the total amount of oxidants, such as $\text{SO}_4^{\cdot-}$ and $\cdot\text{OH}$ in the solution.

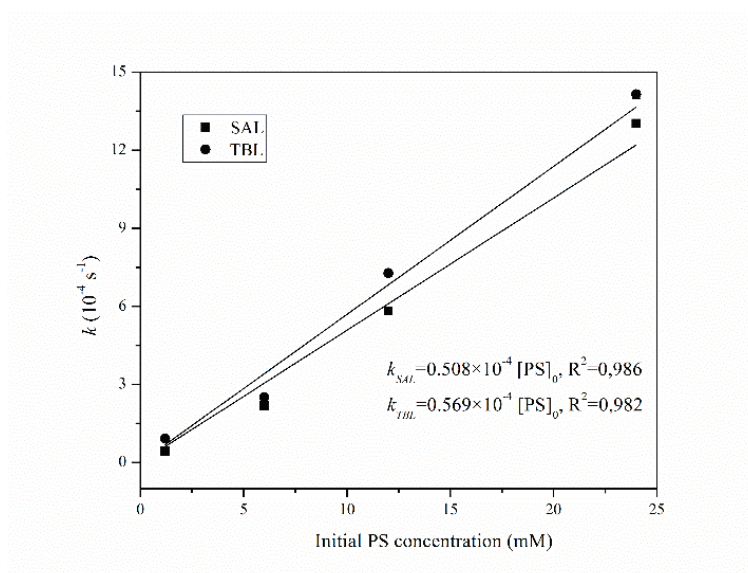
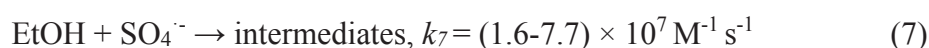
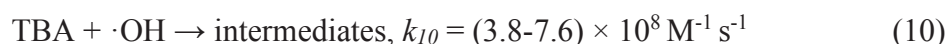
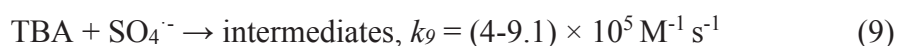
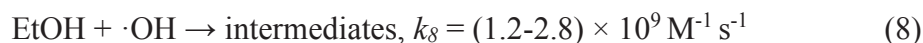


Figure 5.6. Pseudo-first order rate constants for SAL and TBL for different initial PS concentrations ($[\text{SAL}]_0 = [\text{TBL}]_0 = 120 \mu\text{M}$, initial pH = 6.5).

II) Identification of the involved reactive species.

$\text{SO}_4^{\cdot-}$ and $\cdot\text{OH}$ were considered to be the main oxidizing species during the decomposition processes involving SAL and TBL. Thus, to obtain a further insight into the reaction mechanism, experiments were conducted to identify the reactive species by using specific scavengers. Here, EtOH and TBA were used as the scavengers, as this method was intensively used in previous studies and proved to be reliable [40].





As can be seen from Eq 7 to 10, the reaction rate constant of EtOH with $\cdot\text{OH}$ is approximately 50 fold higher than that with $\text{SO}_4^{\cdot-}$, whereas the reaction of $\cdot\text{OH}$ with alcohols that do not contain α -hydrogen, like TBA, is nearly 1000 times greater than that with $\text{SO}_4^{\cdot-}$. Thus, the role played by $\cdot\text{OH}$ during the degradation could be demonstrated by adding an excessive amount of TBA in the reaction system. Then by comparing the difference between the oxidation rates with an excess in TBA or EtOH it could be possible to evaluate the $\text{SO}_4^{\cdot-}$ participation.

Table 5.1 displays the degradation rates of SAL and TBL by simulated sunlight activated PS process in the presence of EtOH and TBA, respectively. Comparing the initial rates in the absence and in the presence of scavengers allows to determine the contribution of $\text{SO}_4^{\cdot-}$ and $\cdot\text{OH}$ in the reaction. Using the quasi-steady-state approximation, one gets the generation and consuming rate of both $\text{SO}_4^{\cdot-}$ and $\cdot\text{OH}$:

$$r_{\text{SO}_4^{\cdot-}} = I_a \Phi = k_{\text{SO}_4^{\cdot-}, \text{SAL}} [\text{SO}_4^{\cdot-}] [\text{SAL}] + k_9 [\text{SO}_4^{\cdot-}] [\text{TBA}] + k_5 [\text{SO}_4^{\cdot-}] [\text{OH}^-] \quad (11)$$

$$r_{\cdot\text{OH}} = k_{\cdot\text{OH}, \text{SAL}} [\cdot\text{OH}] [\text{SAL}] + k_{10} [\cdot\text{OH}] [\text{TBA}] \quad (12)$$

Where I_a is the light intensity absorbed by PS and Φ , is the quantum yield of sulfate radical formation. Thus, the quasi-steady-state concentration of $\text{SO}_4^{\cdot-}$ and $\cdot\text{OH}$ can be written as:

$$[\text{SO}_4^{\cdot-}] = \frac{r_{\text{SO}_4^{\cdot-}}}{k_5 [\text{OH}^-] + k_{\text{SO}_4^{\cdot-}, \text{SAL}} [\text{SAL}] + k_9 [\text{TBA}]} \quad (13)$$

$$[\cdot\text{OH}] = \frac{r_{\cdot\text{OH}}}{k_{\cdot\text{OH}, \text{SAL}} [\text{SAL}] + k_{10} [\text{TBA}]} \quad (14)$$

Based on these, one gets:

$$r_{(SAL)TBA} = k_{OH,SAL}[\cdot OH][SAL] + k_{SO_4^{\cdot-},SAL}[SO_4^{\cdot-}][SAL] = \frac{k_{OH,SAL}[SAL]}{k_5[OH^-] + k_{OH,SAL}[SAL] + k_{10}[TBA]}r_{OH} + \frac{k_{SO_4^{\cdot-},SAL}[SAL]}{k_{SO_4^{\cdot-},SAL}[SAL] + k_9[TBA]}r_{SO_4^{\cdot-}} \quad (15)$$

Here we used the mean values of k_9 and k_{10} from Eq (9) and (10) to calculate the contribution of $SO_4^{\cdot-}$ and $\cdot OH$. For instance, when $[TBA]/[SAL] = 100$, $r_{(SAL)TBA}$ equals to:

$$r_{(SAL)TBA} = 0.085r_{OH} + 0.98r_{SO_4^{\cdot-}} \quad (16)$$

By comparing r_{SAL} (in the absence of TBA) with $r_{(SAL)TBA}$ ($[TBA]/[SAL] = 100$), we could calculate that approximately 10% of SAL removal was attributed to $\cdot OH$, and $SO_4^{\cdot-}$, played a dominant role during the oxidation process. Similarly, for TBL, we calculated that $\cdot OH$ only contributed to about 9% of the total oxidation which is in a good agreement with the fact that at pH 7 $SO_4^{\cdot-}$ is the main reactive species.

5.1.4 Oxidation products.

I) Oxidation products of SAL.

High resolution HPLC-MS analysis under both full scan and product ion scan mode were employed to characterize the structures of the oxidation products. In the case of SAL, four groups of oxidation products were identified in ES^+ (Table 5.2). The product with $m/z = 238.1433$ (corresponding to $[M+H]^+$) has lost 2 H compared to SAL. It was therefore assigned to 2-(*tert*-Butylamino)-1-(4-hydroxy-3-hydroxymethylphenyl) ethanone, in which the CHOH group is replaced into a C=O group. Three peaks with $m/z = 254.1382$ were also detected. They have lost 2 H atoms and gained one O atom compared to SAL. We thus concluded that these compounds are the hydroxylated ethanones for which the addition of $\cdot OH$ can take place at three different positions of aromatic ring. A product with $m/z = 376.1755$ was found. Compared to SAL, it has gained $C_7H_4O_3$. This compound is likely an adduct of the hydroxylated ethanone with the aromatic moiety of SAL constituted by the ring bearing the OH and CH_2OH substituents. Three different peaks were observed, corresponding to the

different possible isomers. In a good agreement, we detected a peak at $m/z = 132.1019$ that is assumed to be the 2-(tert-butylamino)-acetic acid, i.e., the oxidized lateral chain of SAL

II) Oxidation products of TBL.

Only two peaks at $m/z = 322.0949$ were observed in the total ion chromatogram (TIC). They correspond to the gain of SO_4 on the parent compound. The plausible structure is that given in Table 5.2, in which $-\text{OSO}_3\text{H}$ is added to the ring. This is the first time stable adducts produced by sulfate addition to the aromatic ring are detected. In most cases, such an addition occurs at the beginning of the reaction with SO_4^- , afterwards the elimination of the sulfate group takes place to form other intermediates, since sulfate is an excellent leaving group [41]. To further confirm this result, oxidation products of resorcinol and 3,5-DHBA (structurally similar to TBL) with sulfate radical were also identified. For resorcinol, two peaks at $m/z = 204.9805$ were observed from the total ion chromatogram, corresponding to the addition of 96 mass units to the parent compound at three different positions on the ring. For 3,5-DHBA, three peaks of the sulfate addition products were also observed ($m/z = 234.9916$ in negative mode). All these results indicate that SO_4^- reacted with resorcinol and related compounds, TBL and 3,5-DHBA in a similar way.

5.1.5 Mechanisms of oxidation pathways.

The analytical study reveals that the oxidation products of SAL and TBL are very different. The initial step in the UV-PS oxidation is the formation of the phenoxyl radicals. Therefore, the two phenoxyl radicals rearrange differently. For TBL, the dominant pathway is the addition of the sulfate radical on the ring (Figure 5.7A). As a *meta*-substituted phenol, the transformation of TBL into *p*-quinone-methides through an H atom abstraction driven by oxygen, for instance, is inaccessible. Consequently, the phenoxyl radical of TBL is only able to recombine with the other radicals present in the solution. The main recombination reaction is with the sulfate radical but recombination with another phenoxyl radical to form a dimer

could be also possible. Yet, such dimeric products were not detected by HPLC-MS.

Table 5.2. Proposed structure of SAL and TBL (120 μ M) degradation products in the presence of PS (12 mM) after irradiation of 60 min (in positive mode).

| RT (min) | Measured | | Theoretical | | Δ ppm | Formula of natural structure | Proposed structure |
|----------------|-----------|------|-------------|------|--------------|------------------------------|--------------------|
| | exact | mass | exact | mass | | | |
| | $[M+H]^+$ | | $[M+H]^+$ | | | | |
| 0.90 | 240.1584 | | 240.1594 | | -4.1 | $C_{13}H_{22}O_3N$ | |
| 0.72 | 132.1015 | | 132.1019 | | -2.8 | $C_6H_{14}O_2N$ | |
| 1.70 | 238.1433 | | 238.1438 | | -3.3 | $C_{13}H_{20}O_3N$ | |
| 1.17;1.60;1.77 | 254.1382 | | 254.1387 | | -2.6 | $C_{13}H_{20}O_4N$ | |
| 1.74;1.93;2.10 | 376.1748 | | 376.1755 | | -3.0 | $C_{20}H_{26}O_6N$ | |
| 0.90 | 226.1435 | | 226.1438 | | -2.7 | $C_{12}H_{20}O_3N$ | |
| 1.37;1.95 | 322.0949 | | 322.0955 | | -2.1 | $C_{12}H_{20}O_7NS$ | |

R = $CH_2NHC(CH_3)_3$

In the case of SAL, the *ortho* and *para* position of CH₂OH and CHOHR substituents with respect with the OH function makes possible the formation of a quinone-methide structure. Such quinone-methide structure could arise from an H abstraction by oxygen or SO₄⁻, and the addition of the SO₄⁻ on the ring could also take place (Figure 5.7B). However, the main detected primary photoproduct is the carbonylated compound (m/z=238) and the mechanism of the quinone-methide rearrangement into this product needs to be clarified. With this goal, we performed DFT calculations, using 2,4-bis(hydroxymethyl)-phenol as a simplified model. Three intermediates can be proposed (Figure 5), including the sulfate addition on *ortho* position (I) or *para* position (II), as well as the H atom abstraction to form the quinone-methide structure (III). The generation of species I is thermodynamically less favorable due to its relatively high energy level (-38.3 kcal mol⁻¹) with respect to II. In contrast, there is no electronic energy barrier in the entrance channel to form the sulfate additional intermediate II. However, the HPLC-MS data did not reveal the existence of such an additional product. Although there is a very high energy barrier from II→III, we expect that the excess energy is sufficient to overcome the energy barrier towards the thermodynamically favored product III (Intrinsic Reaction Coordinate calculations showed that the Transition State at -15.2 kcal/mol in Figure 5 connected II and III). Note that the proximity of the reactive groups in II (OSO₃⁻ and H in CH₂) may favor reaction II→III before thermal equilibrium is reached for II and thus benefit advantageously of the excess energy.

Then, the intermediate III moves to the final products, species IV (quinone methide) or species V (ketone, aldehyde in the simulations). In Figure 5, energies of IV and V correspond to separated products. Thermodynamically, V is more stable than IV. The transformation of IV to V has been demonstrated in the literature, this process being mediated by H₂O [41]. Including the solvation energy of SO₄⁻ would lower significantly the energies of IV and V.

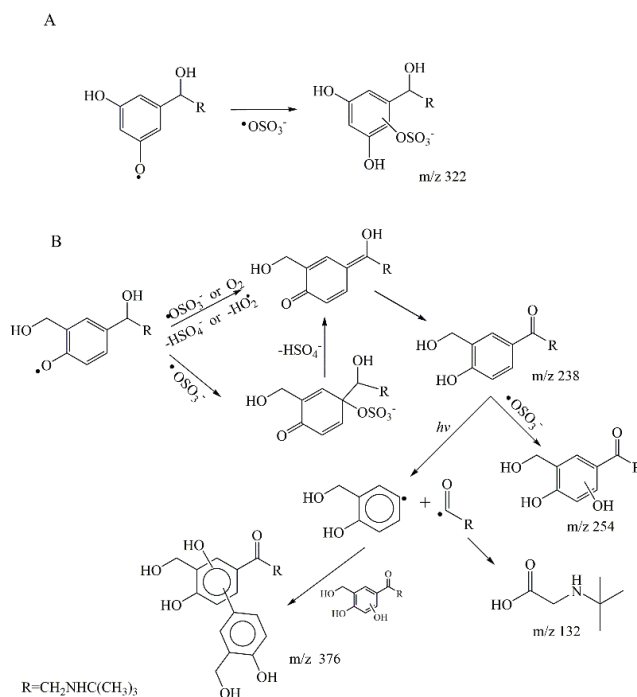


Figure 5.7. Proposed oxidation pathways of TBL (A) and SAL (B) by UV/PS process.

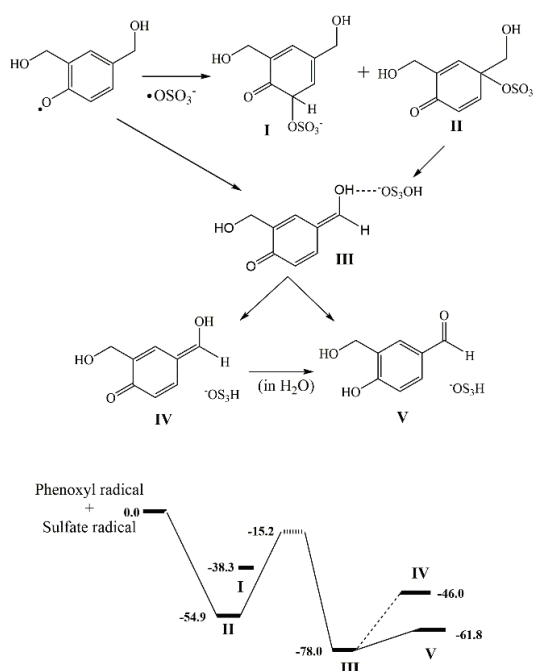


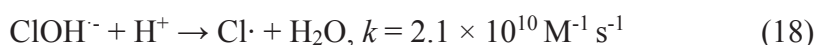
Figure 5.8. Reactions of the phenoxyl radical from SAL. Energy levels are shown in the inset (energies in kcal/mol). The reference energy level is that of the reactants. The bold and dashed lines represent local minima and transition states, respectively (energies of IV and V correspond to separated products. Including the solvation energy of $\cdot\text{OSO}_3^-$ would lower significantly the energies of IV and V).

Thus, based on LFP, HPLC-MS and DFT calculation results, the degradation mechanism of SAL by the sulfate radical shown in Figure 5.7B can be proposed. The main photoproduct deriving from the phenoxyl radical is the carbonylated product ($m/z=238$). This latter can undergo different reactions subsequently, either through attack of a sulfate radical or through photolysis. The formation of the hydroxylated product is a classic pathway of the sulfate radical attack on the phenolic compounds, which is similar to the reaction of phenol with $SO_4^{\cdot-}$, resulting in the production of catechol or hydroquinone[42]. Alternatively, direct electrophilic attack by $\cdot OH$ on the aromatic ring could also contribute to the production of the hydroxylated product. Both hydroxyl and hydroxymethylene group can act as electron donors, thus, the addition of $-OH$ can occur on the three positions remaining on the ring. Moreover, the carbonyl compound can undergo a Norrish type I reaction in which the α -carbon bond is cleaved to give acyl and phenyl radicals. This reaction is likely the result of photolysis rather than an oxidation reaction by sulfate radical. Acyl radical could in turn be oxidized to generate 2-(tert-butylamino)-acetic acid, while the phenyl radical, would react with the $-OH$ addition product (m/z 254) to produce the adduct ($m/z = 376$).

5.1.6. Effects of natural water constituents.

I) Effect of Cl⁻.

Chloride ion could react with $SO_4^{\cdot-}$ to generate new radicals and might have some effects on SAL and TBL oxidation [43-45]:



As shown in Figure 5.9, the k_{obs} of SAL and TBL were not influenced by the addition of Cl⁻ (from 0.5 mM to 0.5 M) compared to the control experiments. Eq 17 shows a possible sink for

$\text{SO}_4^{\cdot-}$ in natural waters rich in chloride ion due to the high rate constant among the reactions. The scavenging of sulfate radical by Cl^- has already been studied by our laboratory using LFP technique, and $\text{Cl}_2^{\cdot-}$ was observed as the new generated species (Eq 19) [46]. However, it was also reported that a rate constant for the reversed reaction similar to the forward rate may therefore push the reaction backward, hence giving rise to few or even no loss oxidation efficiency by sulfate radical [47].

Liang et al. had reported that when Cl^- was present at high level (e.g., $> 0.3 \text{ M}$), the oxidation of trichloroethylene by thermally activated persulfate was inhibited [48]. A possible explanation was that if the concentration of chloride ion was extremely high, the forward reaction of Eq 17 would be more important compared to the reverse one, resulting in a greater degree of consuming of sulfate radicals [48]. When excess chloride ions were present, the chain reactions might occur to regenerate chloride ions and form chlorine (Eq 19 and 20). Therefore, the overall reaction process could be described as Eq 21.

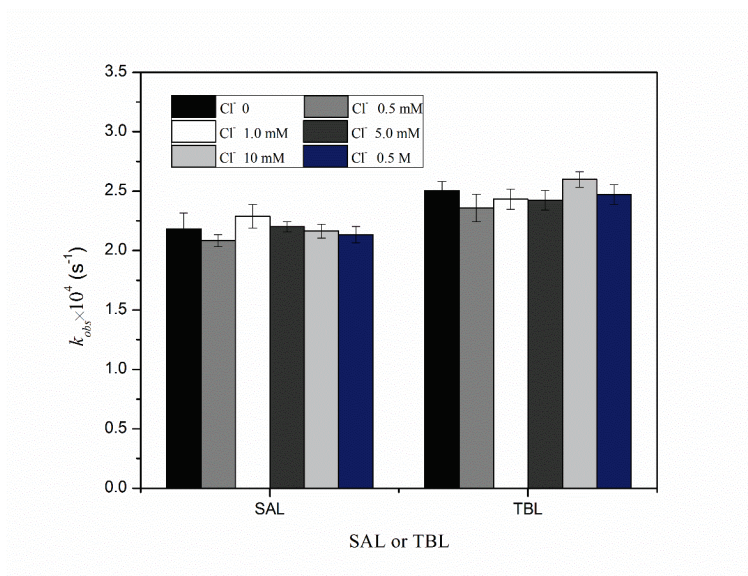
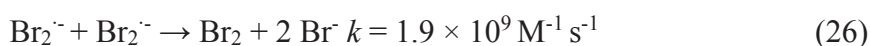
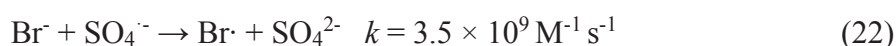


Figure 5.9. Decomposition rate constants of SAL and TBL at various chloride ion concentrations. $[\text{SAL}]_0=120 \mu\text{M}$, $[\text{TBL}]_0=120 \mu\text{M}$, $[\text{PS}]_0=6.0 \text{ mM}$, initial $\text{pH}=7.0$, $t = 90 \text{ min}$.

However, in our work, the degradation rate constants of SAL and TBL remained almost unchanged in the presence of excess Cl^- (0.5 M), suggesting that the high degree of consuming of sulfate radicals by Cl^- were not involved in the oxidation process. Moreover, since no buffer solutions were used in this part of experiments, the results here could also suggest that there was no impact of ion strength on SAL or TBL degradation by simulated sunlight activated PS process.

II) Effect of Br^- .

In sulfate radical based oxidation, bromine atoms ($\text{Br}\cdot$) could be formed from the reaction of Br^- and $\text{SO}_4^{\cdot-}$ with a rate constant of $3.5 \times 10^9 \text{ M}^{-1} \text{ s}^{-1}$ (Eq 22) [18], which is much higher than that of the reaction between Cl^- and $\text{SO}_4^{\cdot-}$ through Eq 17. Unlike Cl^- , $\text{Br}\cdot$ is unstable and can react with additional Br^- or OH^- rapidly to generate $\text{Br}_2^{\cdot-}$ and $\text{HOBr}^{\cdot-}$ (Eq 23 and 24) [49, 50]. The continuous reactions include the formation of Br_2 and HOBr (Eq 25-28), all these reactions would process at rates that are close to diffusion-control limit. Both Br_2 and $\text{Br}_2^{\cdot-}$ are belong to reactive bromine species (RBS), which are electrophilic and trends to react with electron-rich chemicals, such as phenolic compounds.



It has been demonstrated by kinetic modelling that in the presence of a trace level of Br^- , $\text{SO}_4^{\cdot-}$ could be completely scavenged [44]. In this study, different concentrations of Br^- (from 1 to 100 mM) were added in the reaction solutions for SAL and TBL degradation, as shown in

Figure 5.10. The presence of bromide was found to inhibit the SAL and TBL oxidation efficiency, the higher the Br⁻ concentration, the lower the rate constants. At bromide level of 100 mM (1000 times higher than SAL/TBL), we believed SO₄^{•-} was completely scavenged by Br⁻ rather than reacted with the target compounds. Under these circumstances, the degradation of SAL and TBL in Figure 5.10 was attributed to the reactions with new generated reactive species.

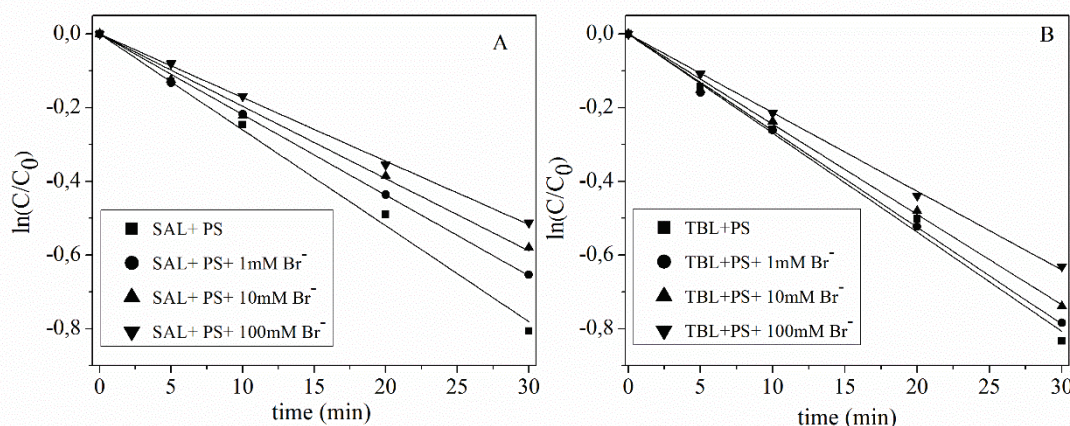


Figure 5.10. Effect of bromide on the oxidation kinetic of SAL and TBL by UV/PS process. [SAL]₀=100 μM, [TBL]₀=100 μM, [PS]₀=6.0 mM, initial pH=7.0.

For example in this study, RBS were considered as the reactive species responsible for the remove of SAL and TBL at high level of bromide, since sulfite radicals were scavenged. Br₂^{•-} is an important intermediate which can form Br₂ either by self-recombination (Eq 26) or reaction with Br[•] (Eq 27), however, in solutions containing 100 μM SAL/TBL (concentration much higher than Br₂^{•-} or Br[•]), reactions of Eq 26 and 27 were negligible due to the competition of SAL/TBL. Thus, the reactions with Br₂^{•-} were regarded as the main pathway

for the degradation of SAL and TBL in the presence of 100 mM bromide.

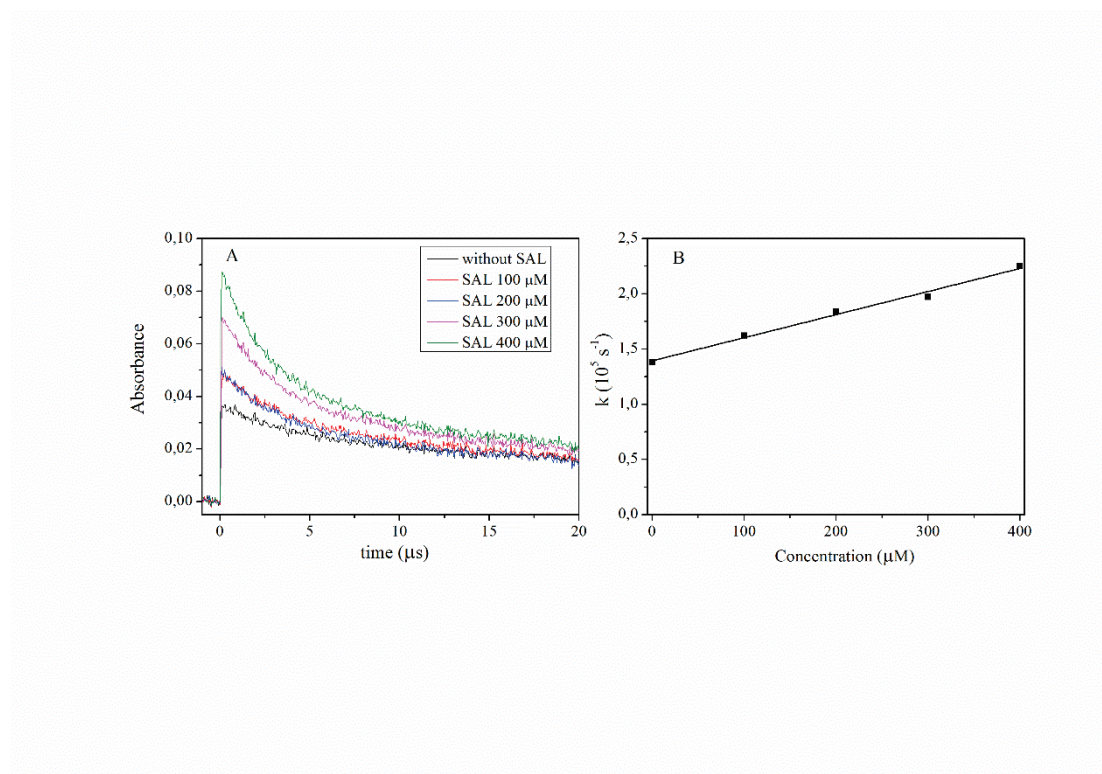


Figure 5.11. Decay of Br₂⁻ transient followed at 370 nm in the absence and presence of SAL (A); The linear relationship of the pseudo-first order decay constant of Br₂⁻ (k , s⁻¹) versus the concentration of SAL (B) ([PS] =10 mM, [Br⁻] =100 mM).

The reactivity of Br₂⁻ towards SAL and TBL were also investigated in this study by using LFP technique. Figure 5.11A shows the transient absorption spectra obtained after 266 nm laser excitation of PS (containing high amount of Br⁻) in the absence or presence of SAL. In the presence of excess Br⁻, SO₄⁻ (maximum absorption at 450 nm) was consumed quickly and a new species was observed, this new species showed maximum absorption around 370-380 nm, which was assigned to Br₂⁻ in accordance with literature [51]. In the absence of SAL, the signal of Br₂⁻ at 370 nm exhibited a decrease with a pseudo-first order constant at 1.38×10^5 s⁻¹, while after the addition of SAL, this transient decay increased to 2.25×10^5 s⁻¹, indicating that Br₂⁻ could react with SAL at a relatively high rate. Using a linear regression, the second order rate constant was estimated at $(2.1 \pm 0.1) \times 10^8$ M⁻¹ s⁻¹ (Figure 5.11B). Similarly, the

reaction rate constant of Br_2^- with TBL was estimated at $(3.9 \pm 0.2) \times 10^8 \text{ M}^{-1} \text{ s}^{-1}$. These values are much smaller than those with $\text{HO}\cdot$ or $\text{SO}_4^{\cdot-}$ (see Table 5.3), leading to the deceleration of SAL/TBL in Figure 5.10.

Table 5.3. Reaction rate constants of different reactive species with SAL and TBL ($\text{M}^{-1} \text{ s}^{-1}$).

| | $\text{SO}_4^{\cdot-}$ | $\cdot\text{OH}$ | $\text{CO}_3^{\cdot-}$ | Br_2^- |
|------------|-----------------------------|-----------------------------|-----------------------------|-----------------------------|
| SAL | $(3.7 \pm 0.3) \times 10^9$ | $(5.3 \pm 0.7) \times 10^9$ | $(4.8 \pm 0.1) \times 10^7$ | $(2.1 \pm 0.1) \times 10^8$ |
| TBL | $(4.2 \pm 0.3) \times 10^9$ | $(5.9 \pm 0.8) \times 10^9$ | $(3.2 \pm 0.2) \times 10^8$ | $(3.9 \pm 0.2) \times 10^8$ |

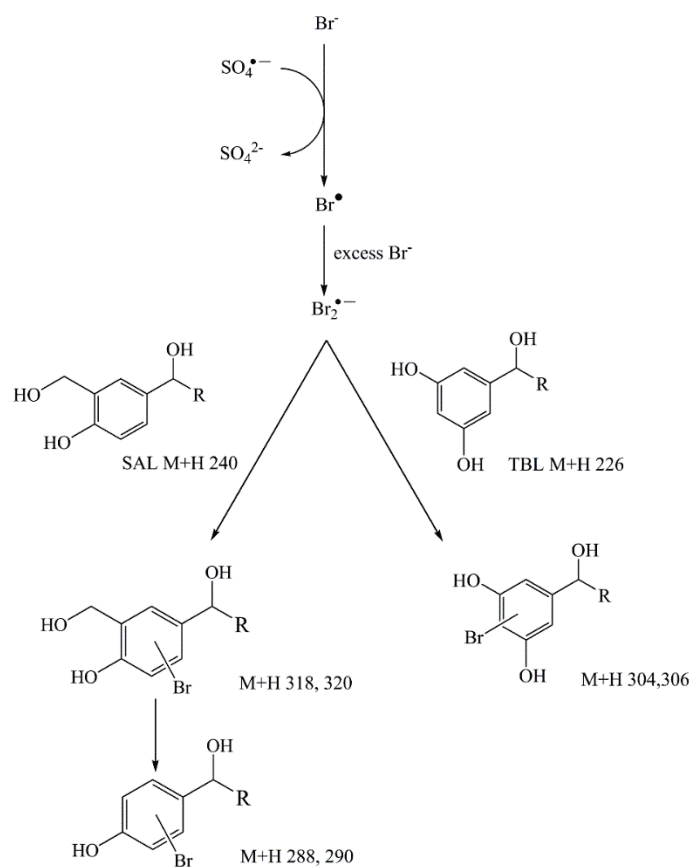
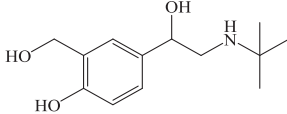
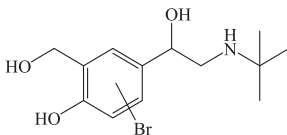
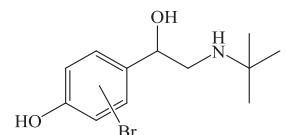
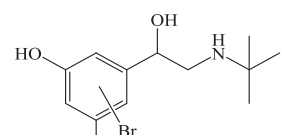


Figure 5.12. Proposed pathways of SAL and TBL in the presence of excess Br^- by UV/PS process ($[\text{SAL}]_0=120 \mu\text{M}$, $[\text{TBL}]_0=120 \mu\text{M}$, $[\text{PS}] =10 \text{ mM}$, $[\text{Br}^-] =100 \text{ mM}$). $\text{R} = \text{CH}_2\text{NH}(\text{CH})_3$.

Table 5.4. Proposed structure of SAL and TBL (120 μ M) degradation products in the presence of PS (12 mM) and excess Br⁻ (0.1 M) after irradiation of 60 min (in positive mode).

| RT (min) | Measured | Theoretical | Δ ppm | Formula of natural structure | Proposed structure | |
|-------------|----------------------------------|----------------------------------|--------------|------------------------------------|--|---|
| | exact mass [M+H] ⁺ | exact mass [M+H] ⁺ | | | | |
| SAL | 0.79 | 240.1584 | 240.1594 | -4.1 | C ₁₃ H ₂₂ O ₃ N |  |
| | 1.10 | 318.0701 | 318.0699 | -0.6 | C ₁₃ H ₂₁ O ₃ NBr |  |
| | | 320.0680 | 320.0678 | | | |
| | 1.27 | 288.0588 | 288.0594 | -2.1 | C ₁₂ H ₁₉ O ₂ NBr |  |
| | | 290.0567 | 290.0573 | | | |
| | TBL | 0.81 | 226.1435 | 226.1438 | -2.7 | C ₁₂ H ₂₀ O ₃ N |
| 1.53 | | 304.0537 | 304.0543 | -2.0 | C ₁₂ H ₁₉ O ₇ NBr |  |
| | 306.0516 | 306.0522 | | | | |

In addition, the oxidation products in Br⁻/UV/PS system were analyzed by high resolution HPLC-MS analysis under both full scan and product ion scan mode. The MS data are listed in Table 5.4, and the proposed pathways of SAL and TBL are illustrated in Figure 5.12. As seen, for SAL, the product with m/z = 318.0701 and 320.0680 was first identified as the addition product of Br atom on the aromatic ring; afterwards, another product with m/z = 288.0588 and 290.0567 was labelled as the secondary reaction product, corresponding to the loss of 30 mass units from the product mentioned above. In the case of TBL, only one product with m/z

= 304.0543 and 306.0522 was detected, which was characterized also as the bromine addition product on TBL.

As an electrophilic oxidant, Br_2^- trends to react with electron-rich chemicals, such as phenolic compounds, it would attack the aromatic ring directly and eventually generate brominated aromatic product, similar result was reported by Liu et al. on the formation of brominated phenol in cobalt catalyzed peroxymonosulfate process of phenol (in presence of Br^-) [52]. As known the brominated aromatic compounds, such as tetrabromobisphenol A (TBBPA), pentabromophenol (PBP) and polybrominated diphenyl ethers (PBDEs) show hepatotoxicity, cytotoxicity and immunotoxicity [53]. Generation of this harmful brominated products in the removal micro-pollutants underlines the potential risks of SR-AOPs in wastewaters containing high level of bromide.

III) Effect of bicarbonate.

The effect of bicarbonate on the degradation of SAL and TBL by activated PS was also investigated in the present study. In presence of (bi)carbonate ions, carbonate radicals (CO_3^-) can be generated through a reaction in which carbonate anions react with hydroxyl and/or sulfate radicals [44]. CO_3^- is a moderate oxidant with a redox potential of 1.59 V and it has been shown to react rapidly with electron-rich aromatic compounds such as aniline and phenols, primarily as an electron acceptor [54]. As shown in Figure 5.13, the degradation rate of SAL was determined as being equal to $2.2 \times 10^{-4} \text{ s}^{-1}$ without HCO_3^- , while, the addition of bicarbonate resulted in a decrease on the removal rates. Increasing bicarbonate level would decrease the oxidation rates. Similar results were also observed in the case of TBL. Degradation rate constants decreased from 2.5 to $2.0 \times 10^{-4} \text{ s}^{-1}$ with bicarbonate concentration increased from 0 to 50 mM. This result could be explained by a scavenging effect of SO_4^- by HCO_3^- to form the less reactive species, CO_3^- , which has been reported many times in the literatures [55-57].

To confirm this finding we determined the second-order rate constant of $\text{CO}_3^{\cdot-}$ with SAL and TBL, the values of $(4.8 \pm 0.1) \times 10^7$ and $(3.2 \pm 0.2) \times 10^8 \text{M}^{-1} \text{s}^{-1}$ were estimated for SAL and TBL, respectively (Table 5.3).

The difference between SAL and TBL in the presence of HCO_3^- could be explained by the different values of second-order rate constants with $\text{CO}_3^{\cdot-}$. The structural difference between SAL and TBL were the methylol with phenolic hydroxyl and the position of phenolic hydroxyl on the aromatic ring, the presence of methylol instead of phenolic hydroxyl might play a critical role. On the basis of previous study, the $-\text{OH}$ substituted benzene derivative was much more reactive towards $\text{CO}_3^{\cdot-}$ than $-\text{CH}_3$ benzene derivative [58]. In general, carbonate radical acted as a selective electrophilic reagent and the reaction could be facilitated by electron-supplying substituents, such as $-\text{OH}$ and $-\text{NH}_2$ [58].

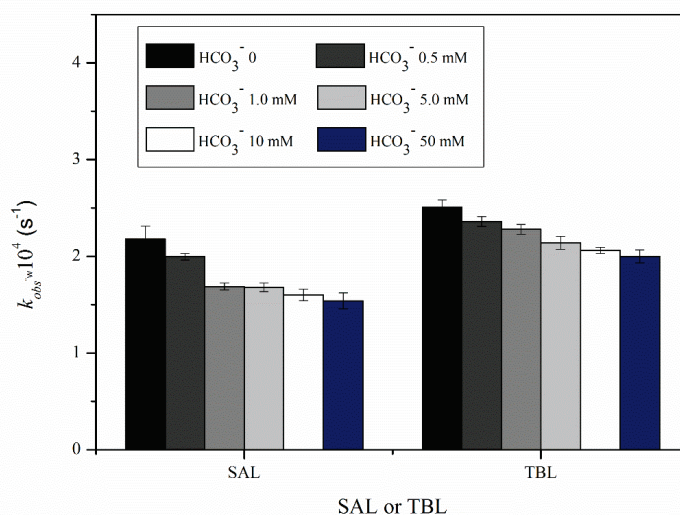
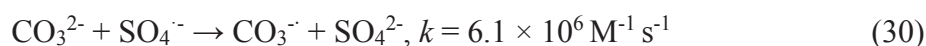
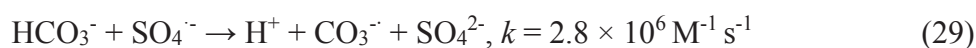


Figure 5.13. Degradation rate constants of SAL and TBL at various bicarbonate ion concentrations. $[\text{SAL}]_0=120 \mu\text{M}$, $[\text{TBL}]_0=120 \mu\text{M}$, $[\text{PS}]_0=6.0 \text{mM}$, $t = 90 \text{min}$.

IV) Effect of dissolved organic matter.

Dissolved organic matter (DOM) which is widely present in natural waters, and

environmental relevant concentration of DOM may range from 0.3 mg to 30 mg L⁻¹ [59, 60]. In this view, the simulated sunlight activated PS induced SAL and TBL degradation were investigated in the presence of SRFA, a common DOM used in aquatic photochemistry, the results are illustrated in Figure 5.14.

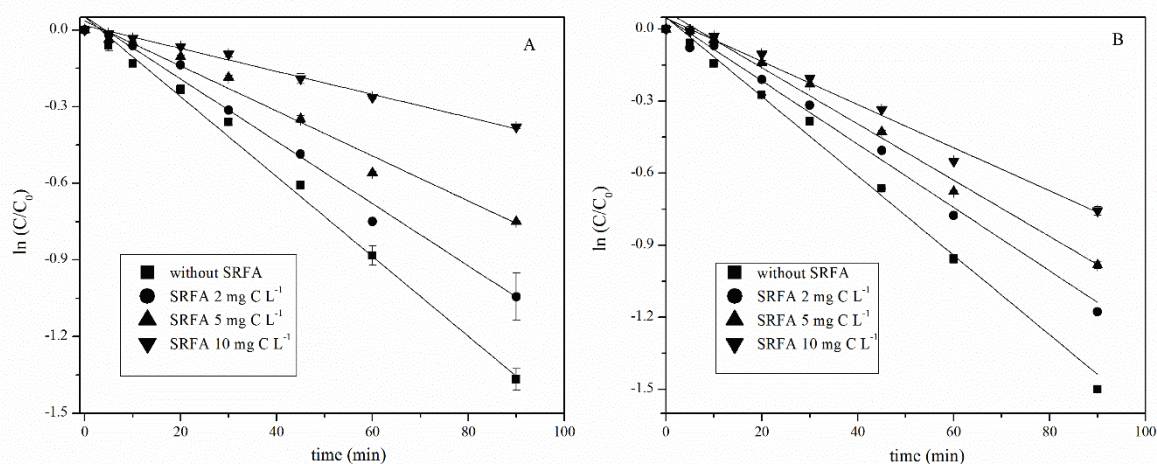
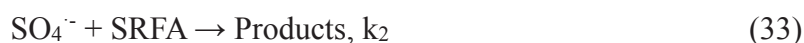


Figure 5.14. Decomposition of SAL (A) and TBL (B) by simulated sunlight activated PS in the presence of different concentration of SRFA. [SAL]₀ = 120 μM, [TBL]₀ = 120 μM, [PS]₀ = 6.0 mM, initial pH=7.0, t = 90 min.

The addition of SRFA decreased markedly the degradation of both SAL and TBL removal, as shown in Figure 6. Specifically, the decomposition rate constant of SAL decreased markedly from 2.2×10^{-4} to $6.2 \times 10^{-5} \text{ s}^{-1}$ with the SRFA concentration increased from 0 to 10 mg C L⁻¹. Concerning TBL, the removal rate constants showed the same tendency since the values decreased from 2.5×10^{-4} to $1.4 \times 10^{-4} \text{ s}^{-1}$ when the concentrations increased from 0 to 10

mg C L⁻¹. The inhibition effect of SRFA could be mainly attributed to two factors. The first one was the light screening factor, SRFA competed photons with PS, leading to less photons available for the activation of PS, as a result, less sulfate radicals were produced. Furthermore, dissolved organic matter was known to be a sink of ·OH and SO₄^{·-} due to some functional groups, which were prone to react with these two radicals [38, 61, 62]. The second-order rate constant of SRFA with SO₄^{·-} and was reported as 1.4×10³ mgC⁻¹ s⁻¹ [19].



Where P represents the target compounds SAL or TBL. In the absence of SRFA, if we assume that sulfate radicals only react with target compound P, the rate of P degradation could be written as:

$$-\frac{d[\text{P}]}{dt} = I_{PS}^0 \Phi \quad (34)$$

Where I_{PS} is the light intensity absorbed by PS and Φ , is the quantum yield of sulfate radical formation. In the absence of SRFA, at the initial step of the reaction, I_{PS} equals to:

$$I_{PS} = \sum_{290}^{340} I_0^\lambda (1 - 10^{-\varepsilon^\lambda cb}) \quad (35)$$

Where I_0^λ is the light intensity of the lamp at a specific wavelength, ε^λ is molar extinction coefficient of PS at the same wavelength (M⁻¹cm⁻¹), c is the PS concentration (M), and b is the path length of the light through the reaction solution (in our reactor, $b = 3.5$ cm). And in the presence of SRFA, I_{PS} becomes:

$$I_{PS} = \sum_{290}^{340} I_0^\lambda \frac{\varepsilon_{PS}^\lambda c_{PS}}{\varepsilon_{PS}^\lambda c_{PS} + \varepsilon_{SRFA}^\lambda c_{SRFA}} (1 - 10^{-(\varepsilon_{PS}^\lambda c_{PS} + \varepsilon_{SRFA}^\lambda c_{SRFA})b}) \quad (36)$$

Therefore, the rate of P degradation in the presence of SRFA at the initial step could be

written as:

$$-\frac{d[P]}{dt} = I_{PS}^0 \Phi \frac{k_1[P]}{k_1[P] + k_2[SRFA]} \quad (37)$$

Based on Eq 36 and 37, the inhibition effects induced by lighting screening and radical scavenging could be evaluated. Light intensities absorbed by PS were calculated (using Eq 36) as 1.27, 1.05, 0.81 and 0.57 10^{-7} Einstein $L^{-1} s^{-1}$ in the presence of 0, 2, 5, 10 mgC L^{-1} SRFA, respectively. The competition of SRFA with TBL or SAL for $SO_4^{\cdot-}$ was found to be of less importance, with SRFA of 10 mgC L^{-1} , the degradation of SAL only decreased approximately 3% from Eq 37. Thus, the inhibition of SRFA on SAL/TBL oxidation by UV/PS was mainly attributed to the lighting screening effect, and the quenching of $SO_4^{\cdot-}$ played a limited role.

5.2. Conclusion.

In summary, the feasibility of photo-activated persulfate for the removal of β 2-adrenoceptor agonists SAL and TBL was verified, and UV/PS was found to be an effective approach for their degradation under natural water conditions (pH 5-8). The LFP technique provided the transient kinetic data such as second-order rate constants, which should be further more reliable than the classic steady-state photolysis method. Our results highlight the potential utility of using LFP. This work also revealed the difference in oxidation mechanisms related to the phenoxy radicals reactivity. Two mechanisms, namely, $-OSO_3H$ addition (TBL) *versus* quinone-methide formation (SAL), were proposed by using LFP, HPLC-MS as well as the model substituted phenols (2-HBA and 4-HBA for SAL, 3,5-DHBA and resorcinol for TBL). This is the first time one demonstrates the selectivity of sulfate radical with different substituted phenols. Chloride (ranging from 0 to 500 mM) exhibited few effect on the degradation kinetics of SAL and TBL, mainly due to the reversed reaction from Cl^{\cdot} and SO_4^{2-} to regenerate Cl^- and $SO_4^{\cdot-}$. Unlikely, the addition of bromide was found to decrease the oxidation efficiencies of UV-PS on both SAL and TBL, sulfate radical would be scavenged by

Br⁻ to form less reactive species, Br₂^{•-}. The LFP technique provided the transient kinetic data of Br₂^{•-} with SAL at $2.1 \times 10^8 \text{ M}^{-1} \text{ s}^{-1}$, and with TBL at $3.9 \times 10^8 \text{ M}^{-1} \text{ s}^{-1}$, which was nearly ten times lower than those with sulfate radical, respectively. In the presence of excess Br⁻, bromine addition products of SAL and TBL were identified by HR-MS, further indicating the involvement of Br₂^{•-}. The presence of bicarbonates attenuated SAL and TBL degradation rates because of the low reactivity of CO₃^{•-} with the target contaminants. The second-order rate constants were estimated at $4.8 \times 10^7 \text{ M}^{-1} \text{ s}^{-1}$ for SAL and $3.2 \times 10^8 \text{ M}^{-1} \text{ s}^{-1}$ for TBL. The presence of NOM also exhibited detrimental effects to the degradation of SAL and TBL, lighting screening effect was regarded as the major factor responsible to the decrease of reaction rates, while sulfate radical scavenging played a very limited role in the UV-PS process. Considering that a large variety of substituted phenols are present in natural waters, the results of this work could help better understand their fates during AOPs treatment.

5.3 References

- [1] L. Zhou, Y. Ji, C. Zeng, Y. Zhang, Z. Wang, X. Yang, Aquatic photodegradation of sunscreen agent p-aminobenzoic acid in the presence of dissolved organic matter, *Water Res.* 47 (2013) 153-162.
- [2] T.A. Slotkin, F.J. Seidler, Terbutaline impairs the development of peripheral noradrenergic projections: Potential implications for autism spectrum disorders and pharmacotherapy of preterm labor, *Neurotoxicol Teratol* 36 (2013) 91-96.
- [3] D. Calamari, E. Zuccato, S. Castiglioni, R. Bagnati, R. Fanelli, Strategic survey of therapeutic drugs in the rivers Po and Lambro in northern Italy, *Environ Sci Technol* 37 (2003) 1241-1248.
- [4] J.P. Bound, N. Voulvoulis, Predicted and measured concentrations for selected pharmaceuticals in UK rivers: Implications for risk assessment, *Water Res* 40 (2006) 2885-2892.

- [5] T.A. Ternes, Occurrence of drugs in German sewage treatment plants and rivers¹, *Water Res* 32 (1998) 3245-3260.
- [6] M.C. Rhodes, F.J. Seidler, D. Qiao, C.A. Tate, M.M. Cousins, T.A. Slotkin, Does pharmacotherapy for preterm labor sensitize the developing brain to environmental neurotoxicants? Cellular and synaptic effects of sequential exposure to terbutaline and chlorpyrifos in neonatal rats, *Toxicol Appl Pharm* 195 (2004) 203-217.
- [7] M. Huerta-Fontela, M.T. Galceran, F. Ventura, Occurrence and removal of pharmaceuticals and hormones through drinking water treatment, *Water Res* 45 (2011) 1432-1442.
- [8] I. Oller, S. Malato, J. Sánchez-Pérez, Combination of advanced oxidation processes and biological treatments for wastewater decontamination—a review, *Sci Total Environ* 409 (2011) 4141-4166.
- [9] M.A. Oturan, J.-J. Aaron, Advanced oxidation processes in water/wastewater treatment: principles and applications. A review, *Crit Rev Env Sci Tec* 44 (2014) 2577-2641.
- [10] L. Zhou, W. Zheng, Y. Ji, J. Zhang, C. Zeng, Y. Zhang, Q. Wang, X. Yang, Ferrous-activated persulfate oxidation of arsenic (III) and diuron in aquatic system, *J. Hazard. Mater.* 263 (2013) 422-430
- [11] M.A. Dahmani, K. Huang, G.E. Hoag, Sodium persulfate oxidation for the remediation of chlorinated solvents (USEPA superfund innovative technology evaluation program), *Water, Air, & Soil Pollution: Focus* 6 (2006) 127-141.
- [12] G. Fang, J. Gao, D.D. Dionysiou, C. Liu, D. Zhou, Activation of persulfate by quinones: Free radical reactions and implication for the degradation of PCBs, *Environ Sci Technol* 47 (2013) 4605-4611.
- [13] D.A. House, Kinetics and mechanism of oxidations by peroxydisulfate, *Chem Rev* 62 (1962) 185-203.

- [14] G.-D. Fang, D.D. Dionysiou, Y. Wang, S.R. Al-Abed, D.-M. Zhou, Sulfate radical-based degradation of polychlorinated biphenyls: effects of chloride ion and reaction kinetics, *J Hazard Mater* 227 (2012) 394-401.
- [15] D. Zhao, X. Liao, X. Yan, S.G. Huling, T. Chai, H. Tao, Effect and mechanism of persulfate activated by different methods for PAHs removal in soil, *J Hazard Mater* 254 (2013) 228-235.
- [16] Y.-C. Lee, S.-L. Lo, P.-T. Chiueh, D.-G. Chang, Efficient decomposition of perfluorocarboxylic acids in aqueous solution using microwave-induced persulfate, *Water Res* 43 (2009) 2811-2816.
- [17] X.-R. Xu, X.-Z. Li, Degradation of azo dye Orange G in aqueous solutions by persulfate with ferrous ion, *Sep Purif Technol* 72 (2010) 105-111.
- [18] P. Neta, R.E. Huie, A.B. Ross, Rate constants for reactions of inorganic radicals in aqueous solution, *J. Phys. Chem. Ref. Data* 17 (1988) 1027-1284.
- [19] H.V. Lutze, S. Bircher, I. Rapp, N. Kerlin, R. Bakkour, M. Geisler, C. von Sonntag, T.C. Schmidt, Degradation of chlorotriazine pesticides by sulfate radicals and the influence of organic matter, *Environmental science & technology* 49 (2015) 1673-1680.
- [20] X. He, S.P. Mezyk, I. Michael, D. Fatta-Kassinos, D.D. Dionysiou, Degradation kinetics and mechanism of β -lactam antibiotics by the activation of H_2O_2 and $Na_2S_2O_8$ under UV-254nm irradiation, *J Hazard Mater* 279 (2014) 375-383.
- [21] P.M.D. Gara, G.N. Bosio, M.C. Gonzalez, N. Russo, M. del Carmen Michelini, R.P. Diez, D.O. Mártire, A combined theoretical and experimental study on the oxidation of fulvic acid by the sulfate radical anion, *Photochemical & Photobiological Sciences* 8 (2009) 992-997.
- [22] P. Nfodzo, H. Choi, Sulfate radicals destroy pharmaceuticals and personal care products, *Environ Eng Sci* 28 (2011) 605-609.

- [23] M.M. Ahmed, S. Barbati, P. Doumenq, S. Chiron, Sulfate radical anion oxidation of diclofenac and sulfamethoxazole for water decontamination, *Chem Eng J* 197 (2012) 440-447.
- [24] C. Tan, N. Gao, Y. Deng, Y. Zhang, M. Sui, J. Deng, S. Zhou, Degradation of antipyrine by UV, UV/H₂O₂ and UV/PS, *J Hazard Mater* 260 (2013) 1008-1016.
- [25] K.A. Rickman, S.P. Mezyk, Kinetics and mechanisms of sulfate radical oxidation of β -lactam antibiotics in water, *Chemosphere* 81 (2010) 359-365.
- [26] R. Matta, S. Tlili, S. Chiron, S. Barbati, Removal of carbamazepine from urban wastewater by sulfate radical oxidation, *Environ Chem Lett* 9 (2011) 347-353.
- [27] T. Zhang, Y. Chen, T. Leiknes, Oxidation of Refractory Benzothiazoles with PMS/CuFe₂O₄: Kinetics and Transformation Intermediates, *Environmental science & technology* (2016).
- [28] O. Brede, S. Kapoor, T. Mukherjee, R. Hermann, S. Naumov, Diphenol radical cations and semiquinone radicals as direct products of the free electron transfer from catechol, resorcinol and hydroquinone to parent solvent radical cations, *PCCP* 4 (2002) 5096-5104.
- [29] M.R. Ganapathi, R. Hermann, S. Naumov, O. Brede, Free electron transfer from several phenols to radical cations of non-polar solvents, *PCCP* 2 (2000) 4947-4955.
- [30] J. Feitelson, E. Hayon, A. Treinin, Photoionization of phenols in water. Effects of light intensity, oxygen, pH, and temperature, *J. Am. Chem. Soc.* 95 (1973) 1025-1029.
- [31] X. Chen, D.S. Larsen, S.E. Bradforth, I.H. van Stokkum, Broadband spectral probing revealing ultrafast photochemical branching after ultraviolet excitation of the aqueous phenolate anion, *The Journal of Physical Chemistry A* 115 (2011) 3807-3819.
- [32] D.W. Silverstein, N. Govind, H.J. van Dam, L. Jensen, Simulating One-Photon Absorption and Resonance Raman Scattering Spectra Using Analytical Excited State Energy

Gradients within Time-Dependent Density Functional Theory, *Journal of chemical theory and computation* 9 (2013) 5490-5503.

[33] V.A. Roginsky, L.M. Pisarenko, W. Bors, C. Michel, M. Saran, Comparative pulse radiolysis studies of alkyl- and methoxy-substituted semiquinones formed from quinones and hydroquinones, *J. Chem. Soc., Faraday Trans.* 94 (1998) 1835-1840.

[34] C. Liang, Z.-S. Wang, C.J. Bruell, Influence of pH on persulfate oxidation of TCE at ambient temperatures, *Chemosphere* 66 (2007) 106-113 %@ 0045-6535.

[35] G.-D. Fang, D.D. Dionysiou, D.-M. Zhou, Y. Wang, X.-D. Zhu, J.-X. Fan, L. Cang, Y.-J. Wang, Transformation of polychlorinated biphenyls by persulfate at ambient temperature, *Chemosphere* 90 (2013) 1573-1580

[36] O.S. Furman, A.L. Teel, R.J. Watts, Mechanism of base activation of persulfate, *Environ Sci Technol* 44 (2010) 6423-6428.

[37] R. Zhang, P. Sun, T.H. Boyer, L. Zhao, C.-H. Huang, Degradation of pharmaceuticals and metabolite in synthetic human urine by UV, UV/H₂O₂, and UV/PDS, *Environmental science & technology* 49 (2015) 3056-3066.

[38] M. Nie, Y. Yang, Z. Zhang, C. Yan, X. Wang, H. Li, W. Dong, Degradation of chloramphenicol by thermally activated persulfate in aqueous solution, *Chem Eng J* 246 (2014) 373-382.

[39] L. Zhou, C. Ferronato, J.-M. Chovelon, M. Sleiman, C. Richard, Investigations of diatrizoate degradation by photo-activated persulfate, *Chem Eng J* 311 (2017) 28-36.

[40] G.P. Anipsitakis, D.D. Dionysiou, Radical generation by the interaction of transition metals with common oxidants, *Environ Sci Technol* 38 (2004) 3705-3712

[41] Y. Chiang, A. Kresge, Y. Zhu, Flash Photolytic Generation and Study of p-Quinone Methide in Aqueous Solution. An Estimate of Rate and Equilibrium Constants for Heterolysis

of the Carbon– Bromine Bond in p-Hydroxybenzyl Bromide, *J Am Chem Soc* 124 (2002) 6349-6356.

[42] G.P. Anipsitakis, D.D. Dionysiou, M.A. Gonzalez, Cobalt-mediated activation of peroxymonosulfate and sulfate radical attack on phenolic compounds. Implications of chloride ions, *Environmental science & technology* 40 (2006) 1000-1007.

[43] R.E. Huie, C.L. Clifton, P. Neta, Electron transfer reaction rates and equilibria of the carbonate and sulfate radical anions, *International Journal of Radiation Applications and Instrumentation. Part C. Radiation Physics and Chemistry* 38 (1991) 477-481.

[44] Y. Yang, J.J. Pignatello, J. Ma, W.A. Mitch, Comparison of halide impacts on the efficiency of contaminant degradation by sulfate and hydroxyl radical-based advanced oxidation processes (AOPs), *Environ Sci Technol* 48 (2014) 2344-2351.

[45] C. Liang, Z.-S. Wang, N. Mohanty, Influences of carbonate and chloride ions on persulfate oxidation of trichloroethylene at 20 °C, *Sci. Total Environ.* 370 (2006) 271-277.

[46] C. George, J.-M. Chovelon, A laser flash photolysis study of the decay of $\text{SO}_4^{\cdot-}$ and $\text{Cl}_2^{\cdot-}$ radical anions in the presence of Cl^- in aqueous solutions, *Chemosphere* 47 (2002) 385-393.

[47] G.V. Buxton, M. Bydder, G.A. Salmon, The reactivity of chlorine atoms in aqueous solution Part II. The equilibrium $\text{SO}_4^{\cdot-} + \text{Cl}_2 \rightleftharpoons \text{SO}_4^{2-} + \text{Cl}_2^{\cdot-}$, *Phys Chem Chem Phys* 1 (1999) 269-273.

[48] C. Liang, Z.-S. Wang, N. Mohanty, Influences of carbonate and chloride ions on persulfate oxidation of trichloroethylene at 20 C, *Sci Total Environ* 370 (2006) 271-277.

[49] J.-Y. Fang, C. Shang, Bromate formation from bromide oxidation by the UV/persulfate process, *Environ Sci Technol* 46 (2012) 8976-8983.

- [50] H.V. Lutze, R. Bakkour, N. Kerlin, C. von Sonntag, T.C. Schmidt, Formation of bromate in sulfate radical based oxidation: mechanistic aspects and suppression by dissolved organic matter, *Water Res* 53 (2014) 370-377.
- [51] V. Nagarajan, R.W. Fessenden, Flash photolysis of transient radicals. 1. X/sub 2//sup- /with X= Cl, Br, I, and SCN, *J. Phys. Chem.:(United States)* 89 (1985).
- [52] K. Liu, J. Lu, Y. Ji, Formation of brominated disinfection by-products and bromate in cobalt catalyzed peroxymonosulfate oxidation of phenol, *Water Res* 84 (2015) 1-7.
- [53] P.O. Darnerud, Toxic effects of brominated flame retardants in man and in wildlife, *Environ Int* 29 (2003) 841-853.
- [54] J. Huang, S.A. Mabury, A new method for measuring carbonate radical reactivity toward pesticides, *Environ Toxicol Chem* 19 (2000) 1501-1507.
- [55] Y. Fan, Y. Ji, D. Kong, J. Lu, Q. Zhou, Kinetic and mechanistic investigations of the degradation of sulfamethazine in heat-activated persulfate oxidation process, *J Hazard Mater* 300 (2015) 39-47.
- [56] Y. Ji, C. Dong, D. Kong, J. Lu, New insights into atrazine degradation by cobalt catalyzed peroxymonosulfate oxidation: kinetics, reaction products and transformation mechanisms, *J Hazard Mater* 285 (2015) 491-500.
- [57] Y. Ji, C. Dong, D. Kong, J. Lu, Q. Zhou, Heat-activated persulfate oxidation of atrazine: Implications for remediation of groundwater contaminated by herbicides, *Chem Eng J* 263 (2015) 45-54.
- [58] S.-N. Chen, M.Z. Hoffman, G.H. Parsons Jr, Reactivity of the carbonate radical toward aromatic compounds in aqueous solution, *The Journal of Physical Chemistry* 79 (1975) 1911-1912.
- [59] Y. Zuo, R.D. Jones, Photochemistry of natural dissolved organic matter in lake and wetland waters—production of carbon monoxide, *Water Research* 31 (1997) 850-858.

- [60] N. Corin, P. Backlund, M. Kulovaara, Degradation products formed during UV-irradiation of humic waters, *Chemosphere* 33 (1996) 245-255.
- [61] Y.-H. Guan, J. Ma, Y.-M. Ren, Y.-L. Liu, J.-Y. Xiao, L.-q. Lin, C. Zhang, Efficient degradation of atrazine by magnetic porous copper ferrite catalyzed peroxymonosulfate oxidation via the formation of hydroxyl and sulfate radicals, *Water Res.* 47 (2013) 5431-5438.
- [62] J.J. Pignatello, E. Oliveros, A. MacKay, Advanced oxidation processes for organic contaminant destruction based on the Fenton reaction and related chemistry, *Crit Rev Env Sci Tec* 36 (2006) 1-84.

Chapter VI

General conclusions and prospects

In this thesis, the reactivity of sulfate radical with natural organic matter (NOM) was initially investigated. NOM is one of the most important constituents in natural water and wastewater, it would react inevitably with $\text{SO}_4^{\bullet-}$ in the application of SR-AOPs. This work estimated the reaction rate constants of $\text{SO}_4^{\bullet-}$ with four selected NOM by recording the decay of $\text{SO}_4^{\bullet-}$ and the formation of new species by means of LFP. The presence of NOM was found to accelerate the decay rate of $\text{SO}_4^{\bullet-}$, and the new generated species were assigned to phenoxyl radicals of NOM. By using a numerical method, the rate constants for $\text{SO}_4^{\bullet-}$ scavenging were calculated at 1.5, 1.8, 1.9 and $3.5 \times 10^3 \text{ s}^{-1} \text{ mgC}^{-1} \text{ L}$ for SRNOM, SRFA, ESFA and NLNOM, respectively. The bleaching rates of these NOM were consistent with LFP measured rate constants. The rate constants of $\bullet\text{OH}$ reaction with different NOMs were reported at $2.7 \times 10^4 \text{ s}^{-1} \text{ mgC}^{-1} \text{ L}$, which is much higher than those with $\text{SO}_4^{\bullet-}$. Thus, due to the scavenging by NOM, AOPs based on $\text{SO}_4^{\bullet-}$ seems more efficient than those based on $\bullet\text{OH}$ in natural water and wastewater (containing NOM), depending on the reaction conditions and the target contaminant.

Iodinated X-ray contrast media diatrizoate (DTZ), β 2-adrenoceptor agonists salbutamol (SAL) and terbutaline (TBL) were selected as our target micro-pollutants. Their reactivity, reaction kinetics and mechanisms with sulfate radical, the effects of natural organic matters were studied systematically in this thesis. The oxidation process was achieved by using simulated sunlight (from a solar simulator Suntest CPS+) activated PS.

Specifically, in the case of DTZ, UV/PS was more efficient than UV/ H_2O_2 process. Sulfate radicals ($\text{SO}_4^{\bullet-}$) was the dominant reactive species in the oxidation process, and the second-order rate constant of sulfate radical with DTZ was calculated as $1.90 \times 10^9 \text{ M}^{-1} \text{ s}^{-1}$ based on laser flash photolysis (LFP) experiments. The results also indicated that increasing initial PS concentration favored the decomposition of DTZ; whereas, degradation of DTZ was not

affected by pH change ranging from 4.5 to 8.5. DOM inhibited DTZ removal rate, while, bicarbonate enhanced it, and chloride ions induced a negative effect above 500 mM. Major oxidation pathways including deiodination-hydroxylation, decarboxylation- hydroxylation and side chain cleavage were proposed. We suggest a direct photodegradation of primary intermediates generated by $\text{SO}_4^{\bullet-}$ attack. These findings demonstrate that halogenated pollutants can readily react with $\text{SO}_4^{\bullet-}$ to form light-absorbing intermediates (ranging from 350 to 500 nm). Thus, this activation method could be a promising approach in the removal of ICMs.

In the experiments dealing with SAL and TBL, the second-order rate constants of sulfate radical reaction with SAL and TBL were measured as $(3.7 \pm 0.3) \times 10^9$ and $(4.2 \pm 0.3) \times 10^9$ $\text{M}^{-1} \text{s}^{-1}$ by LFP, respectively. For both SAL and TBL, phenoxy radicals were found to play key roles in the orientation of the primary pathways. For SAL, a benzophenone derivative was generated by oxidation of the phenoxy radical. However, in the case of TBL, the transformation of the phenoxy radical into benzoquinone was impossible. Instead, the addition of $-\text{OSO}_3\text{H}$ on the aromatic ring was the major pathway. The same reactivity pattern was observed in the case of TBL structural analogs resorcinol and 3,5-dihydroxybenzyl alcohol. Our results revealed that basic conditions inhibited the decomposition of SAL and TBL, while, increasing PS dose enhanced the degradation. Moreover, the effects of natural water constituents, namely, chloride (Cl^-), bromide (Br^-), bicarbonate (HCO_3^-) and natural organic matter (NOM) were investigated, respectively. Our results indicated that chloride exhibited no effect on the oxidation efficiencies of SAL and TBL, while Br^- , HCO_3^- and NOM all showed inhibitory effects. Specifically, the detrimental effect of bromide could mainly be attributed to the scavenging of $\text{SO}_4^{\bullet-}$ to form less reactive species, $\text{Br}_2^{\bullet-}$. By using laser flash photolysis (LFP) technology, the second-order rate constants of $\text{Br}_2^{\bullet-}$ with SAL and TBL were estimated at 2.1 and 3.9×10^8 $\text{M}^{-1} \text{s}^{-1}$, respectively, which were far smaller than those with

$\text{SO}_4^{\bullet-}$ ($3.7 \times 10^9 \text{ M}^{-1} \text{ s}^{-1}$ for SAL and $4.2 \times 10^9 \text{ M}^{-1} \text{ s}^{-1}$ for TBL). In addition, bromine addition products of SAL and TBL were detected in the presence of Br^- by high resolution mass spectrometry (HR-MS), which were believed to be more toxic than the mother compounds. Similar to bromide, HCO_3^- could also quench $\text{SO}_4^{\bullet-}$ to generate carbonate radical ($\text{CO}_3^{\bullet-}$), which was also less reactive than sulfate radical with SAL ($4.8 \times 10^7 \text{ M}^{-1} \text{ s}^{-1}$) and TBL ($3.2 \times 10^8 \text{ M}^{-1} \text{ s}^{-1}$). In the case of NOM, lighting screening effect was regarded as the major factor responsible to the decrease of reaction rates, while sulfate radical scavenging played a very limited role in the UV-PS process.

The present thesis showed that UV activated PS was a promising strategy for the elimination of various micro-pollutants from aqueous solutions. However, it should be noted that in real water matrix such as WWTPs, the presence of different kinds of water constitutes (e.g. bicarbonate, NOM) may scavenge sulfate radical, reducing the oxidation efficiency. In addition, further studies should also better consider the role of secondary reactive species (including light-absorbing intermediates) and the influence of naturally occurring constituents in natural waters, for example, the involvement of $\text{Br}_2^{\bullet-}$ could produce very toxic bromine products. Therefore, before the application of SR-AOPs, a thorough evaluation of the reactivity of target micro-pollutants with sulfate radical, the effects of water constitutes and the toxicity of intermediates is of great importance in order to optimize treatment process as well as evaluate the potential ecological risks.

Appendix

List of published papers during PhD period.

1. **Lei Zhou**, Ya Zhang, Qi Wang, Corinne Ferronato, Xi Yang*. Jean-Marc Chovelon**, Photochemical behavior of carbon nanotubes in natural waters: reactive oxygen species production and effects on •OH generation by Suwannee River fulvic acid, nitrate, and Fe (III). *Environmental Science and Pollution Research*. 2016, 23, 19520–19528.
2. **Lei Zhou**, Qi Wang, Ya Zhang, Yuefei Ji, Xi Yang*. Aquatic photolysis of β 2-agonist salbutamol: kinetics and mechanism studies. *Environmental Science and Pollution Research*. 2016, 24, 5544–5553.
3. **Lei Zhou**, Corinne Ferronato, Jean-Marc Chovelon*, Mohamad Sleiman, Claire Richard*. Investigations of diatrizoate degradation by photo-activated persulfate. *Chemical Engineering Journal*. 2017,311, 28-36.
4. **Lei Zhou**, Ya Zhang*, Rongrong Ying, Guoqing Wang*, Tao Long, Jianhua Li, Yusuo Lin. Thermo Activated Persulfate Oxidation of Pesticide Chlorpyrifos in Aquatic System: Kinetic and Mechanistic Investigations. *Environmental Science and Pollution Research*. 2017, 24, 11549–11558.
5. **Lei Zhou**, Mohamad Sleiman, Corinne Ferronato, Jean-Marc Chovelon*, Claire Richard*. Reactivity of sulfate radicals with natural organic matters. *Environmental Chemistry Letters*. 2017

